Surface nano-structured materials to control bacterial contamination

Petya Stoyanova Petkova

A thesis submitted in fulfilment of the requirements for degree of

International Doctor of Philosophy

at the

Universitat Politècnica de Catalunya

Supervised by Dr. Tzanko Tzanov

Group of Molecular and Industrial Biotechnology (GBMI)

Department of Chemical Engineering

Universitat Politècnica de Catalunya

Terrassa (Barcelona)

2016

This thesis was financially supported by:

Ayudas para la formación de profesorado universitario (FPU)

Ref beca: FPU 12/06258

A pilot line of antibacterial and antifungal medical textiles based on a sonochemical process, FP7-228730

Group of Molecular and Industrial Biotechnology

На моето семейство
To my family

Abstract

The spread of bacteria and infections, initially associated with an increased number of hospital-acquired infections, has now extended into the community causing severe and difficult to diagnose and treat diseases. Additionally, many of those diseases are evoked by bacteria that have become resistant to antibiotics. Overcoming the ability of bacteria to develop resistance will potentially reduce the burden of these infections on the healthcare systems worldwide and prevent thousands of deaths each year.

At present, there is a great interest in manufacturing antimicrobial materials that would provide bacteria-free environment. The nano-scale particles are promising candidates to fight bacterial pathogens, since developing of resistance to their action is less likely to occur. Nanoparticles (NPs) can be incorporated into polymeric matrices to design a wide variety of nanocomposites. Such nano-structures consisting of inorganic and inorganic/organic NPs represent a novel class of materials with a broad range of applications.

This thesis is about the development of antibacterial nano-structured materials aimed at preventing the spread of bacteria. To achieve this, two versatile physicochemical and biotechnological tools, namely sonochemistry and biocatalysis were innovatively combined. Ultrasound irradiation used for the generation of various nano-structures and its combination with biocatalysts (enzymes) opens new perspectives in materials processing, here illustrated by the production of NPs coated medical textiles, water treatment membranes and chronic wound dressings.

The first part of the thesis aims at the development of antibacterial medical textiles to prevent the bacteria transmission and proliferation using two single step approaches for antibacterial NPs coating of textiles. In the first approach antibacterial zinc oxide NPs (ZnO NPs) and chitosan (CS) were deposited simultaneously on cotton fabric by ultrasound irradiation. The obtained hybrid NPs coatings demonstrated durable antibacterial properties after multiple washing cycles. Moreover, the presence of biopolymer in the NP hybrids improved the biocompatibility of the material in comparison with ZnO NPs coating alone.

In the second approach, a simultaneous sonochemical/enzymatic process for durable antibacterial coating of cotton with ZnO NPs was carried out. The enzymatic treatment provides better adhesion of the ZnO NPs and, as a consequence, enhanced coating stability during exploitation. Likewise to the antibacterial coatings obtained in the first approach, the antibacterial efficiency of these textiles was maintained after multiple intensive laundry

regimes used in hospitals. The NPs-coated cotton fabrics inhibited the growth of the most medically relevant bacteria species.

In the second part of the thesis, hybrid antibacterial biopolymer/silver NPs and cork matrices, were enzymatically assembled into an antimicrobial material with potential for water remediation. Intrinsically antibacterial amino-functional biopolymers, namely CS and aminocellulose were used as doping agents to stabilize colloidal dispersions of silver NPs (AgNPs), additionally providing the particles with functionalities for covalent immobilization on cork to impart durable antibacterial effect. The biopolymers promoted the antibacterial performance of the obtained nanocomposites in conditions simulating a real situation in constructed wetlands.

In the last, third part of the thesis, a bioactive nanocomposite hydrogel for wound treatment was developed. Sonochemically synthesized epigallocatechin gallate nanospheres (EGCG NSs) were incorporated and simultaneously crosslinked enzymatically into a thiolated chitosan hydrogel. The potential of the generated EGCG NSs for chronic wound treatment was evaluated by assessing its antibacterial properties and inhibitory effect on myeloperoxidase and collagenase biomarkers of chronic wound infection. Sustained release of the EGCG NSs from the biopolymer matrix was achieved. The latter, coupled with the good biocompatibility of the hydrogel suggested its potential for chronic wound management.

Keywords: antibacterial nanoparticles, chitosan, antibacterial coatings, medical textiles, ultrasound, water disinfection, nanocomposites, natural phenolics, enzymatic crosslinking, hydrogels, wound healing

Table of Contents

Abbreviation list

A

AgNPs	silver nanoparticles
$AgNO_3$	silver nitrate
$NaBH_4$	sodium borohydride
AC	aminocellulose
ICP – AES	inductive coupled plasma atomic emission spectroscopy

B

B. subtilis	Bacillus subtilis

C

CS	chitosan
CuNPs	copper nanoparticles
CuO NPs	copper oxide nanoparticles
CFU	colony forming units

D

DNSA	3,5-dinitrosalicylic acid
DLS	dynamic light scattering
DS	degree of substitution

E

E. coli	Escherichia coli
EGCG	epigallocatechin gallate
EGCG NSs	epigallocatechin gallate nanospheres
EDS	energy dispersive X – ray spectroscopy
ECM	extracellular matric

F

FTIR	Fourier transform infrared spectroscopy
FPU	filter paper assay

G

GAE	gallic acid equivalents

H

HAI	healthcare associated infections
HRP	horseradish peroxidase
HRSEM	high resolution environmental scanning electron microscope

M

MeO	metal oxide
MeO NPs	metal oxide nanoparticles
MgO NPs	magnesium oxide nanoparticle
MMPs	metalloproteinases
MPO	myeloperoxidase
MPRA	methicillin-resistant *Staphylococcus aureus*

N

NPs	nanoparticles
NSs	nanospheres
NCs	nanocapsules
NB	nutrient broth
$NaBH_4$	sodium borohidride

P

P. aeruginosa	Pseudomonas aeruginosa

R

ROS	reactive oxygen species

S

S. aureus	Staphylococcus aureus
SPR	surface plasmon resonance
STEM	scanning transmission electron microscopy

T

TiO_2 NPs	titanium dioxide nanoparticles
TBA	2-iminothiolane hydrochloride (Traut's reagent)
TC	thiolated chitosan
TEM	transmission electron microscope

U

US	ultrasound
UV	ultraviolet

W

WHO	World Health Organization

X

XPS	X-ray photoelectron spectroscopy

Z

ZnO	zinc oxide
ZnO NPs	zinc oxide nanoparticles
ζ	zeta potential

Figure, table and scheme captions

1 Introduction

Antibiotic resistance is a growing public health concern worldwide. Each year the number of people who acquire infections caused by antibiotic resistant bacteria increases, resulting in increased number of deaths. Antibiotics are the most commonly prescribed drugs to treat infections caused by bacteria. However, the emergence of new resistant microorganisms has accelerated alongside with their misuse and overuse, which contribute to the antibiotic resistance around the globe. Direct or indirect contact with a source of infectious pathogens e.g. environmental surfaces, healthcare settings, food and water supplies brings about the spread and transmission of pathogens. Therefore, an efficient strategy to address the threat of antimicrobial resistance should be aimed at: i) the prevention and control of the spread of bacteria and infections, and ii) the development of new bactericides to which bacteria cannot easily acquire resistance.

Recent approaches addressing this challenge explore non-traditional antibiotic agents such as antimicrobial nanoparticles (NPs) and nanosized carriers for target drug delivery. Antimicrobial NPs are found to be effective in inactivating various microorganisms. A variety of chemical and physical synthetic routes have been exploited for the NPs synthesis. Among them, the use of ultrasound (US) is currently positioned as one of the most powerful tools in nano-structured materials synthesis. Moreover, the US irradiation has been successfully applied to homogeneously coat the surface of variety of solid substrates, including textiles, glass and nylon. It has been demonstrated that the microjets and shock waves produced after cavitation collapse are able to drive the NPs at such high velocities towards the solid substrate that fusion and strong adherence by physical or chemical interactions with the surface occurs during collision. Another promising approach exploiting US is the combination of ultrasonic energy and enzymatic treatments as a strategy to boost the enzyme activity e.g. to accelerate the mass transfer during some of the textiles' manufacturing steps and thus, shorten the processing time. Both innovative tools (US and biocatalysts) could be also employed, alone or in combination, to create antibacterial surfaces and devices.

This thesis aims at designing of nano-functionalized materials able to prevent/reduce the bacterial spread. The rationale of the work is the integration of nano- and bio-technological approaches with sonochemistry. The innovative combination of antimicrobial NPs, biopolymers, enzymes, and sonochemical irradiation is exploited to develop the following nano-structured surfaces and devices: i) medical textiles coated with antibacterial metal oxide NPs and biopolymer/metal oxide nano-hybrids, ii) antibacterial biopolymer/metal NPs-

cork composites for water disinfection, and iii) bioactive nanocomposite hydrogels for wound treatment.

2 State-of-the-art

2.1 The global threat of antimicrobial resistance. Hospital-associated infections

"Antimicrobial resistance is resistance of a microorganism to an antimicrobial drug that was originally effective for treatment of infections caused by it."[1] The antimicrobial resistance threatens the effective prevention and treatment of an ever-increasing range of infections caused by resistant microorganisms, including bacteria, fungi, viruses and parasites. Those microorganisms are able to withstand the attack of antibacterial drugs, antifungals and antivirals, so that conventional treatments become ineffective and infections persist, increasing the risk of transmission.

The development of resistant strains is a natural occurrence that happen when resistant markers are exchanged between them or when microorganisms replicate themselves erroneously. The use and misuse of antimicrobial drugs accelerates the emergence of drug-resistant strains. Poor infection control practices, inadequate sanitary conditions and inappropriate food-handling encourage the further spread of antimicrobial resistance. The World Health Organization (WHO) warns that at present the so called "post-antibiotic era", in which common infections and minor injuries can kill, is a very real possibility due to the fact that resistance to common bacteria has reached alarming levels worldwide.[1]

The mechanisms by which antimicrobials act involve interference with proteins,[2] nucleic acid synthesis,[3] and inhibition of cell-wall synthesis i.e. the peptidoglycan biosynthesis.[4,5] However, bacteria have evolved genetic and biochemical ways of resisting these antimicrobial actions and to develop a tolerance to the antimicrobial drugs by several ways:[6]

- enzymatic inactivation of the drugs by beta-lactamases, acetylases, adenylases, and phosphorylases,
- limiting the drug access by virtue of membrane characteristics,
- altering the drug target so that the antimicrobial no longer binds to it,
- by passing the drug's metabolism,
- increasing the expression of efflux pumps.

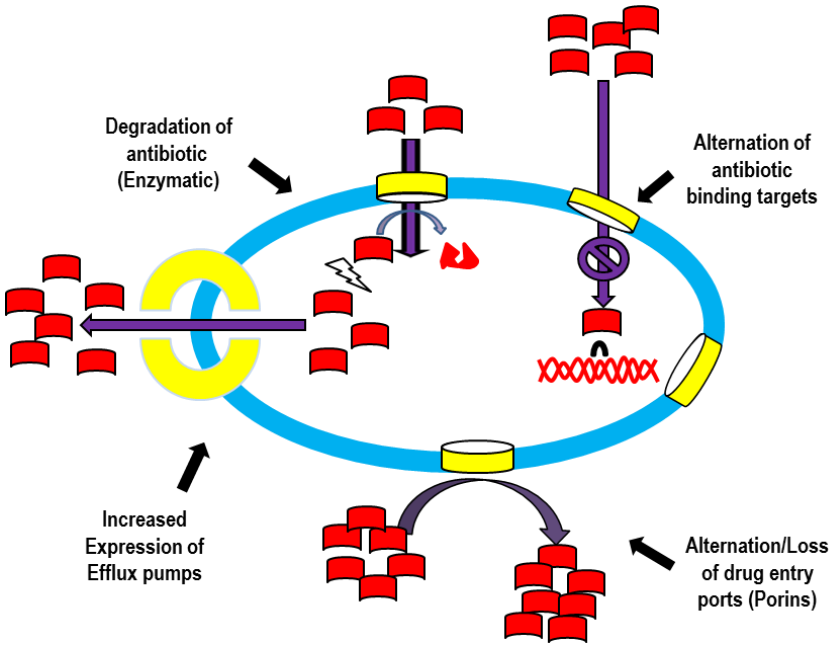

Figure 2.1 Bacterial antibiotic resistance mechanisms. Red blocks indicate antibiotics. Yellow channels indicate drug entry ports/porins. Mechanisms of bacterial resistance include the alteration of drug binding targets (DNA), degradation of antibiotics by enzymatic action, expression of efflux pumps on the cell membrane, and alteration or loss of porin/drug entry ports. The latter two mechanisms reduce the intracellular concentration and permeability of the drug into the cell.[6]

The resistance mechanisms develop by enterococci and staphylococci are of particular clinical significance as these are among the most frequent causes of infections in the healthcare units. The Enterococcus includes some of the most important nosocomial multidrug-resistant organisms, and these pathogens usually affect patients who are debilitated by other, concurrent illnesses and undergoing prolonged hospitalization.[7] The surveillance data indicate that the Enterococcus is the third most commonly isolated pathogen (12% of all hospital infections), behind only coagulase-negative staphylococcus and *Staphylococcus aureus* (*S. aureus*).[8] The mechanisms underlying antibiotic resistance in enterococci may be intrinsic (universally found within the genome of the species) and acquired (through mutation of intrinsic genes or horizontal exchange of genetic material encoding resistance determinants) and it includes i) intrinsic resistance to β-lactams, lincosamides (clindamycin) and streptogramins (quinupristin, dalfopristin) aminoglycosides, aztreonam, cephalosporins, imipenem, and trimethoprim-sulfamethoxazole; ii) tolerance to all cell-wall-active antimicrobials; and iii) acquired resistance to β-lactams (penicillin),

aminoglycosides, glycopeptides (vancomycin), chloramphenicol, erythromycin, tetracycline, streptogramins, daptomycin and linezolid.[9,10]

The resistance of staphylococci includes i) beta-lactamase production, ii) secretion of novel beta-lactamases, iii) expression of novel penicillin-binding proteins to which penicillins bind poorly, and iv) increased production or altered affinity to existing penicillin-binding proteins. As aforementioned (Figure 2.1), there are many mechanisms adopted for the development of resistance from bacteria and it is of great concern to prevent/reduce the spread of antimicrobial resistant pathogens in order to limit the occurrence of hospital acquired infections.

Hospital acquired infections, also called nosocomial infections, can be defined as infections that patients develop during the course of receiving healthcare treatment, being not present and without evidence of incubation at the time of admission to a healthcare setting. These also include infections acquired in the hospital, but appearing after the patients' discharge as well as vocational infections among personnel of the healthcare facility. The terms hospital-acquired or nosocomial infections are now replaced by healthcare associated infections (HAI) due to the diverse healthcare facilities currently available to patients.[1,11]

During hospitalization the patient is exposed to a variety of microorganisms and within hours after the admission, the patient's flora begins to acquire the characteristics of the surrounding bacterial environment. There are two sources causing HAI - endogenous or exogenous. The endogenous sources include body sites that are normally inhabited by microorganisms e.g. urinary and gastrointestinal tracts. While the exogenous sources include those that are not part of the patient such as visitors, medical personnel, equipment and the healthcare environment.

The development of clinical disease and thus, the frequency of nosocomial infections, depends of many factors such as patients susceptibility and microorganisms characteristics. Immunocompromised patients and patients with chronic diseases undergo invasive examinations and treatments. Such patients are having increased susceptibility to infections with opportunistic pathogens, part of the normal bacterial flora in the human. For example, commensal bacteria such as cutaneous coagulase-negative staphylococci cause intravascular line infection and intestinal *Escherichia coli* (*E. coli*) are the most common cause of urinary infection, if the natural host is compromised.[12] The HAI infections occur:

- up to 48 hours after hospital admission,
- up to 3 days after discharge,
- up to 30 days after an operation.[12]

The HAI are a major financial issue in the European healthcare system and were recognized as a major threat associated with medical care. On average, nosocomial patients stay in the hospital 2.5 times longer than patients without infection, hence, adding more than 10 million patients in hospitals in Europe per year. The alarming statistics show that 1 in 10 patients is affected by HAI which as a consequence leads to a substantial increase in health care costs each year.[13] Moreover, the HAI are important contributors to morbidity and mortality. Their significance as a public health problem increases with increasing economic and human impact due to: the increasing numbers and crowding of people, more frequent impaired immunity (age, illness, treatments), and most importantly the increasing bacterial resistance to antibiotics.[12] Among the numerous risk factors for acquiring a nosocomial infection, the length of hospital stay is the most important.

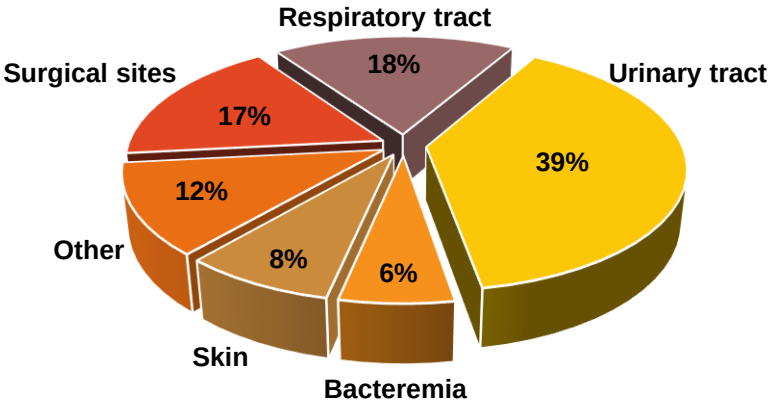

Figure 2.2 Sites of the most common nosocomial infections.[12]

Bacteria that cause nosocomial infections can be transmitted in several ways: i) from the permanent or transient flora of the patient (the bacteria cause infection because of transmission to sites outside the natural habitat, damage to tissue (wound) or inappropriate antibiotic therapy that allows overgrowth), ii) bacteria transmission from another patient or member of the hospital staff (via direct contacts between the patients and contaminated staff, via air or objectives when contaminated with patients' bacteria), and iii) microorganisms surviving in the hospital environment (water, food, linen, equipment and

supplies used).[12] Thus, major efforts of the healthcare organizations nowadays are aimed at preventing HAI and other adverse events in order to improve the healthcare delivery.

2.2 Strategies for prevention and control of hospital-associated infections

The prevention of nosocomial infections requires an integrated and monitored programme which includes: i) limiting transmission of organisms and the risk of endogenous infections by minimizing invasive procedures, ii) controlling environmental risks for infection, and iii) promoting optimal antimicrobial use and surveillance of infections.[12] It was shown that the implementation of the infection control programmes could reduce the occurrence of nosocomial infections by 32 %.[14] Thus, the attention to the preventive strategies may significantly reduce disease transmission rates. Frequent hand washing remains the single most important intervention in infection control. The use of gloves, gowns, and masks together with the employment of adequate sterilization and disinfection practices have a role in preventing infections.[15]

Despite the completion of the previously stated prevention strategies, the problem of infections related to medical implants and devices persists as their role in the disease transmission remains undefined. The virulent microorganisms can readily colonize surfaces of materials, such as white coats, bed sheets, stethoscopes and catheters among others.[15] Moreover, bacteria can grow in colonies which encapsulate itself with a protective extracellular polymeric matrix forming biofilms. The biofilm structure becomes much harder to combat than circulating bacteria due to the intrinsic resistance of these structures to antimicrobial agents and host defense mechanisms.[16] Thus, there is a strong need to mitigate bacterial colonization by imparting antibacterial surface properties or by equipping the medical surfaces with features that prevent bacterial attachment.

Several surface modification approaches aimed at introducing surface-mediated antibacterial properties are focused on improving the currently marketed materials or on designing of new ones (Figure 2.3).

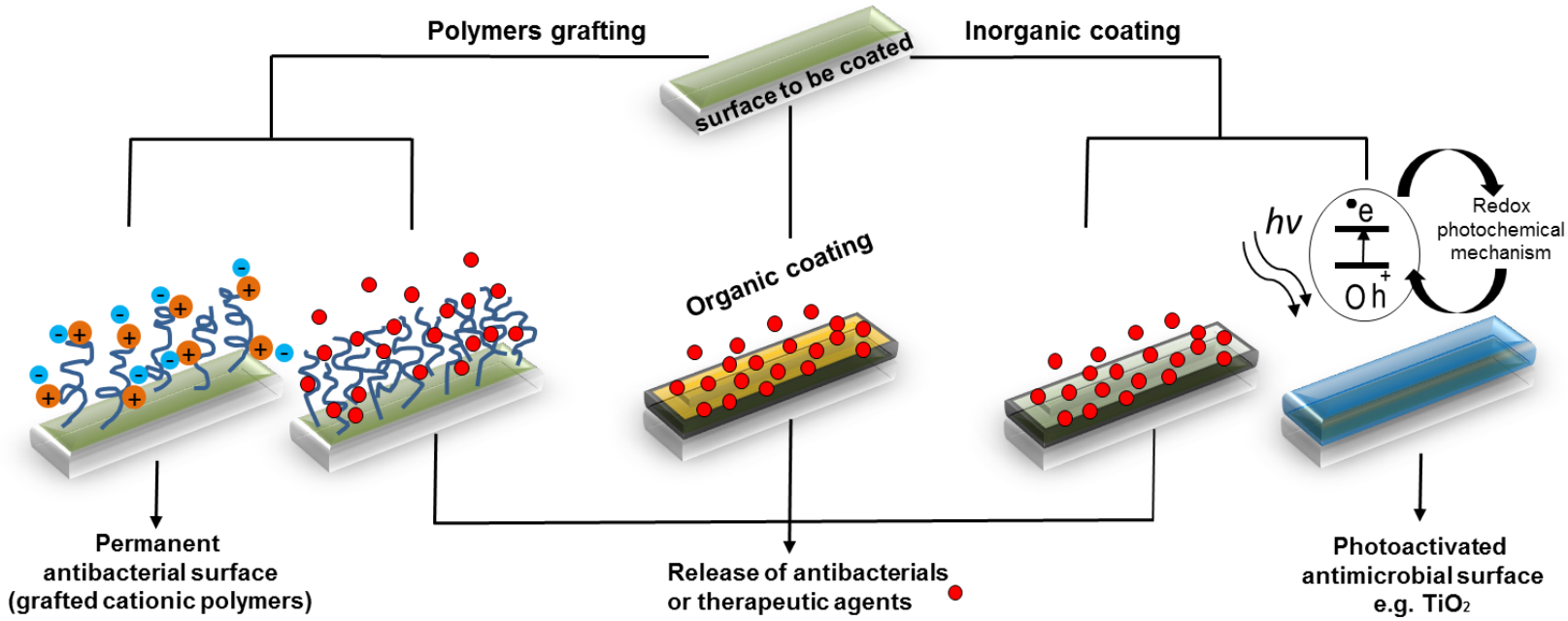

Figure 2.3 Surface modification approaches in medical devices aimed at obtaining antibacterial properties (adapted from[17]).

Important efforts have been directed at designing surfaces that release antibacterial agents. In this line, polymers and polymer coatings present a potentially interesting approach when controlled drug release of organic or inorganic antimicrobial actives is envisaged. Drug release from a matrix has intrinsic disadvantages involving the duration and effectiveness of the antibacterial action, since they are limited by drug loading and release kinetics. This issue, however, can be overcome by applying strategies to control the release of actives from the matrices. Such approaches include the covalent immobilization of the active molecules on the surface or their loading into polymer matrices (which allows their controlled release as the polymer degrades). The designing of inorganic (or hybrid organic-inorganic) coatings, in which both an antibacterial activity (from the surface) and antimicrobial compound release are possible is another promising strategy.[17]

The development of antimicrobial biomaterials and coatings based on nanosized particles is of great interest in the fields of bionanotechnology and applied nanomaterials due to their extraordinary size-dependent physical and chemical properties. At present, the nanomaterials are rapidly being commercialized and have become indispensable in many areas of human activity such as biology and medicine.[18]

2.3 Antibacterial nanoparticles

Nanoparticles (NPs) are microscopic particles having at least one dimension in the order of 100th of nm or less. However, in the literature often the term "*nano*" is used for any particles in the size range 1–1,000 nm especially when referring to organic structures design for e.g. drug delivery applications or structures composed from more than one type of molecules.[19,20]

The nano-structures are consider as a bridge between bulk materials and atomic or molecular structures. The bulk material usually have constant physical properties regardless of its size, but at the nano-scale often this is not the case.

In the fields of science and technology the nanomaterial can be used for a wide variety of applications since they possess unique and beneficial chemical, physical, and mechanical properties. The application of different nanoscale materials is getting importance in areas such as electronic storage systems,[21] civil engineering,[22] chemistry,[23] biomedicine and molecular biology,[24,25] vehicles for gene and drug delivery,[26,27] biomagnetic separation,[28] agro-food industry,[29] textile engineering,[30] and semiconductor physics[31], providing novel technological advances. Nowadays, a close attention receives the usage of antibacterial nanomaterials, such as chitosan (CS) NPs, proteins, metal-containing NPs e.g. metal and

metal oxides (MeO) NPs etc. Some of these nano-scaled particles act with multiple simultaneous mechanisms against microbes (Figure 2.4) which makes the development of resistance to these NPs unlikely, because multiple simultaneous gene mutations in the same bacterial cell would be required for that resistance to develop.[32] The antimicrobial NPs can be used effectively by coating them on the surfaces that require antimicrobial functions, for instance, on medical devices, textiles and water treatment filters.[33]

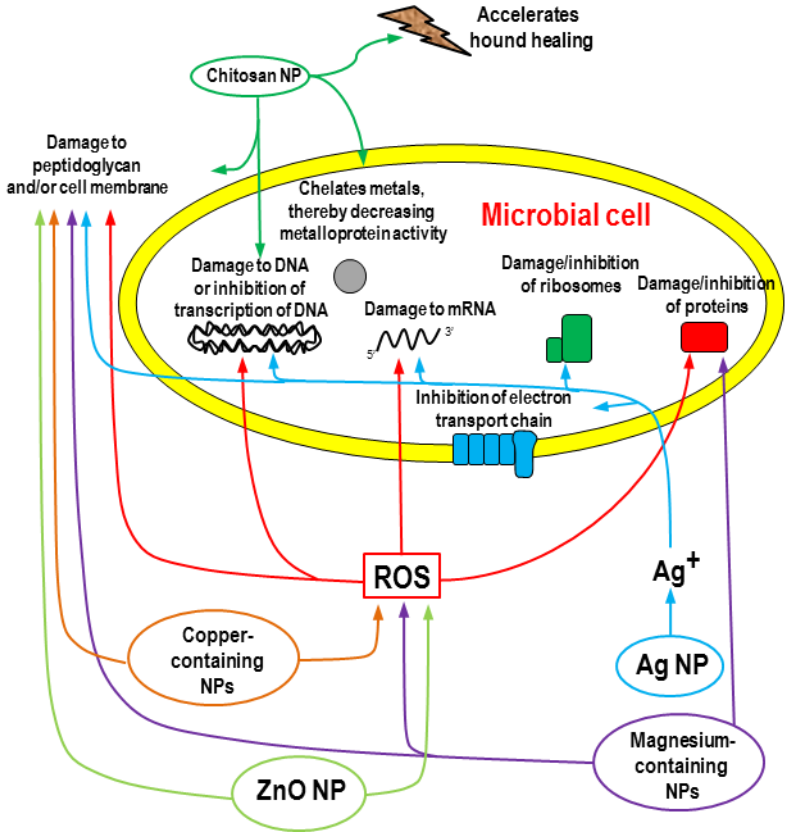

Figure 2.4 Multiple mechanisms of antimicrobial action of, chitosan-containing NPs (chitosan NPs), silver-containing NPs (AgNPs), zinc oxide-containing NPs (ZnO NPs), copper-containing NPs, and magnesium-containing NPs; ROS refers to reactive oxygen species (adapted from[32]).

2.3.1 Synthesis of nanoparticles. Sonochemistry - a versatile tool for nanoparticles synthesis and antimicrobial nano-functionalization of surfaces

Different physical and chemical processes are currently used to synthesize metal NPs, with desired size, size distribution and morphology/shape. While some methods are bottoms up (synthesis), some are called top down ("milling"). Top down methods involve braking the larger materials (bulk or micro structures) into NPs, while bottom up methods start form homogeneous solution or gas to build up the nano-structure (particle, layer, wire etc.). The synthesis methods include liquid and gas phase processes such as micro-emulsion, reverse micelle process, novel spray methods and sol-gel assisted *in-situ* techniques.

Some of the most common techniques used to prepare biodegradable NPs (nanospheres (NSs) and nanocapsules (NCs)) include coacervation and phase separation, emulsification diffusion, solvent displacement and solvent evaporation, sol-gel encapsulation, supercritical fluid technology, spray drying and spray congealing.[34] However, the majority of the synthesis routes for generation of polymeric nanoscale biomedical materials are based on emulsification techniques, and are achieved either directly from a macromolecule, or through a polymerization reaction during the preparation.[35,36] Selection of an appropriate route depends on different factors including the particle size, their thermal, chemical and physiological stability, and the requirement of an organic solvent and surfactants in the reaction. The latter two are being directly associated with the biocompatibility of the final product. However, whenever referring to the industry, the main requirements to the NPs synthesis process are to be low-cost, environmentally friendly and to be suitable for both continuous operation and a high production rate.

Sonochemistry is a research field in which due to the application of powerful ultrasound (US) radiation molecules undergo a chemical reaction. The US irradiation of liquids (20 KHz–10 MHz) creates conditions important for the improvement of the stoichiometric and catalytic chemical reactions by increasing the reactivity, in some cases, nearly by a million-fold. The greatest advances in sonochemistry, however, reside in the production of new materials with unusual properties. The synthesis capacity of US comes from the acoustic cavitation phenomenon, which consists of the formation, growth and the implosive collapse of bubbles in a liquid.[37] The dynamics of i) cavity growth, through the diffusion of solute vapor into the volume of bubble, and ii) collapse, which occurs when the bubble size reaches its maximum, are highly dependent on the local environment and are different in homogeneous liquids and near the liquid-solid interface. The implosions of cavities inside which gases and vapors are

compressed, generate intense heat that raises the temperature of the liquid surrounding the cavity and creates local hot spots.[38] It is claimed that upon the collapse of bubbles, temperatures of nearly 5000 °C and local pressures as high as 500 atmospheres are obtained (Figure 2.5A). Since the collapse of bubbles occurs in less than nanoseconds, the heating and cooling rates during cavitation are greater than 10^9 K/s.[39]

In general, no chemical reactions happen when US irradiation is applied to solid and solid-gas systems as the cavitation phenomenon takes place only in liquids. Thus, the chemical effects of US fall into three areas: i) homogeneous sonochemistry of liquids, ii) heterogeneous sonochemistry of liquid-liquid or liquid-solid systems, and iii) sonocatalysis (initiation of a catalytic reaction by irradiation with US).[39] The source of homogeneous sonochemistry is the localized hot spot, while related phenomena occur with cavitation in liquid-solid systems. There are two important aspects - microjets and shock waves - derived from cavitation observed nearby surfaces. The cavitation and the shock waves, created by US can accelerate solid particles to very high velocities, as the non-spherical collapse of the cavities drives high speed microjets of liquid directed towards the surface (Figure 2.5B).

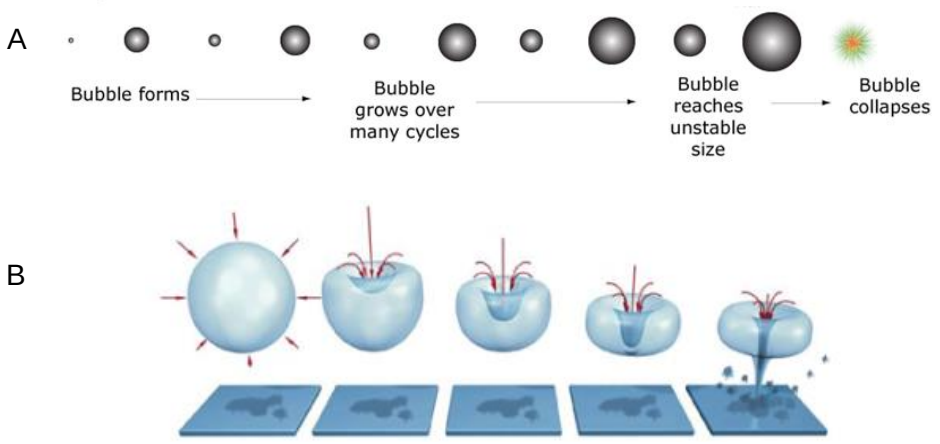

Figure 2.5 A) Bubble formation, growth and subsequent collapse over several acoustic cycles. A bubble oscillates in phase with the applied sound wave, contracting during compression and expanding during rarefactions,[40] B) Collapsing bubbles near a surface experience non-uniformities in their surroundings that results in the formation of high-velocity microjets.[41]

These extreme conditions cause the rupture of chemical bonds and enhance mass transport and thus, cause changes in the surface morphology, reactivity and composition. In the process of formation of nanomaterials, their solid state is determined by the high cooling

rates coupled with the type of precursors used. In the case, when volatile precursors are used, gas phase reactions are predominant and the formed NPs are amorphous.[42] On the other hand, when for the synthesis of NPs the precursor is a non-volatile compound, the reaction occurs in the liquid phase and in this case the products formed could be nanoamorphous or nanocrystalline.[38] The latter depends upon the temperature of the ring region, where the reactions take place. In the former case, the volatile precursor (e.g. a volatile organometallic compound) will produce free metal atoms generated by bond dissociation due to the high temperatures created during bubble collapse. These atoms can be injected into the liquid phase and nucleate to form NPs or other nano-structured materials if appropriate templates or stabilizers are present in the solution. Nonvolatile precursors may still undergo sonochemical reactions, even outside of the collapsing bubbles by undergoing reactions with radicals or other high energy species produced from the sonolysis of vapor molecules inside the collapsing bubbles that then diffuse into the liquid phase to initiate a series of reactions (e.g. reduction of metal cations, Figure 2.6).[43]

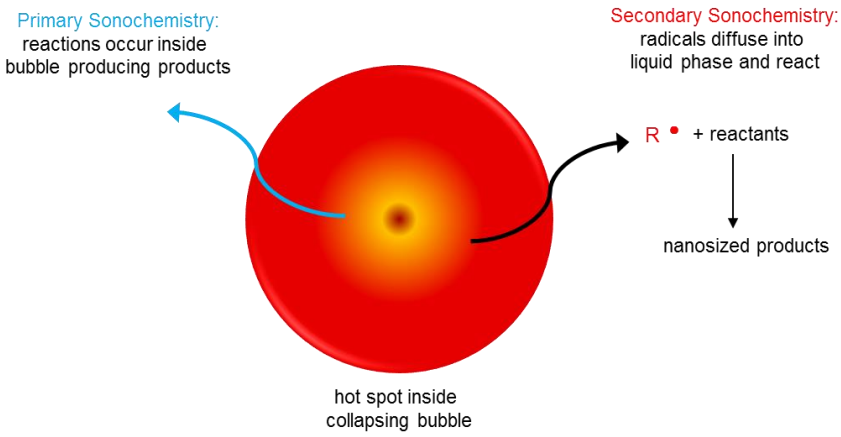

Figure 2.6 Primary sonochemistry and secondary sonochemistry for preparation of nanomaterials. An example of primary sonochemistry is the generation of metal atoms from sonolysis of weak metal–carbon bonds from volatile organometallic compounds inside the collapsing bubble that then diffuse into the bulk liquid to form functional nanomaterials. Secondary sonochemical products may arise from chemically active species (e.g., organic radicals from sonolysis of vapour) that are formed inside the bubble, but then diffuse into the liquid phase and subsequently react with solution precursors to form a variety of nano-structured materials.[43]

The importance of sonochemistry in the fields of material science and nanotechnology rises up through its advantages for i) preparation of amorphous NPs, ii) formation of

proteinaceous and polymer micro- and nano-particles, iii) insertion of nanomaterials into mesoporous materials, and iv) deposition of NPs on metal, ceramic and polymeric surfaces. The advantages of US over the conventional methods for NPs preparation include shorter reaction times, milder reaction conditions, higher yields, improved selectivity and clean reactions.[44–47] Moreover, sonochemical routes often do not employ any binding agents or stabilizers. For instance, Gedanken and coworkers have readily synthesized by US irradiation different metallic NPs and core-shells with encapsulated metal without using coupling agents.[48–51]

The extreme conditions attained during bubble collapse (localized hotspot through adiabatic compression or shock wave formation within the gas phase) have been exploited to decompose chemical bonds and generate a variety of nano-structured materials such as metal,[52,53] MeO/metal hydroxides[54–62] metal sulfides,[63] metal nitrides,[64] metal carbide NPs[65,66] bimetallic NPs,[67–71] semiconductor NPs,[72,73] metal-polymer composites,[74,75] ceramic materials[69,76] and others.[62,77] For the generation of these structures acetate,[53,58,60,73,78] aqueous metal salts solution,[61,72,79] ammonia complexes[57,63] and organometallic precursors[55,65,77,80,81] have been used.

The sonochemical synthesis of nanostructured materials is also extremely versatile as various forms of nanophase materials can be generated simply by changing the reaction conditions, e.g. temperature, concentration of precursors, sonication power and time.[44,57,60,69,82–84] Nanowires,[85–87] nanorings,[52,88,89] nanotubes,[72,88] nanorods,[88,90–92] nanoplates,[52,74] nested inorganic fullerenes[93], spheres,[63,94] nanocylinders[95] and many others structures, such as whiskers-like,[72,96] flower-like[94,97] and wormhole-like[98] are among the shapes of sonochemical products. For instance, by controlling the process parameters zinc oxide (ZnO) nanostructures with different morphology were synthesized by Jung et al.[94] ZnO nanorods and nanocups were obtained by changing the concentration of the precursors (zinc nitrate hexahydrate and hexa-methylenetetramine) and sonication time, while triethyl citrate was used as an additional chemical to synthesize ZnO nanodisks. For the synthesis of ZnO nanoflowers and NSs, zinc acetate dihydrate and ammonia–water were used as zinc cation and hydroxide anion precursors, respectively. In this case, for the synthesis of ZnO NSs triethyl citrate was added to the above mixture. Recently, US-assisted anionic biosurfactants (rhamnolipids and surfactin)-template route was developed to synthesise α-HH nano-$CaSO_4$.[44] Control over the crystal polymorph, size and shape of nano-$CaSO_4$ was achieved by adjusting the molar ratio of $(NH_4)_2SO_4/CaCl_2$ and the mass ratios of

rhamnolipid/H_2O, surfactin/H_2O and rhamnolipid/surfactin. It was observed that with increasing the biosurfactants/H_2O ratios, crystal length and aspect ratio decreased whereas by increase the surfactin ratio, the crystal morphology gradually changes from long rods to hexagonal plate and then to plate-like structures. The preferential adsorption of rhamnolipid on the side facets and surfactin on the top facets contributes to the morphology control. In this study, the US approach was found to be superior to conventional *in situ* deposition technique used for the synthesis of nano-$CaSO_4$ in terms of energy efficiency, processing time, yield and crystallization habit (crystal shape, morphology and *l/w* aspect ratio).

Surface modification has been recognized as one of the most advanced and intriguing methods to build tailored nanomaterials. One of the benefits of coating NPs on 2D and 3D surfaces is the avoidance of the release of the NPs to the environment. The coated nanomaterials provide a very high surface area and possess chemical and physical properties that are distinct from those of the individual components. Moreover, the sonochemistry is a method that enables to simultaneously produce NPs and deposit them on the substrates in one single step. Gedanken and co-workers have defined two routes for the NPs deposition on substrates under US: i) ‘‘throwing stones’’ mode of deposition[99] and ii) *in situ* mode of deposition.[100,101] In the “throwing stones” mode of deposition, the substrates are coated with preliminarily synthesized NPs or commercial NPs, while in the *in situ* mode the substrates are coated with NPs that were directly synthesized during the sonochemical reaction. An additional route for the deposition of NPs very similar to the *in situ* coating method was found for the sonication of aqueous solutions of either inorganic[102] or organic compounds.[103] For instance, it was found that the sonication of aqueous solutions of inorganic compounds (NaCl, $CuSO_4$, KI) resulted in the formation of salt NPs, but not metal or MeO NPs (as in the case of *in situ* method).[102]

The sonochemical coating is performed by the “bombardment” of 2D and 3D solid surfaces (ceramic, polymeric, glass, metal, textiles and paper) by liquid microjets carrying NPs. These microjets are formed when the acoustic bubble collapses near a solid surface. In the one-step sono-process the newly formed NPs (or commercial one) are embedded physically into the solid surface by the microjets moving at speeds >200 m/sec. This process produces a uniform homogenous and stable coating of NPs on surfaces with different functional groups. Various metal NPs were deposited with the aid of US on different organic and inorganic supports, such as polystyrene[104], poly(methyl methacrylate),[105,106] silica,[107–111] and alumina.[112] For example, a nanocomposite from silver/nylon 6,6 has been produced from an

aqueous solution of silver nitrate ($AgNO_3$) in the presence of ammonia and ethylene glycol by an US-assisted reduction method. Larger NPs (50 – 100 nm) were finely dispersed onto the polymer surface, while smaller NPs (20 nm) have penetrated the surface and distributed inside the polymer grains. The obtained nanocomposites were stable to washing and were used as a master batch for the production of nylon yarns by melting and spinning processes. The produced nylon fibers have demonstrated good antibacterial performance towards Gram-positive *S. aureus* and Gram-negative *Pseudomonas aeruginosa* (*P. aeruginosa*) bacteria.[113] Zinc oxide NPs (ZnO NPs) were deposited on a glass slides by sonochemical irradiation of the Zn^{2+} ions precursor in a water–ethanol mixture.[114] The leaching of NPs was tested in water, or ethanol and/or acetone solutions. The results demonstrated that the sonochemically deposited ZnO NPs are strongly anchored to the glass, as no NPs were detected in the leaching solutions after 7 days of incubation. Recently, Kiel et al. reported on sonochemical preparation of salt NPs from an aqueous solution of NaCl, $CuSO_4$ and KI and simultaneous deposition on glass microscope slide, a parylene-coated glass slide, or a silicon wafer.[102] It was found that the increasing of the initial ions concentration and US treatment time, lead to enlarged NPs and appearance of aggregates on the substrate surfaces.

The application of US to produce high performance nanocomposite coatings on steel was also demonstrated by several research groups. For example, Zn-Ni-Al_2O_3 nanocomposite coatings on low carbon steel were fabricated using eletrodeposition technique with the aid of US by Zheng and co-workers.[115] It was shown that the US vibration significantly improved the uniform dispersion of nano-alumina particles in the matrix and increased the nano-alumina content incorporated in the Zn-Ni-Al_2O_3 nanocomposite coating. Further, the anticorrosion properties and the hardness of Zn-Ni-Al_2O_3 composite coatings were improved significantly as compared to the Zn-Ni alloy, which was related to the nano-aluminia content and dispersion in the matrix. Soloviev and co-workers have generated silver NPs (AgNPs) by reduction of $AgNO_3$ by ethylene glycol and simultaneously coated them on stainless steel plate.[116] They found that the adherence of the particles on the steel substrate is not as good as in the case when soft substrates are used. Moreover, by increasing the distance between the substrate and the sonochemical horn the coating was found to be unstable and easily washed. The metal flat surfaces usually provide fewer possibilities for direct functionalization especially without any additives as compared to polymeric materials. This leads to lower coating stability and thus, decreased life-time at use of the product.

The sonochemical process enables also to coat the inner walls of hollow tubing e.g. AgNPs were deposited in a one-step US process on tubing made of rubber, PVC, Teflon and polyethylene.[117] In another approach enzyme NPs of α-amylase were also *in situ* generated and immobilized onto polyethylene films via high-intensity US.[118]

Sonochemical methods have also been applied to solve the stability problem of magnetic NPs[119,120] through their sonochemical coating with polymers or deposition on surfaces. The US irradiation was used as a way to prevent the agglomeration of the magnetite particles and accelerate the hydrolysis and condensation of tetraethyl orthosilicate.[121,122] The method resulted in homogeneously coated NPs due to the improved mass transfer of silica sols to NPs surface. It was found that the thickness of the silica layer over the NPs could be easily controlled by the sonication time.[121] The challenges in synthesis of iron air-stable structures were also overcome by sonochemistry. Air-stable iron NPs were synthesized and deposited on the surface of carbon spherules by US.[49] The process consist of sonochemical decomposition of $Fe(CO)_5$ in diphenylmethane. This approach was previously applied by Nikitenko and co-workers, who synthesized highly magnetic, air-stable iron-iron carbide NPs by using power US.[123] Their finding showed that during the sonolysis of neat diphenylmethane a polymer-like solid product is formed, which coats the surface of iron NPs formed simultaneously from $Fe(CO)_5$. Recently, the synthesis of magnetically recyclable thin-layer MnO_2 nanosheet-coated Fe_3O_4 nanocomposites with photocatalytic properties by combined hydrothermal/US approach was also reported.[124]

2.3.2 Metal and metal oxide nanoparticles

Because of their biocidal activity, metals have been widely used for centuries as antimicrobial agents. Nano-metal and metal based compounds such oxides or salts are claimed to be more biocidal (at very low concentrations) than many conventional antibiotics, which utilization at high concentrations can induce adverse effects and toxicity to human cells.[125,126] Moreover, the use of antibacterial NPs is also among the most promising strategies to overcome the microbial drug resistance.[127] The generally accepted mechanism of metallic NPs antibacterial action involves generation of reactive oxygen species (ROS) including hydrogen peroxide (H_2O_2), OH^{-} (hydroxyl radicals), and O_2^{-2} (peroxide), followed by the disruption of the bacterial cell membrane (Figure 2.4).[126,128–131] These killing mechanisms are usually less prone for the development of antimicrobial resistance.[33]

However, while for some of the metallic NPs the mechanism of antibacterial activity is widely investigated and clarified, for others still remains a subject of debate. The bactericidal effect of those nanosystems depends on several parameters such as NP's size, stability and concentration.

Many studies indicate that smaller NPs have better antibacterial performance than the bigger ones. Morones *et al.* have reported on the AgNPs size effect against Gram-negative bacteria.[132] They investigated particles in the range of 1–100 nm and had found that the NPs in a direct interaction with the bacteria preferentially had a diameter of ~1–10 nm.

Another factor that could play a role for the antibacterial properties of the NPs is their shape. For instance, the shape dependent antibacterial performance against Gram-positive *Streptococcus iniae* and *Streptococcus parauberis* and Gram-negative *E. coli* and *Vibrio anguillarum* bacteria was observed for the copper oxide NPs (CuO NPs).[133] The tested NPs shapes included surface morphologies such as rice grain-like, needle-like and plate-like. Among these differently shaped CuO nanomaterials, the plate-like CuO displayed better antibacterial activity than grain or needle shaped nano-CuO.

Recently, Perelshtein and co-authors have reported that the antibacterial properties of metal oxide NPs (MeO NPs), namely ZnO and CuO, depends on their crystalline structure, whereas the presence of more defects and less organized structure leads to higher toxicity.[134] Their study compared the activity of commercial and sonochemically produced NPs. A significant increase in the production of ROS was found in the more defective, sonochemically prepared metal nanooxides, as compared to the commercial ones with the same particle size range.

The bactericidal efficiency of the metallic NPs may be also affected by the type of microorganism i.e. to be strain-specific. For instance, *E. coli*, *S. aureus* and *Bacillus subtilis* (*B. subtilis*) bacteria strains susceptibility to silver and copper NPs (CuNPs) was studied.[135,136] The *E. coli* and *S. aureus* were more susceptible to the effect of the AgNPs compared to the CuNPs, while *B. subtilis* depicted the highest sensitivity to NPs compared to the other strains and was more adversely affected by the CuNPs.[135] The greater biocidal efficiency of AgNPs for *E.coli* (Gram-negative) than to *S. aureus* (Gram-positive) was attributed to the difference in cell wall structure between Gram-negative and Gram-positive microorganisms.[137]

The antibacterial properties of metal NPs were largely studied against human pathogenic bacteria such as *P. aeruginosa*, *E. coli*, *S. aureus*, *Klebsiella pneumoniae* and the antibiotic resistant bacteria as methicillin-resistant *Staphylococcus aureus* (*MRSA*). For instance,

copper,[138] CuO,[131,139] zinc[140,141] and ZnO,[142] titanium[143] and TiO_2,[144] MgO,[145] gold,[146] alginate[147] and silver[140,143,146] are among the NPs that antibacterial effectiveness against bacteria, viruses and other eukaryotic micro-organisms have been proved.
Silver and zinc NPs supported on various suitable materials, such as carbon, polyurethane foam,[148] polymers and sepiolite[149] have been effectively used for biological applications due to their bactericidal properties. In the medicine, materials comprising nano-silver are used also to prevent bacteria colonization on catheters,[150] contact lenses,[151] dental materials,[152] medical instruments,[153] and human skin.[154]

The application of AgNPs in the medical and pharmaceutical fields is widely exploited due to their high thermal stability, low volatility and low toxicity to human cells. The AgNPs are among the approved by the U.S. Food and Drug Administration nano-devices for antibacterial wound dressings. Silver-containing materials can be also employed to eliminate microorganisms on textile fabrics,[155,156] or they can be used for water treatment purposes.[157] In fact, by far silver is the most widely used antimicrobial material incorporated in the form of nano-silver in functional textiles. For example, powdered AgNPs were prepared using alkali dissolved starch as reducing and stabilizing agent followed by applying these particles to cotton fabrics. The developed material showed potential as wound dressing material as it demonstrated good antibacterial and anti-inflammatory properties.[158] In another approach, AgNPs impregnated paper as point-of-use device for microbial purification of drinking water was designed. The embedded in the blotter paper NPs release was minimal, with values under the WHO limit of 0.1 ppm for silver in drinking water.[159]

Composite metal-metal NPs have been also applied in biomedical areas as antibacterial agents as well as for bioseparations, targeted drug delivery and magnetic resonance imaging. The combined use of silica NPs with the other biocidal metals such as silver has been extensively studied in the recent years. For example, the production of novel antimicrobial silver–silica nanocomposite material was reported.[160] The results revealed that the nanocomposite have better antimicrobial effect against a wide range of microorganisms compared to conventional materials, such as silver nitrate and silver zeolite. In another study, silica nanowire substrates decorated with Ag- or CuNPs have demonstrated strong antibacterial activity against *E. coli*. However, while silver decorated silica nanowires were found to be biocompatible with human lung adenocarcinoma epithelial cell line A549, the copper decorated silica nanowires showed high cytotoxicity.[161] In another study, the antibacterial activity of nanostructured ZnMgO was compared to its pure nano-ZnO and

nano-MgO counterparts. Among the three oxides, the ZnO nanocrystals were found to be the most effective antibacterials against both Gram-positive (*B. subtilis*) and Gram-negative (*E. coli*) tested bacteria. The magnesium oxide NPs (MgO NPs) revealed moderate activity, whereas the ZnMgO NPs indicated high specific antibacterial activity to *B.subtilis*. It was shown that the ZnO NPs alone were toxic when applied to human HeLa cells, while MgO NPs and the mixed oxide did not induce any cell damage, which suggested that nano-structured ZnMgO could be used as a safe new therapeutic for bacterial infections.[162] However, the studies to evaluate the biological toxicity of nano-metals still continue, since hazard issues should be considered when using MeO antimicrobials as a therapy in humans.[163–165] Optimizing the metal concentrations to non-hazardous levels without affecting their functional properties would be a way to diminish the cytotoxic effect of these systems. This target is achievable by combining metal NPs with antimicrobial polymers that enhance their stability and efficacy. Thus, a hybrid nanomaterial comprising metal NPs and antimicrobial biopolymer is expected to exhibit low toxicity coupled to high antimicrobial efficiency even in low particles concentration. Such composites have already been used as drug delivery devices and antibacterial coatings.[166] For example, complexing metal NPs with chitosan (CS), a biopolymer with intrinsic antimicrobial properties,[167] resulted in enhanced antibacterial performance,[168] homogeneous NPs distribution on solid surfaces and improved cytotoxicity profiles due to the low dissolution rates of the metal from such complexes.[168,169]

2.3.3 Hybrid polymer/metal nanoparticles

Inorganic NPs are frequently engineered with an organic surface coating to improve their physicochemical properties. Metal NPs are used due to both - their enhanced antimicrobial behavior as compared with traditional materials and their capacity to be embedded into polymer matrices. However, there lies a main question in preparing metal based NPs stable enough during their exploitation or storage. Owing to the decreased particles' size and the increased surface area all nano-structured materials possess an excess surface energy in comparison with the bulk counterparts, and thus are thermodynamically unstable or metastable. For example, irreversible aggregation is observed for aqueous suspensions of unprotected silver and gold particles.[170] Thus, one of the great challenges is to overcome the surface energy and to prevent the NPs aggregation which is driven by reduction of overall surface energy (in order to reach thermodynamic stability i.e. lowest energy state). Traditionally the aggregation is overcome through the spontaneous adsorption on the particle surface of different coating materials or by involving of stabilization process i.e.

reducing of the metal ions in presence of polymers, hydrogels and surfactants. Whenever the surface of the NPs is modified by molecules or coated with a thin layer of other materials (with different constituents), they show enhanced properties compared to the non-functionalized uncoated particles.[171] However, it is worthy to mention that even NPs with high colloidal stability can change their physicochemical properties *in vivo*. The stability in a mammalian organism remains unknown as following internalization by cells, the NPs are typically localized inside highly acidic endosomes and/or lysosomes and the polymer shell could be degraded upon the activities of different enzymes.[172]

Various commercially available polymers including poly(methacrylic acid),[173] poly(maleic anhydride alt-1-tetradecene),[174] poly(acrylic acid),[175,176] poly(ethylene glycol)[177] and poly-(allylamine hydrochloride)[176] have been used as coating materials on the surface of metallic NPs. Introducing polymers with specific characteristics to the surface of the NPs is also a strategy for developing of novel functional hybrid nanomaterials due to the polymer's physicochemical properties (solubility, hydrophilicity and hydrophobicity).[178]

While some of the polymers are being applied only as stabilizers, another are preferred due to their specific properties e.g. desired functional groups. For example, the polymeric shells containing functionalities such as phenyl, ammonium, or thiol pending groups (derived from poly(dimethylpropargylamonium chloride), or poly(phenylacetylene-co-allylmercaptan), respectively) have been used to tune hydrophilic and hydrophobic properties and solubility of the target core shell systems based on noble metal NPs (gold NPs, AgNPs, platinum NPs).[179]

The designing of hybrid nanocomposites comprising of natural polymers (biopolymers) with antimicrobial activity and inherent biodegradability and biocompatibility (e.g. chitosans)[180,181] and metal NPs is highly appealing because of the individual antibacterial activity of both components. For instance, CS-Ag NPs bionanocomposites have shown to possess higher antibacterial activity than any of the components acting alone against Gram-negative *E. coli*[182] and Gram-positive *S. aureus*[183] bacteria. Biopolymers bearing amino moieties are intrinsically antimicrobial and impart positive charge onto the metal surface to lower the particles aggregation over a wide pH range, thereby extending the shelf life of these systems.[184,185] Moreover, the inclusion of amino functionalities brings about reactivity to the otherwise inert metal NPs, necessary for permanent immobilization of the hybrid biopolymer-metal NPs onto different surfaces. Covalent immobilization on solid substrates is not only employed to facilitate the recovery, but also the NPs reuse.[184,186]

Furthermore, naked metal based NPs are reported to be toxic to human cells and to potentially induce oxidative stress processes in the body.[187,188] It was demonstrated that the surface coating of those NPs with a biopolymer shell is an effective way to improve/enhance their biocompatibility.[189,190] The latter makes them suitable for various biological and biomedical applications. For example, recent studies have focused on dual-action NPs for inactivation of pathogens under magnetic hyperthermia. Antibacterial NPs for magnetic hyperthermia coated with shells of oleic acid, polyethyleneimine and polyethyleneimine-methyl cellulose have been synthesized and their antibacterial and antibiofilm properties were evaluated against *E. coli* and *S. aureus* bacteria.[191] Such nano-structures have shown potential against antibiotic resistant strains like *MRSA*.[192] The antibacterial properties of hyperthermia agents appeared to be highly desired as this would decrease the bacterial infections co-locallized with cancer.[192,193]

2.3.4 Nanoparticles as drug delivery system

One of the most promising applications of nanomedicine technology is the development of nanoparticulate drug delivery systems for diseases monitoring, control, treatment, and diagnosis. Among all investigated in this field nano-scaled structures probably the most promising candidates are the biodegradable NPs. The main advantages of such particles are their biocompatibility and ability to deliver effectively drug to a target site and as a consequence, to increase the therapeutic benefit while minimizing side effects. Those nano-structures are aimed to provide the stability of the drug and are characterized with specific control release properties.

In general, the nano-scaled structures used in the field of biotechnology and medicine for administration of bioactives range in particle size between 10 and 500 nm and rarely exceed 700 nm.[20] The nanosize of these particles allows various communications with biomolecules on the cell surfaces and within the cells, in a way that can be decoded and designated depending on the biochemical and physiochemical properties of these cells.[194] Therefore, the nano-devices in drug delivery system and noninvasive imaging offered various advantages over conventional pharmaceutical agents.[194,195] To be used at their full capacity the designed nano systems have to be stable, biocompatible, and selectively directed to specific sites in the body after systemic administration.

Nano-scale structures for drug delivery applications in different shapes could be prepared from different materials and biomolecules such as metals,[196] proteins,[197] lipids,[198]

biopolymers[27] etc. Depending on the selected method of NPs preparation, the obtained nano-structures could be NCs or NSs. The NCs are vesicle structures in which the drug is confined to a cavity surrounded by a nontoxic polymeric membrane or coating, while the NSs are systems in which the drug is uniformly dispersed. The active therapeutic could be attached to the NPs shell, entrapped or dissolved, depending on the NPs target application. In addition, the shell of the NPs could be made from molecules which possess specific activity and can act directly from the NPs surface. When designing such nano-devices the controlled release of pharmacological actives to the targeted site of action at the therapeutically optimal rate and dose regimen has been a major goal.

The nano-scale pharmaceuticals could be administrated alone or when incorporated into different carriers such as films, solid foam, nanofibrous matrix, or hydrogels. In the research area, a wide range of natural–origin polymers are being applied as carriers systems for active biomolecules or as cell carriers with application in the tissue engineering field. Polymers such as polysaccharides, due to their bio-characteristics, namely biocompatibility and similarity to the extracellular matrix (ECM) are classify as one of the most attractive options to be used in the tissue engineering field and drug delivery applications. Moreover, the polymeric scaffolds can be designed to release different bioactives and be can be easily engineered as possess different functional groups available for modification.

2.4 Antibacterial nanocomposites to prevent bacterial contamination and transmission

In order to prevent/reduce the transmission of microbial infections, it is necessary to develop materials with antioxidation, antibacterial and antifungal properties. Cost-effective and biocompatible materials have been used in the production of antibacterial nanocomposites that are able to prevent the transmission of bacteria and infections. Such nanocomposites find a wide application as hygienic products, for food packaging, water purification systems, filters, and medical equipment.

2.4.1 Antibacterial nanoparticles-coated medical textiles

The high potential of the nano-structured materials was illustrated by producing of functional textiles. High performance antibacterial nanocomposites resulted from the surface modification of textiles with metallic and organometallic nanomaterials. However, the

development of stable hybrid NPs coatings on textiles, almost exclusively involves the use of precursors, chemical pre-treatment, or additional processing steps, such as thermal curing, which renders the production technology rather complicated, time-consuming, and cost-inefficient.[199,200] For example, in a multi-step process, CS was covalently attached to previously oxidized cellulose, followed by the incorporation of ZnO microparticles into the CS layer by 'equilibration-cum-hydrothermal' approach.[201] Another time-consuming process was employed to impart both antimicrobial and UV protection properties to cotton by padding with zinc oxide/chitosan NPs (ZnO/CS NPs) suspension followed by squeezing, high-energy drying and curing.[202]

Considering the fact that fiber and film processing are the most difficult procedures of molding polymeric materials, bulk modification of continuous multi-filament yarns is an extremely sensitive process. The achieving of optimum process conditions is a main requirement. For example, Dastjerdi and colleagues have conducted (on a pilot plant scale) the bulk modification of filament yarns with various concentrations of nano-composite fillers via melt mixing of the two different silver-based nanocomposite fillers (silver/zinc and Ag/TiO_2), and polymer powder in three different mixing methods - single and twin screw extruder as well as master batch preparation. Besides that the technique is considered as high-quality and environmental-friendly, it is limited to synthetic fibers and the particles situated in the central part of the filaments do not contribute to the antibacterial performance.[203]

The sonochemistry has appeared as an efficient, simple, and fast technique for coating of different solid surfaces with NPs, overcoming the aforementioned manufacturing hurdles, namely the need of pre- or post-treatments and consequently long processing times.[114,204] Moreover, the application of high intensity US also prevents the NPs aggregation, whereas the obtained coatings are extremely stable and uniformly deposited on the substrates[30] and it is nowadays widely employed for synthesizing and embedding of antibacterial NPs into textile materials in a single process. For example, Gedanken and coworkers have demonstrated the successful application of US as a method for the antimicrobial finishing of various textiles with metal and MeO NPs in a one-step process.[100,101,204–206] The mechanism proposed for the deposition is based on the local melting of the substrate due to the high rate and temperature of the NPs thrown towards the solid surface by the sonochemical microjets (Figure 2.7).[101] Antibacterial properties were imparted to the cotton bandages by the sonochemical synthesis and deposition of CuO NPs onto their surface. For the generation of CuO NPs, copper(II)acetate monohydrate was used as precursor. The

antibacterial efficacy of the nanocomposites was demonstrated against *E. coli* and *S. aureus* bacteria strains. Regarding the mechanism responsible for the antibacterial action of the NPs it is worthy to mention that the Cu^{2+} ions did not have antibacterial properties (in comparison with Zn^{2+} released from ZnO NPs). The authors attributed the antibacterial activity of nano-CuO to the generation of active species responsible for damaging the bacteria's cells.[204] The same research group has also demonstrated that the antibacterial performance of sonochemically CuONPs coated cotton textiles withstand 65 washing cycles at temperature regimes used in hospitals.[207] This research was in line with the industrial need to fabricate antibacterial textiles for hospital uses. Such materials answer the problem of the hospital-acquired infections as they are able to prevent/reduce the bacteria spreading in the hospital healthcare units.[208]

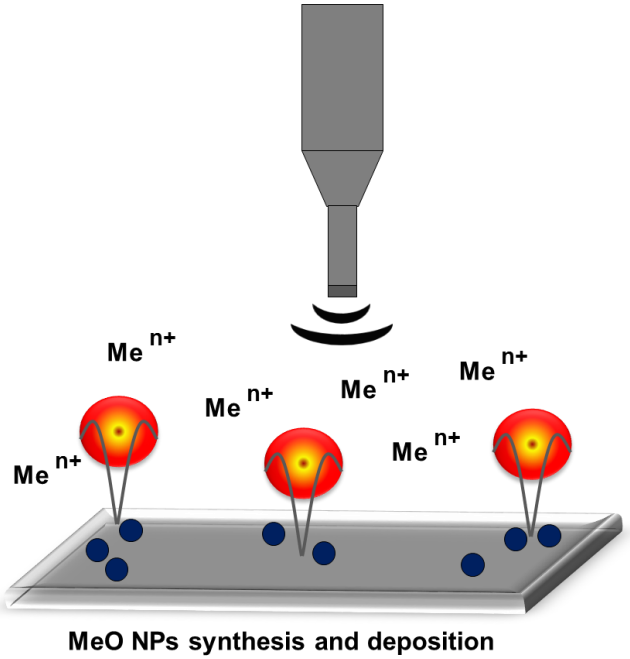

Figure 2.7 Scheme of the sonochemical deposition of MeO NPs on a solid substrate[209]

Our group has reported on a two-step process comprising cellulase pre-treatment followed by sonochemical synthesis and deposition of ZnO NPs on cotton fabric.[141] The enzymatic activation was combined with sonochemical synthesis/deposition of NPs in order to increase the number of anchoring points (reducing sugar ends) available to the NPs on the cotton surface. The positive effect of the enzyme pre-treatment on the stability of the ZnO coatings was demonstrated after repeated washing cycles at hospital laundry regime (92°C).

Moreover, the fabrics coated with NPs after preliminary treatment with enzyme showed uniform NPs dispersion along the fibres, and particle sizes in lower nanometric range in comparison with non-treated fabric. Perelshtein *et al*. have applied one-step sonochemical process to obtain antimicrobial coatings of titanium dioxide NPs (TiO_2 NPs) on cotton. The produced nano coatings displayed antimicrobial effect (when light illuminated) against common antimicrobial pathogens.[100] In another study, ZnO NPs were synthesized and simultaneous deposited on the surface of cotton bandages using US irradiation. The formed ZnO NPs were homogeneously dispersed on the cotton surface. In line with the concerns for the NPs toxicity, the authors performed leaching test for evaluating the stability of the coatings. It was found that the concentration of zinc ions in the leaching solution increases by increasing the temperature, however, no NPs presence in the solution was detected by transmission electron microscope (TEM) and dynamic light scattering (DLS) analysis. These findings indicated that during the sonochemical process the NPs were strongly anchored to the textile substrate.

The coating of fabrics with polymer NPs by US was also demonstrated. Tannic acid NPs were synthesized from an aqueous solution without the use of stabilizers and embedded on to cotton textiles in a one-step sonochemical process.[103] The obtained materials possessed antimicrobial and anti-inflammatory properties. The anti-inflammatory properties were assessed in terms of inhibition of inflammatory enzymes (myeloperoxidase (MPO) and collagenase) activities. It was found that the inhibitory effect of the tested specimens was directly proportional to the concentration of organic compound used for bandage coating. The authors assumed that tannic acid NPs exhibited their functions from the surface of the cotton bandages.

In recent years, Morsali and coworkers have demonstrated in several studies the NPs coating of polyester and silk fibers through sequential dipping steps in alternating bath of metal salts under US.[156,210,211] For example, silver bromide NPs were coated onto polyester fabrics by sequential dipping steps in alternating bath of potassium bromide and $AgNO_3$ under US irradiation.[156] It was demonstrated that the NPs size and morphology depend on the US power, sequential dipping steps and precursor concentration. The results suggested that an increasing of the sequential dipping steps and salts concentration lead to an increasing of the particles size, while an increase in the sonication power is accompanying with decreasing the size of the particles.

2.4.2 Potential of sonochemical processing in manufacturing of functional materials

The use of US in laboratory reactions is becoming commonplace, and the extension of the technology to industrial-scale reactions is likely to follow. Underlying these developing technologies are the recent advances in our understanding of the nature of cavitation and the chemical effects of US. The sonochemical coating route could be easily scaled-up to meet the requirements of large-scale textile coatings. Recently, the European project SONO (FP7-228730, http://www.fp7-sono.eu/), where our group was a key partner, demonstrated the development of a pilot line for the production of medical antibacterial textiles based on sonochemistry. The antibacterial efficiency of the produced medical textiles have been reported in several research papers[30,204,208] and in validated in a clinical study.[209]

Pilot scale installation for sonochemically assisted coating of textile fabrics with various kinds of NPs was designed by Abramov *et al.* (Figure 2.8).[30] The principle of the developed machine (operating in a roll-to-roll mode) involved feeding the fabric through a gap between two flat vibrating plates driven by magnetostrictive transducers. The speed of the moving fabric could be regulated between 0.004 and 0.050 m/s. Up to 50 m of fabric can be continuously coat with CuO and ZnO NPs using this pilot machine. The obtained textiles were characterized in terms of coating morphology, structure and stability to washing. The antibacterial assay of the coatings demonstrated that the loading of the nano-oxide appear to be decisive for their biocide performance. The obtained cotton fabrics displayed good antibacterial activity towards *E. coli*, *K. pneumoniae*, *S. aureus* and *MRSA.*[212]

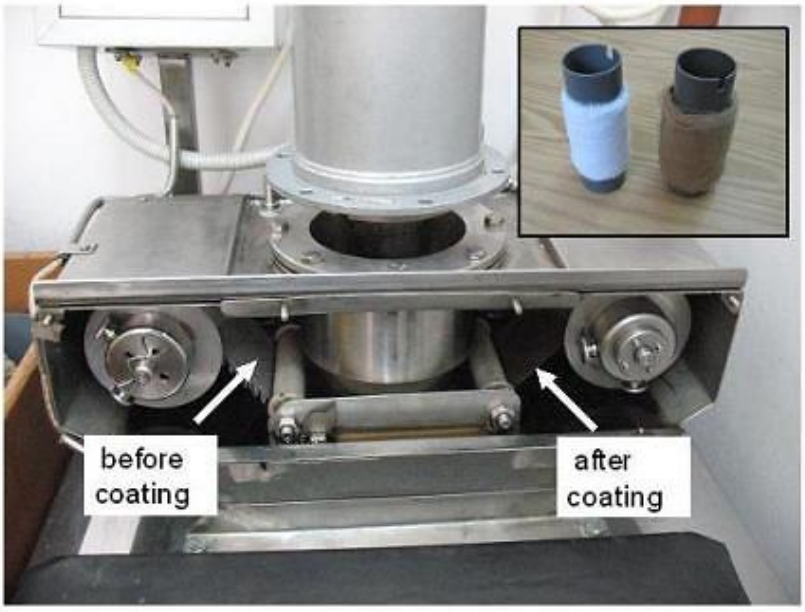

Figure 2.8 Photo of the roll-to-roll sonochemical pilot installation. In the inset the CuO-coated and uncoated spools are shown. The front panel is open to show the change in the color of bandage after coating with CuO NPs. In the inset, one can observe that with the deposition of CuO NPs the color of the bandage changed from white to brown. When the ZnO is deposited on the bandage, the white color is retained.[30]

2.4.3 Antimicrobial nanocomposites for water disinfection

Constructed wetlands in various designs are the most versatile systems for removal of pesticides, heavy metals, polycyclic aromatic compounds and pharmaceutical residues.[214–217] Currently, a major issue with these systems is related to the additional microbial contamination, especially the growth of undesired pathogen bacteria.

Microbiologically unsafe water is a global problem and among major causes of preventable morbidity and mortality. The WHO reports that by 2025 half of the world's population will be living in water-stressed areas with access only to inadequate drinking water.[218] One such example is microbiologically contaminated water associated with transmission of so-called bacteria waterborne diseases such as diarrhea, cholera, dysentery and typhoid fever.[219] Annually 2.2 million diarrheal disease deaths are being linked with the consumption of contaminated water.[220] The concerns about these diseases have even worsened during the last years due to the effects of global warming, namely extreme rainfall and flooding that contribute to the inordinate microbial proliferation in surface and groundwater.[221,222]

Strategies to efficiently recover wastewater acceptable for domestic or recreational purposes are therefore considered of global importance.

Some conventional methods for treating microbiologically unsafe water, e.g. boiling, reduce most waterborne pathogens and it is nowadays widely used to disinfect household water.[223] However, these methods are only efficient for small volumes. Whenever the purification of larger volumes is required, the disinfection process involves the use of chemicals, such as chlorine, chloramines, iodine or ozone.[224,225] Among them, the most accepted is the chlorination due to its efficiency and low price. Nevertheless, chlorine disinfection leads also to the formation of by-products as trihalomethanes,[223,226,227] which are related with developing certain cancers or adverse reproductive outcomes.[228,229] Many researchers are therefore investigating new sustainable techniques to disinfect large volumes of water without endangering the environment and the human health.[230,231]

Recently, considerable interest has arisen in the application of nanotechnology for water purification. In particular, functional antibacterial NPs and their potential for disinfection or microbial control in system level water treatment. Nanomaterials are providing novel opportunities to develop more efficient and cost effective nano-structured and reactive membranes for water purification. Several nanomaterials, such as silver, CS, and TiO_2, have found applications as antimicrobial agents in diverse products and industrial processes, including for water treatment.[224] Among all, nano-silver have been widely used for water filtration applications to inactivate bacteria[232] and viruses.[233,234] Moreover, AgNPs have been demonstrated to possess remarkable antimicrobial properties when employed in very low concentrations without harmful side effects.[235–238] Another NPs that have great potential as water purification catalysts and redox active media are the TiO_2 NPs. TiO_2 NPs can be employed as both oxidative and reductive catalysts to degrade organic and inorganic pollutants; to reduce toxic metal ions under UV and as antibacterial agents for water purification.[239240]

However, for disinfection purposes the NPs immobilization on preferably low-cost materials is necessary, where the permanent NPs binding ensures the disinfection efficiency during long-term exploitation.[241] For example, cellulose acetate hollow fiber membrane loaded with AgNPs for water treatment were prepared via dry-jet wet-spinning technique. The fibers were active against *E. coli* and *S. aureus* after being immersed in water bath for 180 days, despite that 60 % of the initially loaded silver remained. However, during filtration the silver content in the hollow fiber was depleted quickly within 5 days and the material lost it antibacterial activity against both tested bacteria strains, meaning that silver content must

be periodically replenished after permeation.[232] In another approach, a two-step process was used to design composite membranes on a glass support consisting of 50 nm thick chitosan layer on a poly(acrylic acid)/poly(ethylene glycol) diacrylate layer. The obtained material possess antibacterial activity towards *S. aureus* and *E. coli* bacteria, and the antibacterial activity of the membrane improved with increasing chitosan content.[242] In a similar way, nano-composite membranes incorporating other functional (e.g. catalytic, photocatalytic and antimicrobial) NPs into water treatment membranes can be developed. The strategies for the NPs immobilization of onto various 2D or 3D macroscopic surface mainly involve the NPs modification with polymers or molecules containing functional groups allowing their further anchoring on a target surface. However, for achieving this goal the use of facile and environmentally friendly method is an important issue. The potential application of bio-catalysts (enzymes) could results into direct immobilization of various functionalized NPs onto different substrates under mild conditions.

2.4.4 Antimicrobial hydrogels for wound treatment

Wide range of new functional dressing materials are frequently introduced to target different aspects of the wound healing process as a result of the existing variety of wound types (acute or chronic). The ideal wound dressings are defined as those capable to achieve rapid healing at reasonable cost coupled with minimal inconvenience to the patients. The wound treatment should be based on the controlled-release delivery of active substances directly into wound sites which promotes the wound healing process such as grow factors,[243,244] antimicrobials[245] or inhibitors of deleterious enzymes found in wounds.[246] Many of the new topical dressings are based on novel polymers and are employed for drugs' disposal due to their physical characteristics (e.g. fluid affinity, water uptake, rheological properties) but mainly because of their suitability for delivery of therapeutic agents when maintaining the wound surfaces moist.

Hydrogels are three-dimensional structures with high water content often comprising covalently cross-linked hydrophilic polymers. The extent of cross-linking allows for tuning of physical, chemical and biological properties, which in the case of biopolymers are usually coupled with the intrinsic biocompatibility and similarity with the ECM of various tissues. Hence, biopolymer hydrogels are used for a wide range of biomedical applications such as drug carriers or composite matrices for tissue engineering.[247,248] For instance, they appear attractive alternatives to conventional wound dressings to overcome their common

disadvantages such as low flexibility, lack of porosity and high adherence to wound surface that provokes painful removal.[249] Additionally, the hydrogel-based wound materials provide and maintain beneficial for wound healing moisture environment.

Compounds with intrinsic antimicrobial properties, e.g. polyphenolic molecules or metal oxides, could be added to polymer mixtures prior to gelation, targeting their sustained or controlled release from the hydrogel platform.[250,251] In one such approach, plant polyphenols were encapsulated for protection and delivered from the biopolymeric NPs or matrices to improve the resistance of cells to oxidative stress, and to inhibit bacteria growth and deleterious chronic wound enzyme activities.[246,252] Their processing into nanoscale particles is yet another attempt to improve their bioavailability and increase the efficiency in order to reduce the administration doses.[253] Further integration of the NPs within a hydrogel platform aiming their protection and controlled/sustained release is expected to aid in the development of more efficient drug delivery systems for e.g. medical applications.[251]

Polysaccharides, such as cellulose and starch, are the most abundant natural polymers in the biosphere. Naturally occurring alginate and chitosan are well known wound management materials due to their biological and haemostatic properties, which also facilitate the wound healing process.[254] These are often applied in combination with pharmaceutical agents as bioactive dressings capable for sustained, and thus prolonged delivery of actives to the wound site.[255] CS and its derivatives are potentially exploitable in the surface modification of colloidal carriers to modulate the bio-distribution of drugs and/or control their absorption.[256–258] CS materials have been widely used as a topical dressing to treat wound and burn infections not only because of its intrinsic antimicrobial properties, but also by virtue of its ability to deliver extrinsic antimicrobial agents to wounds and burns. Another, promising approach for designing of hydrogel wound dressings are based on collagen or glycosaminoglycans (GAG) such as hyaluronan and chondroitin sulfate, which are found in the ECM.[259,260] The GAG molecules can be chemically modified, creating new bio-materials with important bio-medical applications e.g. delivery of growth factors to the wound or as scaffolding material for tissue regeneration.[261,262] Dressings prepared from chemically-crosslinked GAG hydrogel films acts as bio-interactive wound dressings participating actively in the wound healing process rather than simply being passive barriers to desiccation.

To achieve the polymer gelation different physical and chemical cross-linking strategies have been employed. The physical cross-linking can be achieved by changing the physical entanglements or by non-covalent physical associations, such as secondary forces

(hydrogen, ionic, or hydrophobic bonding).[263,264] For example, the physical characteristics of the hydrogels could be modulated to the desired ones by changing pH, ionic strength and temperature of gelation.[265,266] It was demonstrated that the mechanical properties of collagen gels are easily tuned by varying those parameters.[267] In another study, it was shown that the ionotropic gelation method for formation of crosslinked CS can be modified from ionic cross-linking to deprotonation by adjusting the pH of tripolyphosphate. In such conditions the CS ionic cross-linking takes place at lower pH, while the deprotonation mechanism occur when higher pH is used.[268] A powerful approach for the generation of new materials with desired properties are the supramolecular interactions. Such hydrogel materials based on supramolecular self-assembly synthesis attracted special interest in the biological and electronics fields. The supramolecular self-assembly of cyclodextrins and polymers has led to the development of novel supramolecular hydrogels for drug delivery applications. For example, supramolecular hydrogel suitable for relatively long-term sustained controlled release were formulated based on the complexation *α*-cyclodextrin with various triblock copolymers bearing a hydrophobic block.[263,269] The general advantage of physically cross-linked hydrogels lies on a forming a gel without the need for chemical modification or the addition of cross-linking entities which make them suitable for *in vivo* practices. However, such networks held together by physical interactions only form mechanically weak scaffolds, resulting in fast erosion or degradation which limits their applications.[270] Because of these it is difficult to decouple hydrogels variables such as gelation time, network pore size, chemical functionalization, and degradation time, restricting the design flexibility.[271] The presence of non-homogeneities, free chain ends or chain loops and defects due to the formation of clusters of molecular entanglements, or hydrophobically- or ionically-associated domains can be also observed. A low viscosity liquid phase or syneresis of the hydrogel after the gel formation is another drawback of solely physical networks.[272] For these reasons, chemically cross-linkable systems allowing the formation of covalent bonds *in situ* have been developed. The chemical cross-linking process requires the addition of small molecules or conjugated directly to reactive pre-polymers. Chemical cross-linking of biopolymers to produce hydrogels results in higher mechanical properties compared to the physically assembled materials. However, the residual toxic chemicals and organic solvents employed often make them unsuitable for biomedical applications due to the toxic effects on human cells.[273,274] The formation of free radicals or the nonselective reactivity with nucleophiles found in biomolecules such as proteins can cause undesired side reactions such as inflammation.[275,276] As an alternative, covalently cross-linked gels could be obtain *in situ* via

enzyme-catalyzed reactions applying mild conditions and avoiding the use of harsh chemicals.[277,278] Such enzyme cross-linking systems are exploitable for encapsulation of various bio-entities (e.g. active agents and/or cells) and for further application in the pharmaceutical industry.[279] For example, peroxidase-catalyzed oxidation of CS derivatives was used for the preparation of biocompatible hydrogels for cartilage tissue engineering and drug delivery.[280,281] The sustained release of therapeutic proteins produced by genetically engineered to secrete an anticancer drug (interleukin-2) cells through 4 % gelatin hydrogels enzymatically cross-linked by microbial transglutaminase was recently reported. The findings in this study have demonstrated that the enzymatically cross-linked hydrogels were not only biocompatible, but also have suitable transport properties that would facilitate the design of sustained drug release devices.[282]

3 Objectives of the thesis

The main objective of this thesis is the *development of antibacterial nanocomposite coatings and materials aimed at reduction/prevention the transmission of infections and bacteria*. The increasing bacterial resistance to the most powerful antibiotics and the frequent occurrence of nosocomial infections are of great concern since microbial contamination is a serious issue involving multiple human environments, including the health care and biomedical industries, water purification systems, and food packaging and storage. The nanoparticles based materials and coatings represent one of the most promising strategies for overcoming microbial resistance. To this end, the following specific objectives have been set up:

- **The development of antibacterial medical textiles by a sonochemical process**. The use of antibacterial textiles is in the list of preventive measures to reduce the bioburden in clinical settings and consequently diminish the risk of healthcare associated infections.
  - **Development of stable hybrid nanocoatings on medical textiles using a one step sonochemical approach**. The combination of biopolymers and metal oxide nanoparticles to develop hybrid nanocoatings is expected to provide enhanced antibacterial efficiency and improved biocompatibility due to the synergistic effect of both compounds. The exploitation of ultrasound coating technology will assure the nanocoating uniformity and stability.
  - **Improving the uniformity and adhesion of the antibacterial nanoparticles onto textiles by a simultaneous sono-enzymatic coating process**. The ultrasound will be employed to boost the rate of the enzymatic hydrolysis and create on the cotton surface a larger number of reducing sugar ends for better nanoparticles adhesion and durability of the antibacterial effect.

- **Development of hybrid biopolymer-metal based nanoparticles and nanocomposites for water disinfection**. Amino-functional biopolymers will be used as doping agents to stabilize concentrated colloidal dispersions of silver nanoparticles, additionally providing the particles with functionalities for covalent immobilization. Further, antimicrobial material with potential for water remediation will be designed via enzyme-assisted assembling of the hybrid biopolymer-silver nanoparticles and phenol bearing filter matrices.

- **Formation of nanocomposite hydrogels for localized delivery of nano-therapeutics to wounds**. Biopolymer (thiolated chitosan) hydrogels will be loaded with sonochemically processed nanoscale phenolics serving as active compound in an enzyme-assisted gelation process. The developed nanocomposite is aimed at modulating the enzymes activity and microbial load in chronic wounds.

4 Materials and Methods

4.1 Reagents

Bleached woven 100 % cotton fabric (144 g/m2, warp/weft density 25/21 threads/cm) was provided by Davo, Romania. Low molecular weight chitosan (15 kDa, 87 % DDA) supplied by Kitozyme (Belgium) was used in the preparation of ZnO/CS and Ag/CS hybrid NPs and was dissolved prior to use in 1 % acetic acid. Water dispersion of ZnO NPs (size <100 nm), potassium sodium tartrate tetrahydrate, sodium hydroxide, 1,1-diphenyl-2-picrylhydrazyl radical (DPPH•) and 3,5-dinitrosalicylic acid (DNSA) were purchased from Sigma-Aldrich (Spain).

Granulated cork with mean particle size of ~0.5 cm was provided by the Catalan Cork Institute. Silver nitrate ($AgNO_3$), sodium borohidride ($NaBH_4$), hydrochloric acid, sodium hydroxide and ethanol were of analytical grade, purchased from Sigma-Aldrich (Spain). Microcrystalline cellulose (Fluka, Avicel PH-101) dried at 105 °C for 2 h was used for the 6-deoxy-6-(ω-aminoethyl) aminocellulose (AC, ~15kDa) preparation. First, tosyl cellulose was prepared using the synthesis method of Rahn et al.,[283] obtaining the product with a degree of substitution (DS) of 0.8. Ethylendiamine was then added in excess and the mixture was stirred for 3 h at 100 ºC. After precipitation in H_2O the conjugate was filtered, washed several times with isopropanol and H_2O, and finally dried in vacuum.

For the preparation of chitosan hydrogels, chitosan with average Mw of 20 kDa and acetylation degree of 18.54 % was provided by KitoZyme (Belgium). Ellman's reagent (5,5'-dithiobis(2-nitro-benzoic acid)), 2-iminothiolane hydrochloride (Traut's reagent, TBA) and epigallocatechin gallate (EGCG) were purchased from Sigma-Aldrich (Spain).

4.2 Enzymes

Cellulase formulation Kappacell ETU 39 for biopolishing of cotton textiles (5.86 mg/mL protein, 1.2 mM glucose equivalents released per min, averaged over 60 min, pH optimum 5 - 8) was purchased by Kapp-Chemie GmbH & Co. KG (Germany). Horseradish peroxidase (HRP, 1 U will oxidize 1 µmole of 2,2'-Azino-bis(3-ethylbenzthiazoline-6-sulfonic acid) per minute at pH 5.0 and 25 °C) isolated from horseradish roots (Amoracia rusticana) was purchased from Sigma-Aldrich.

Laccase (EC 1.10.3.2 Trametes sp. laccase, Laccase L603P) was provided by Biocatalysts, UK. Laccase activity was determined by oxidation of 5 mM 2,2'- azino-bis(3-

ethylbenzthiazoline-6-sulfonic acid) (ABTS) substrate in 0.1 M succinic acid/succinate buffer (pH 5.0), followed by an absorbance increase at 420 nm and 50 ºC, to obtain 0.14 U/mg protein, where one unit is defined as the amount of enzyme necessary to oxidize 1 µmol of ABTS per min ($\varepsilon 420 = 36{,}000\ M^{-1}\ cm^{-1}$). Protein content was determined using the Bradford method, obtaining 0.125 mg protein per mg solid.

MPO from human leukocytes (1550 U/mg solid: 1 U will produce an increase in absorbance at 470 nm of 1.0 per minute at pH 7.0 and 25 °C, calculated from the initial rate of reaction using guaiacol as a substrate) was from Planta Natural Products (Austria). EnzChek® kit was purchased from Life Technologies (Spain).

4.3 Bacteria

Gram-positive S. aureus (ATCC 25923) and Gram-negative *E*. coli (ATCC 25922) were used in the antimicrobial activity assays. Plate count agar, Baird-Parker agar, egg yolk emulsion and all other reagents for cell culture studies were purchased from Sigma-Aldrich unless otherwise specified.

4.4 Experimental methods

4.4.1 Simultaneous sonochemical coating of textiles with antibacterial ZnO/chitosan nanoparticles

4.4.1.1 Ultrasound-assisted coating of cotton

The sonochemical coating process was carried out using an ultrasonic transducer (Ti-horn, 20 kHz, 750 W, Sonics and Materials VC750, USA). The power (21.5 W) and intensity (0.43 W/cm^3) were determined calorimetrically by measuring the time-dependent temperature increase in the ultrasonic vessel. The coating of the cotton samples (0.70 ± 0.05 g, approx. 5 x 10 cm) was performed during 30 min at 20 ± 2 °C and 35 % amplitude, in a glass jacked vessel containing 50 mL ZnO NPs aqueous solution (0.2, 2 or 20 mM) and 0.3 % (w/v) chitosan. After sonication, the samples were thoroughly washed with distilled water to

remove the loosely fixed particles and chitosan. Control samples were prepared by deposition of ZnO NPs alone.

4.4.1.2 Quantification of deposited ZnO

The amount of ZnO embedded on the fabrics was determined after extraction with 0.5 M nitric acid. The concentration of solubilized Zn2+ ions was probed by inductive coupled plasma atomic emission spectroscopy (ICP – AES) analysis using ULTIMA JY2501 (France). The obtained results are reported as mean values ± standard deviation (n = 3).

4.4.1.3 Characterization of the coatings and nanoparticles

The surface morphology of the coatings and size of the deposited NPs were studied with high resolution scanning electron microscope (HRSEM) model Quanta 200 FEG from FEI (USA). Additionally, the presence of zinc and chitosan on the coated fabric was detected by energy dispersive X – ray spectroscopy (EDS). ZnO/CS mass and molar ratios were determined by X-ray photoelectron spectroscopy (XPS) on a SPECS system equipped with an Al anode XR50 source operating at 150 mW and a Phoibos 150 MCD-9 detector (Germany). The morphology of the ZnO NPs in the remaining after the sonochemical process suspensions was investigated by a Ziess Neon FIb microscope (Carl Zeiss, Germany) in scanning transmission electron microscopy (STEM) mode operating at 30 kV acceleration voltage. The samples for observation were drop-casted on a TEM holey carbon grid. Additionally, STEM images were taken to evaluate the leaching of the NPs from the fabrics. Prior to STEM analysis the coated fabrics were incubated for 1 h in 0.3 mM KH_2PO_4 solution at 37 °C and 230 rpm.

4.4.1.4 Antibacterial tests

Antimicrobial activity of the coated samples was assessed according to the standard shake flask method, recommended by the American Society for Testing and Materials (ASTM) for permanently immobilized active agents on fabrics (ASTM-E2149-01). The method provides quantitative data for measuring the reduction rate in number of colonies formed, converted to the average colony forming units per milliliter of buffer solution in the flask (CFU/mL). For preparation of *E. coli* and *S. aureus* suspensions, a single colony from the corresponding

stock bacterial cultures was used. The culture was then inoculated overnight in 20 mL sterile nutrient broth (NB, Sharlab, Spain) in a 100 mL Erlenmeyer flask and incubated at 37 ºC and 110 rpm. The inoculated bacterial culture was diluted with sterile buffer (0.3 mM KH_2PO_4) until solution absorbance of 0.28 ± 0.01 at 475 nm was reached, which corresponds to 1.5 ÷ 3.0 x 10^8 CFU/mL. This bacterial culture was then diluted appropriately into sterile buffer solution to obtain a final concentration of 1.5 ÷ 3.0 x 10^5 CFU/mL (working bacterial dilution). Thereafter, the cotton fabrics (0.035 g) were incubated with 5 mL of bacterial suspension at 37 ºC and 230 rpm. For determination of the inoculum cell density the suspensions were withdrawn before introducing the textile sample and after 15, 30 and 60 min in contact with the fabrics. These suspensions were serially diluted in sterile buffer solution, plated on a plate count agar and further incubated at 37 ºC for 24 h to determine the number of surviving bacteria. Antimicrobial activity is reported in terms of percentage of bacteria reduction calculated as the ratio between the number of surviving bacteria before and after the contact with the coated textiles using the following formula:

Bacteria reduction (%) = ((A-B) / A) x 100 (Equation 4.1)

where A and B are the average number of bacteria before and after the contact with the coated textiles, respectively.

The durability of the antibacterial effect was evaluated after performing 10 washing cycles in a laboratory dyeing machine (Ahiba Nuance, Datacolor) at 75 °C, 30 rpm, for 15 min with 0.1 g/L non-ionic surfactant Cotemol NI (Colorcenter, Spain), in liquor to good ratio 30:1.

4.4.1.5 Cell culture

The BJ-5ta cells (human foreskin fibroblasts, ATCC-CRL-4001) were maintained in 4 parts Dulbecco's Modified Eagle's Medium (DMEM, ATCC) containing 4 mM of L-glutamine (ATCC), 4500 mg/L glucose, 1500 mg/L sodium bicarbonate and 1 mM sodium pyruvate, and 1 part of Medium 199 supplemented with 10 % (v/v) of fetal bovine serum (FBS) and 10 g/mL Hygromycin B, at 37 ºC in a humidified atmosphere with 5 % CO_2. The culture medium was replaced every 2 days. At pre-confluence, cells were harvested using trypsin-EDTA (ATCC-30-2101, 0.25 % (w/v) trypsin / 0.53 mM EDTA solution in Hank's BSS without calcium or magnesium) and seeded at a density of 4.5 x 10^4 cells/well in a 96-well tissue culture-treated polystyrene plate (Nunc, Spain).

4.4.1.6 Cytotoxicity evaluation by indirect contact

Coated fabric samples (25 mg) were first sterilized under UV light for 1 h. The samples were then placed in contact with 3 mL of complete growth medium (DMEM) in a CO_2 incubator at 37 °C for 1 and 7 days. At the end of these periods, the samples were removed and the growth media withdrawn. Medium without the contact with the cotton was used as a negative control, whereas a 30 % dimethyl sulfoxide (DMSO) prepared in fresh culture medium was used as a toxicity positive control.

The previously seeded cells were put into contact with the withdrawn culture media and incubated at 37 °C in a humidified atmosphere of 5 % CO_2 for 24 h. The cells were further examined for signs of toxicity using Alamar Blue assay kit (AlamarBlue®, Invitrogen). Resazurin, the active blue ingredient of the kit, is a nontoxic, cell permeable compound that, once in a viable cell, is reduced to red colored resorufin. AlamarBlue® was diluted in culture medium and added to each well after aspirating the culture medium containing the samples. After 4 h incubation at 37 ºC the absorbance at 570 nm was measured, using 600 nm as a reference wavelength, in a microplate reader Infinite M200, Tecan (Austria). The quantity of resorufin formed is directly proportional to the number of viable cells. The error bars for each data are the standard deviation of three independent measurements. No cell viability was detected after the contact with the positive control regardless of the incubation time (data not reported).

4.4.2 Simultaneous sonochemical enzymatic coating of textiles with antibacterial ZnO nanoparticles

4.4.2.1 Cellulase activity measurements

The cellulase activity was measured using the filter paper (FPU) assay.[284] Reactions were carried out in 50 mL test tubes with Whatman No. 1 filter paper strip (1 x 6 cm, 50 mg) in 1.0 mL distilled water and 0.5 mL enzyme formulation. The mixtures were incubated at temperatures ranging from 20 to 65 °C for 1 h. Thereafter, a colorimetric reagent (DNSA) was added to quantify the amount of reducing sugars. The DNSA solution was prepared by dissolving 120 g sodium potassium tartrate in 80 mL of previously heated (60 °C) 0.2 M

NaOH, prior to addition of 200 mL of 96 mM DNSA and volume completion to 400 mL with distilled water. The reaction mixtures were placed in a boiling water bath for 5 min, cooled to room temperature and diluted with 20 mL distilled water prior to measuring the absorbance at 540 nm with Infinite M200 (Tecan, Austria) multiplate reader. All experiments were performed in triplicate.

4.4.2.2 Enzyme stability in US field

One mL of cellulase product diluted to 50 mL with water was subjected to US irradiation (20 kHz, 21.5 W, 17.30 W/cm^2, 0.43 W/cm^3 and 35 % of amplitude) for 30 min at temperatures ranging from 20 to 60 °C. After the treatment, enzyme aliquots (0.5 mL) were incubated for 1 h at 55 °C with Whatman No. 1 filter paper strip (1 x 6 cm) and the reducing sugars released were measured using the FPU assay as previously described. The residual enzyme activity was calculated as a percentage of the activity of the enzyme not exposed to US. The possible effect of the sonochemical treatment on the tertiary and secondary structure of cellulase was assessed by measuring the intrinsic fluorescence of the enzyme as a result of protein unfolding and denaturing. For the purpose of the assay, cellulase water solutions not exposed (control) and exposed to US treatment (30 min) were evaluated. The fluorescence was measured at room temperature (25 ± 1 °C) with Quanta Master 4 spectrofluorometer (PTI, USA) at 280 nm excitation wavelength (slit = 2 nm), 300 - 450 nm emission wavelength (slit = 2 nm) and 1200 nm/s of scanning speed.

4.4.2.3 Effect of the US parameters on the enzyme performance

To study the hydrolytic potential of the cellulase toward cellulose substrate under sonication, the US amplitude of vibration (and thus intensity) was varied to determine its effect on the yield of the enzyme catalyzed reaction expressed in reducing sugars concentration. For this aim, 1 mL of cellulase solution (diluted to 50 mL with water) was subjected to ultrasonic irradiation at different US amplitudes (range of 20 – 40 %) for 30 min at 55 °C and in presence of 0.5 g of Whatman No. 1 filter paper as a substrate. Thereafter, the liberated reducing sugars were determined using the aforementioned method (section 2.4.2.1., FPU assay). Control treatments without enzyme were carried out in parallel. All results are reported as mean values ± standard deviation (n = 3).

4.4.2.4 Ultrasound-enzyme assisted coating of cotton with ZnO NPs

The sonochemical coating was carried out using an ultrasonic transducer Ti-horn (20 kHz, Sonics and Materials VC750, USA). The US intensity (17.30 W/cm^2), density (0.43 W/cm^3) and power (21.5 W) used for the textile treatment were calorimetrically determined as described in 2.4.1.1. The cotton samples (5 x 10 cm, approx. 0.7 g) were immersed in the ultrasonic pot containing 50 mL ZnO NPs aqueous solution (1 mM) and 2 % of weight of fabric (owf) cellulase formulation and the coating of the cotton samples was carried out during 30 min at 55 ± 2 °C and amplitude of 35 %. To maintain the fabric at the bottom of the US pot without using any additional accessories, the fabric sample was cut bigger than the diameter of the pot (4 cm). Thereafter, the sample was folded in a way that its diameter is slightly wider than the diameter of the pot, thereby once placed at the bottom of the pot the contact/friction of its edges with the walls prevents it from moving during the sonochemical process. The sample area exposed to the US irradiation was used for the further experiments. The ultrasonic horn was dippen 1 cm in the ZnO dispersion at a distance from the fabric (at the bottom of the ultrasonic pot without any additional support) of approximately 3 cm. Thereafter the samples were thoroughly washed with distilled water to remove the loosely fixed particles. Controls were prepared by sonochemical deposition of ZnO NPs in presence of temperature-denatured enzyme.

4.4.2.5 Characterization of the coatings

The quantification of the amount of ZnO deposited on the fabrics (by ICP – AES) and the surface morphology studies of the coatings (by HRSEM) were carried out as described previously in section 4.4.1.2. For both washed and unwashed samples, the HRSEM images (section 4.4.1.2) were obtained from fabrics treated in three independent experiments. ImageJ software was used to build three size histograms of the ZnO NPs deposited on to the fabrics.

4.4.2.6 Antibacterial test

The antibacterial performance of the coatings were assessed as previously described in Section 4.4.1.4

4.4.3 Enzyme-assisted functionalization of cork surface with antibacterial biopolymer/silver hybrid nanoparticles

4.4.3.1 Preparation of biopolymer-doped silver nanoparticles

Biopolymers, CS and aminocellulose (AC) were dissolved to reach 0.8 % (w/v) in 1 % CH_3COOH (CS) and distilled water (AC). The pH of the solutions were adjusted to 5 by adding 2 M NaOH in case of CS and 1 M HCl in case of AC. AgNPs synthesis was carried out by chemical reduction of Ag^+ to elemental silver (Ag) using $NaBH_4$ (17.5 mg/mL in dH_2O), starting from aqueous solutions of $AgNO_3$ (5 mg/mL) in presence of CS or AC. First, 2 mL of $NaBH_4$ was added to 30 mL of a biopolymer solution under vigorous stirring, and then $AgNO_3$ was slowly added to reach the final volume of 50 mL.

4.4.3.2 Characterization of biopolymer-doped silver nanoparticles

The hybrid structures were characterized using ζ potential for the particles charge, DLS for the mean particle size, UV-Vis spectrophotometry to check for the presence and intensity of the AgNPs surface plasmon resonance (SPR) band, and STEM to visualize the particles and evaluate their stability in the obtained dispersions. ζ potential was measured using Malvern ®Zetasizer Nano ZS, DLS measurements were performed using DL135 Particle Size Analyzer (Cordouan Technologies, France). Three samples of each AgNPs dispersion (in absence and presence of CS of AC) were processed acquiring 5 measurement cycles with 1 % signal-to-noise ratio. The data were analyzed using NanoQ 1.2.1.1 software. UV-Visible spectra were recorded between 300-600 nm for the dispersions diluted 100 times in distilled water using a Cary 100 Bio spectrophotometer (Varian). The AgNPs in the dispersions were visualized by a Zeiss Neon FIB microscope (Carl Zeiss, Germany) in STEM mode operating at 30 kV acceleration voltage. The samples for observation were drop-casted on a TEM holey carbon grid.

4.4.3.3 Immobilization of the hybrid biopolymer-doped AgNPs onto cork

Prior to the treatment with biopolymer-doped AgNPs, the cork granules were cleaned with aqueous solution of HCl (pH 2), distilled H_2O, NaOH solution (pH 10) and finally with 96 % EtOH, and dried at 60 ºC for 12 h. Thereafter, 1 g of the material was placed in a mixture containing 18 mL of AgNPs dispersion (pure, doped with CS or doped with AC – immediately after their preparation), 18 mL of 0.1 M succinic acid/succinate buffer (pH 5), and 0.5 mL of

laccase (final concentration 0.1 U/mL). The reaction was allowed to proceed for 24 h at 50 °C and 30 rpm in a laboratory dying machine Ahiba (Datacolor). Control samples were also prepared using the same treatment conditions without laccase (in presence of hybrid biopolymer-AgNPs) and with laccase and CS or AC alone (without AgNPs). The treated cork was washed thoroughly with water to remove the loosely fixed particles and $NaBH_4$ from the material, and finally dried at 50 ºC for 12 h.

Fourier transform infrared spectroscopy (FTIR) was used to analyze the surface of the treated cork. IR spectra of the samples were collected in the range of 4000-600 cm^{-1} using Perkin-Elmer Spectrum 100 (USA) equipped with universal ATR sampling accessory, performing 64 scans for each spectrum. Scanning electron microscopy (SEM) was performed to examine the morphology of the AgNPs-biopolymer hybrids immobilized onto cork and to examine the presence of bacteria on the non-modified cork (control) and on the cork-AgNPs-CS composite. The micrographs with magnification ×30K were obtained using a Zeiss Neon FIB microscope (Carl Zeiss, Germany) operating in SEM mode.

4.4.3.4 Antimicrobial activity of AgNPs embedded cork matrices

The antimicrobial performance of treated cork matrices was assessed against *E. coli* and *S. aureus* using the dynamic shake ASTM E 2149-01 test, as described in section 2.4.1.4. The results were expressed as log_{10} of CFU/mL of buffer solution in the flask. Besides the unwashed matrices (only rinsed with water after the treatment), the antibacterial performance of the untreated and treated cork was evaluated after immersing those in water for 1, 2 and 5 days at room temperature while stirring (100 rpm) to mimic the environment in which the materials are intended to be used, i.e. water flow in constructed wetlands. Finally, the antimicrobial activity after 5 days washing is also expressed as a reduction percentage of the survived bacteria colonies. The results were expressed as log reduction in CFU counts.

To study the viability of the bacteria accumulated on the cork surface, unmodified and functionalized with AgNPs-CS cork pieces were incubated with *E. coli* contaminated water for 16 h. Thereafter, the cork samples were washed with sterile distilled water. To grow the alive bacteria, five of the washed cork granules were placed on Coliform agar and incubated at 37 °C for 24 h, while another five granules were used for SEM measurements in order to detect the presence of bacteria on the materials' surface. Before the SEM analysis the

bacteria accumulated on the cork were subjected to fixation procedure preserving their initial structure. Briefly, the samples were placed in 4% paraformaldehyde in phosphate-buffered saline (PBS) for 30 min, then washed twice with sterile PBS, and placed in 25, 50, 75 and 96% ethanol for 10 min. The fixation was conducted at room temperature.

4.4.4 Enzyme-assisted formation of nanospheres-embedded hybrid biopolymer hydrogels for wound healing

4.4.4.1 Nanospheres preparation and characterization

NSs were generated by applying 20 kHz ultrasonic irradiation (0.43 W/cm^3 intensity and 35 % amplitude) on the interface of water/oil mixture (15:6 (v/v)) containing 0.5 mM EGCG for 3 min at 4 ºC. The NSs suspended in the aqueous phase were thereafter subjected to several cleaning steps after centrifugation (2000 rpm for 15 min) to remove the oil phase. Three samples of each NSs suspension were assayed by DLS at room temperature to determine the mean sphere size of the obtained phenolic NSs as described in section 2.4.3.2. The NSs morphology was evaluated using a NIKON Eclipse Ti−S fluorescence microscope (Nikon Instruments, Inc., The Netherlands). The phenol groups of EGCG NSs and free solution were estimated according to the Folin-Ciocalteu method for determination of total phenol content [285] by monitoring the reaction at 760 nm in a microplate reader (Infinite M200, Tecan, Austria) and the results were expressed in gallic acid equivalents (GAE). Prior measuring the absorbance, the samples were filtered through Millex® GP 0.22 µm PES filters (Merck Millipore Ltd., Spain) after which 200 µL of the filtrates were transferred to a 96-well microplate.

4.4.4.2 Myeloperoxidase inhibition

The MPO inhibition with the EGCG NSs and free solution was measured using guaiacol as a substrate. The samples were serially diluted in 50 mM phosphate buffer, pH 6.5 (in a concentration range of 0.0025 to 0.001 mM) and further 450 µL of each dilution was incubated for 1 h with 20 µL of 0.60 U MPO and 30 µL of guaiacol (167 mM) at 37 °C. The mixtures were then filtered through Millex® GP 0.22 µm PES filters (Merck Millipore Ltd., Spain) and 200 µL of the filtrates were transferred to a 96-well microplate. The reaction was

started by adding 22 µL of 1 mM H_2O_2 and the absorbance increase was followed at 470 nm for 90 s.

4.4.4.3 Collagenase inhibition

The collagenase activity was measured using EnzChek® kit. Briefly, 80 µL of the EGCG free solution or NSs suspension, 100 µL of collagenase (0.5 U/mL) and 20 µL gelatin-fluorescein conjugate (to a final substrate concentration of 100 µg/mL) were incubated at room temperature protected from light. After 6 h the fluorescence was measured (493/528 nm) using a microplate reader Infinite M200, Tecan (Austria). For each sample, the background fluorescence values derived from the controls without the enzyme were subtracted. The measurements were performed in triplicate and the results are expressed as the percentage of collagenase inhibition compared to the control without EGCG.

4.4.4.4 Antioxidant activity

Radical scavenging activity of the EGCG NSs and free solution were determined by measuring the decrease in absorbance of 1,1-diphenyl-2-picrylhydrazyl radical (DPPH•) at 517 nm. Different dilutions of the samples (100 µL) were incubated with 2.5 mL of DPPH• solution (9.84 mM) in methanol at room temperature in dark for 30 min. All experiments were carried out in triplicate. The antioxidant activity was calculated using the following formula:

DPPH inhibition (%) = [1 – (A/Ao)] x 100

where A0 is the absorbance of the negative control (DPPH solution alone) and A is the absorbance in presence of the EGCG solution/NSs suspension.

4.4.4.5 Antibacterial tests

S. aureus growth inhibition assay was performed in presence of the EGCG NSs or free solution. For the preparation of S. aureus suspension, a single colony from the corresponding stock bacterial culture was used. The culture was then inoculated overnight in 20 mL sterile NB (Sharlab, Spain) in a 100 mL Erlenmeyer flask and incubated at 37 °C and 110 rpm. In order to obtain the bacteria stock solutions the inoculated bacterial culture

was diluted with NB until reaching the absorbance of 0.01, monitored at 600 nm. Thereafter, 250 µL undiluted (0.5 mM) and diluted (0.25; 0.1; 0.05; 0.025 mM) in NB EGCG NSs/solution were incubated with 250 µL of bacteria stock solution for 24 h at 37 °C and 230 rpm. After, the suspensions were serially diluted in NB, plated on a Baird-Parker agar, and further incubated at 37 °C for 24 h to determine the number of surviving bacteria colonies. Antimicrobial activity is reported in terms of percentage of bacteria reduction calculated as the ratio between the number of surviving colonies before and after the contact with the samples using Equation 4.1 (Section 4.4.1.4), where A and B are the average number of bacteria colonies at 24 h for bacteria incubated without (control sample) and with EGCG NSs/solution, respectively.

4.4.4.6 Thiolation of chitosan

The incorporation of thiol groups into chitosan was carried out following the procedure of Bernkop-Schnürch et al.[286] First, chitosan was dissolved in CH3COOH (1% v/v) and TBA was added at the chitosan:TBA ratio 5:2 (w/w). The pH was then adjusted to 6 with 5 M NaOH. In order to avoid the oxidation of free thiols to -S-S- during the coupling reaction, dithiotreitol was added in a final concentration of 100 mM. The reaction mixture was stirred for 24 h at room temperature. The obtained thiolated chitosan (TC) conjugate was purified by 24 h lasting different dialysis steps: first three times against 5 mM HCl containing 1 % NaCl, then two times against 5 mM HCl. Thereafter, TC and the control (non-thiolated chitosan) were freeze-dried and stored at 4°C until further use. The free thiol content in the TC conjugate was determined spectrophotometrically using Ellman's reagent[287] and found to be 878±14 µmol/g of conjugate.

4.4.4.7 Hydrogels preparation and characterization

Hydrogels were obtained by enzymatic cross-linking between 46 to 660 sec at room temperature, using horseradish peroxidase (9.65 U/mL) and hydrogen peroxide as an oxidizing agent. For the hydrogels containing EGCG NSs, the spheres were dispersed in 2 % TC solution in a spheres:TC 10/90 (v/v) ratio prior to cross-linking. The gelation time (the time which it takes for the formation of gel) was determined using a vial tilting method by regarding the gel state when the solution does not flow for 1min after inverting a vial.[288] The

morphology of the obtained hydrogels was studied by scanning electron microscopy (SEM, JSM 5610 scanning electron microscope (JEOL Ltd, Japan)).

4.4.4.8 Swelling ratio and in vitro degradation of chitosan hydrogels

TC hydrogels were cut into pieces of 3 mg and thereafter immersed in 2 mL distilled water. The samples were taken out at predetermined time intervals and weighed after removing the water adhered on their surface by gently blotting with filter paper. The swelling degree (DS) was determined using the following formula:

DS (%) = [(Ww – Wi)/Wi] x 100

where, Wi and Ww are the initial weight and weight of the wet sample, respectively (n=6 for each time point).

To study the hydrogel degradation in water, hydrogels were previously freeze-dried and thereafter equally weighted (3 mg) prior to immersion in 2 mL distilled water at 37 °C. The samples were removed after 1, 7, 14, and 21 days and again freeze-dried. The percent mass loss was calculated as follows:

Degradation (%) = [(Wi – Wd)/Wi] x 100

where, Wi and Wd are the initial dry weight and the dry weight of the sample, respectively (n=6 for each time point).

4.4.4.9 In vitro NSs release

To study the release of EGCG NSs from TC platform, hydrogel pieces (0.2 g) loaded with NSs were incubated in 1 mL distilled H_2O. The release of phenol NSs into the incubation solution was followed spectrophotometrically at 280 nm (EGCG NSs wavelength of maximum absorbance) at determined time intervals. The results are presented as an average percentage (of three repetitions) of the phenols released from hydrogels.

4.4.4.10 Cell culture

The BJ-5ta cells (human foreskin fibroblasts, ATCC-CRL-4001) were maintained as described in section 2.4.1.5. and were further used to assess the samples' cytotoxic effect after direct contact with the cells as detailed below.

4.4.4.11 Cytotoxicity evaluation by AlamarBlue Assay

Cells were seeded at a density of 4.5×10^4 cells/well on a 96-well tissue-culture-treated polystyrene plate (Nunc) one day before the experiments. Thereafter, cells were exposed to solutions of EGCG NSs, TC and their mixture in the concentrations 10 times lower that those used for the hydrogel preparation at a final volume of 150 µL and incubated at 37 °C in a humidified atmosphere with 5% CO_2. After 24 h contact, the NSs were removed and the cells were washed twice with PBS and stained for signs of toxicity using AlamarBlue assay. To do so, 100 µL of 10% (v/v) AlamarBlue reagent in DMEM was added to the cells and incubated for 4 h at 37 °C, after which the absorbance at 570 nm was measured, using 600 nm as a reference wavelength, in a microplate reader. The quantity of resorufin formed is directly proportional to the number of viable cells. BJ5ta cells relative viability (%) was determined for each sample and compared with that of cells incubated only with cell culture medium. H_2O_2 (500 µM) was used as a positive control of cell death. Data are expressed as the mean of three measurements, with a standard deviation as a source of error.

5 Results and Discussion

5.1 Sonochemical coating of medical textiles with antibacterial ZnO/chitosan hybrid nanoparticles

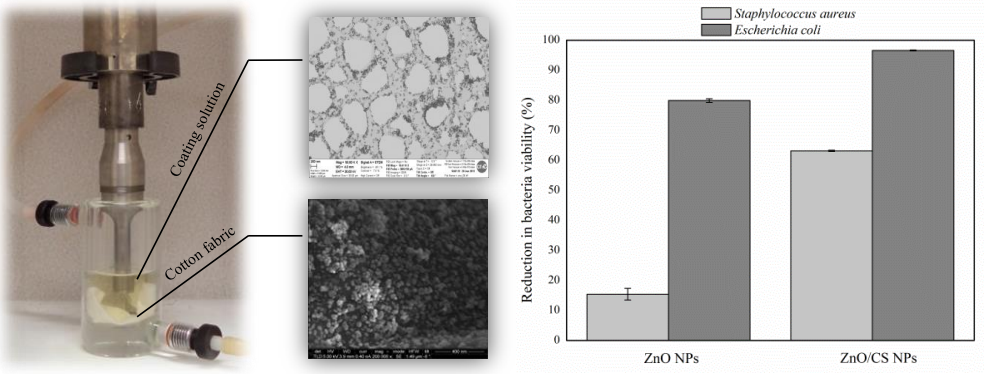

This section is based on the following publication:

Petkova P, Francesko A, Fernandes MM, Mendoza E, Perelshtein I, Gedanken A, Tzanov T, Sonochemical coating of textiles with hybrid ZnO/chitosan antimicrobial nanoparticles. *ACS Applied Materials & Interfaces*, 2014, 6 (2), pp 1164–1172

5.1.1 Introduction

The properties of hybrid polymer-metal nanocomposites are influenced by the components interactions which affect the composite shape, size distribution and stability. Chitosan (CS) strongly complexes, unlike other natural compounds, with metal ions due to its free amine groups.[289,290] Two models are proposed for hybrid CS and metal ions structures: “pendant model” where ion is bound to only one amino group of CS,[291] and “bridge model” where ion is bound to several nitrogen atoms and hydroxyl groups of one or bridging more CS chains.[292] This ability of CS was explored in our previous study[293] to sonochemically synthesize zinc oxide (ZnO)/CS NPs (ZnO/CS NPs) and simultaneously deposit them on cotton fabrics. Here, the study is extended to the optimization of the sonochemical process in terms of metal oxide (MeO) concentration and reaction time in order to obtain efficient and durable antimicrobial textiles that do not cause toxic effects to human cells.

Such development is in the scope of a general strategy to decrease the occurrence of nosocomial infections in clinical settings through sustainable manufacturing of efficient antimicrobial hospital textiles. The sonochemical process is carried out in aqueous solutions, in line with the current focus on development of environmentally friendly manufacturing technologies. The durability of the antimicrobial effect is also evaluated after multiple high-temperature washing cycles used in hospitals against two medically relevant bacterial species – *S. aureus* and *E. coli*.

5.1.2 Characterization of the coated fabrics

ICP measurements were performed for determination of zinc on the cotton treated with different ZnO NPs concentrations in the presence and absence of CS. As expected, increased ZnO NPs concentration in the coating process led to higher amount of zinc deposited on the fabric (Figure 5.1A). On the contrary, considerably less amount of zinc was detected on the fabrics treated in presence of CS. Moreover, the EDS analysis of the hybrid coatings detected the presence of N and Zn on the fabric, thereby confirming the deposition of both CS and ZnO (Figure 5.1B).

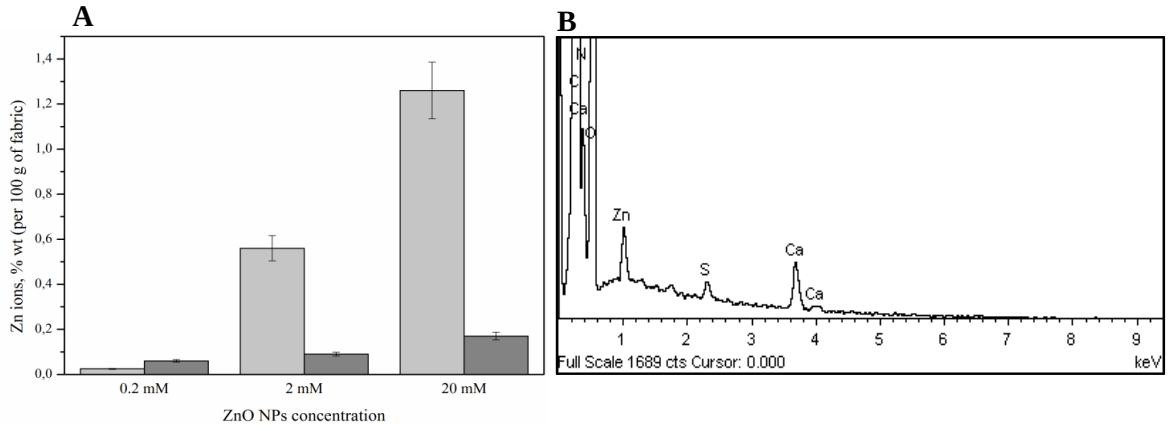

Figure 5.1 (A) Amount of zinc sonochemically deposited on cotton fabrics from solutions of ZnO NPs, in absence (light grey bars) and presence (dark grey bars) of 0.3 % (w/v) CS, and (B) EDS spectrum of cotton coated with 2 mM ZnO in presence of CS.

XPS analysis was conducted to determine the molar and mass ratios of ZnO/CS on the cotton fiber surface. Due to the large experimental groups, XPS results presented herein are for the hybrid 2 mM ZnO NPs/CS coating. The energy spectrum of the photoelectrons, produced by the x-rays photoelectronic effect allows the determination of the sample composition (up to 10 nm sampling depth). The position of the peaks (binding energies of electron orbitals) in the spectrum and their relative areas are used to quantitatively identify the composition of the sample surface (Figure 5.2A). Figure 5.2B shows high - energy resolution carbon C 1s spectrum obtained for the hybrid coating. Three peaks are assigned to the different chemical bonds of carbon atoms, namely C-O (286.21 eV), C=O / O-C-O (287.29 eV) and C-H / C-C (284.80eV). The N 1s spectrum peaks (Figure 5.2C) with binding energies of 399.35 eV and 401.9 eV were assigned to the chitosan amino and protonated amino groups, respectively. Zn 2p 3/2 spectrum is presented with only one peak with binding energy at 1021.97 eV (Figure 5.2D).[293] Atomic concentrations obtained from XPS analysis

for Zn (14.87 %) and N (85.13 %) were used for calculation the molar (14.19) and mass (0.08) ratios of ZnO/CS within the hybrid coating.

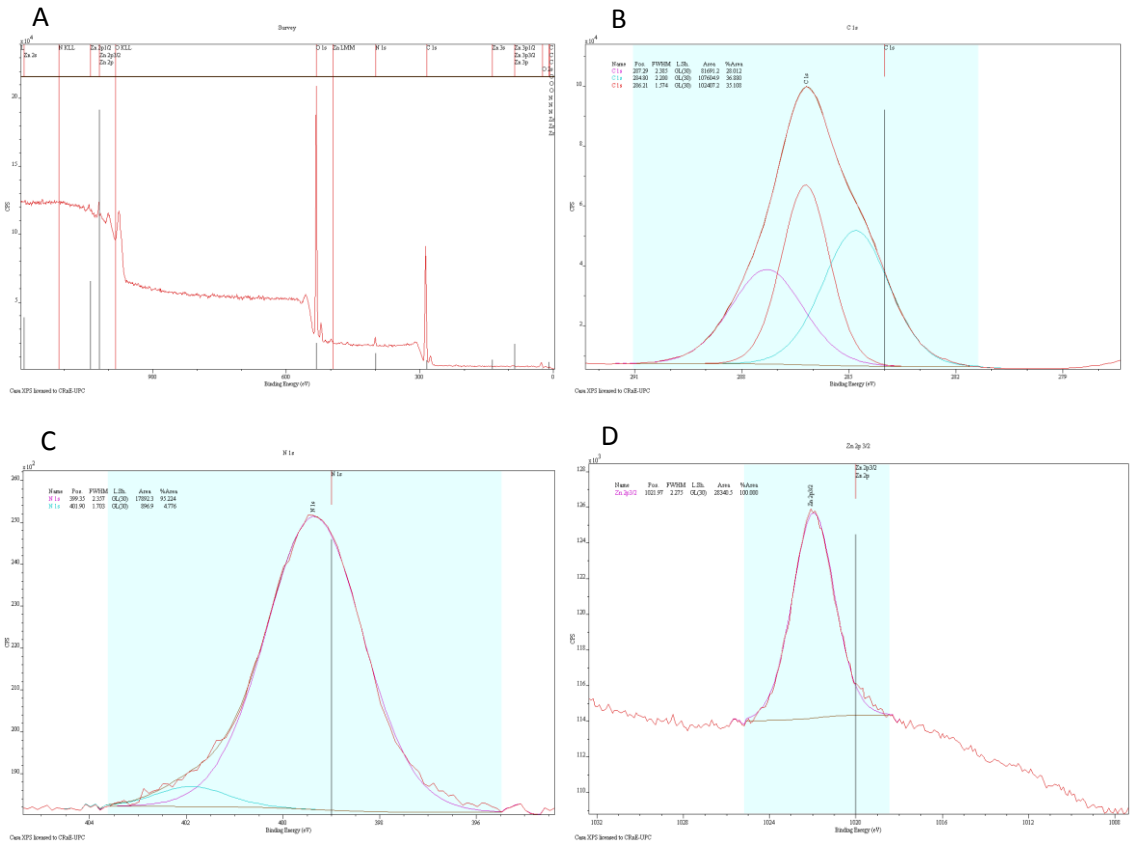

Figure 5.2 N and Zn XPS spectra of cotton sonicated in the presence of 2mM ZnO NPs and CS.

The HRSEM surface analysis of the sample coated only with ZnO showed a dense layer of NPs on the fibers (Figure 5.3A, B). Comparatively lower amount of NPs with bigger average size was found on the fabric treated with ZnO/CS system (Figure 5.3C, D), in good agreement with the ICP data. It is hard to distinguish between the individual and hybrid ZnO/CS particles, because chitosan itself is able to form nanospheres under sonochemical irradiation that are similar in shape to the ZnO NPs.[293] Indeed, the pure CS coating (Figure 5.3E, F) appeared quite similar morphologically to the hybrid coating. Nevertheless, the NPs within the hybrid coating were bigger in size than the pure ZnO or CS particles, indicating that these probably were comprised of both components. It was reported that the mean diameter of CS NPs increased when metal ions were loaded to the polymer.[294] On the other hand, the effect of CS on the metal NPs is resumed in its action as a controller of the nucleation or stabilizer.[295,296]

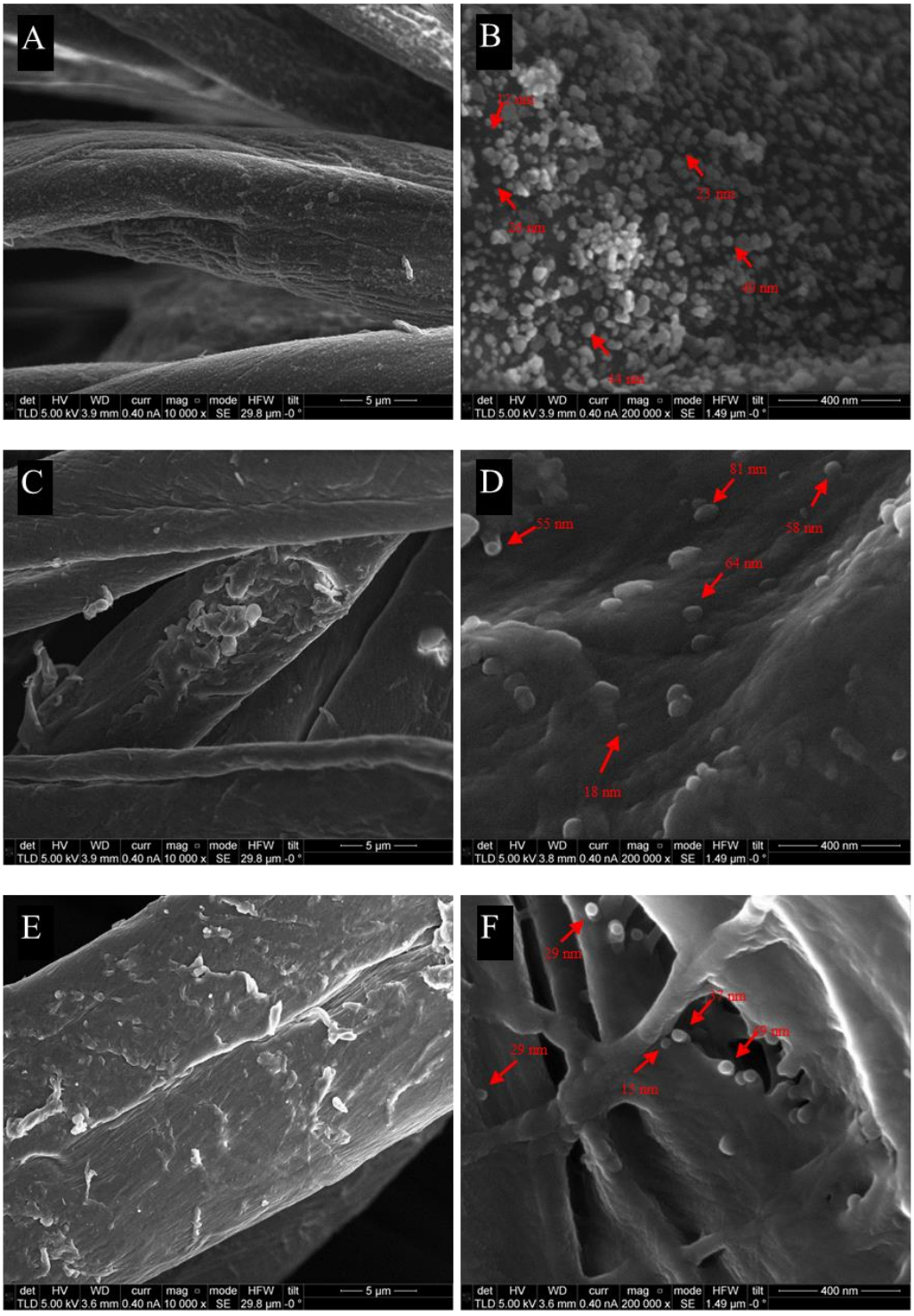

Figure 5.3 HRSEM micrographs of cotton fabrics coated with ZnO (A, B), ZnO/CS (C, D), and CS (E, F). Composition of the starting solution: 2 mM ZnO NPs and 0.3 % (w/v) CS. The images on the left were taken with 10 000x, whereas the right-side images were taken with 200 000x magnification.

To explain the differences in the amounts of ZnO deposited on the fibers, the remaining after the sonochemical process solutions were evaluated for the presence of ZnO NPs using STEM. Given the lower amount of Zn detected on the fabrics treated in presence of chitosan, it was expected that higher amount of MeO particles would be found in the corresponding remaining solution compared to the one remained after coating in absence of chitosan. Surprisingly, the ZnO NPs density was also lower in the solution left after the hybrid coating (Figure 5.4A). The lower amount of NPs both on the fabric and in the remaining solution could be explained only if the effect of pH on the solubility of both ZnO and CS is considered. ZnO dissolution occurs over a wide pH range,[297] whereas the oxide is stable at pH 7.2 due to a minimal interference of the dissolution products. On the other hand, due to inter-molecular and intra-molecular hydrogen bonding, chitosan can be dissolved only in aqueous solutions of organic or mineral acids below pH 7. At these conditions the stability of ZnO rapidly decreases due to reaction with acidic substances. It is thus expected that the addition of CS dissolved in CH_3COOH to ZnO aqueous suspension will decrease the pH of the system and affect the ZnO stability. After CS addition the pH of the ZnO NPs suspension indeed dropped from 8.2 to 6.9. Zn^{2+} complexation could also contribute to the lowering of the system pH. Similar behavior was already reported for various metal ion systems containing CS.[298–300] The complex reaction could be described according to the Lewis acid-base theory, where the acid (Zn^{2+}) is an acceptor of a pair of electrons, provided by the base (CS).[298] Thus, the physicochemical properties of the individual composite components most probably dictate the formation of Zn^{2+}/CS complex within the hybrid coatings. On the other hand, no NPs leaching was detected from the coated fabrics, revealing high stability of both ZnO and the hybrid coatings (Figure 5.4B).

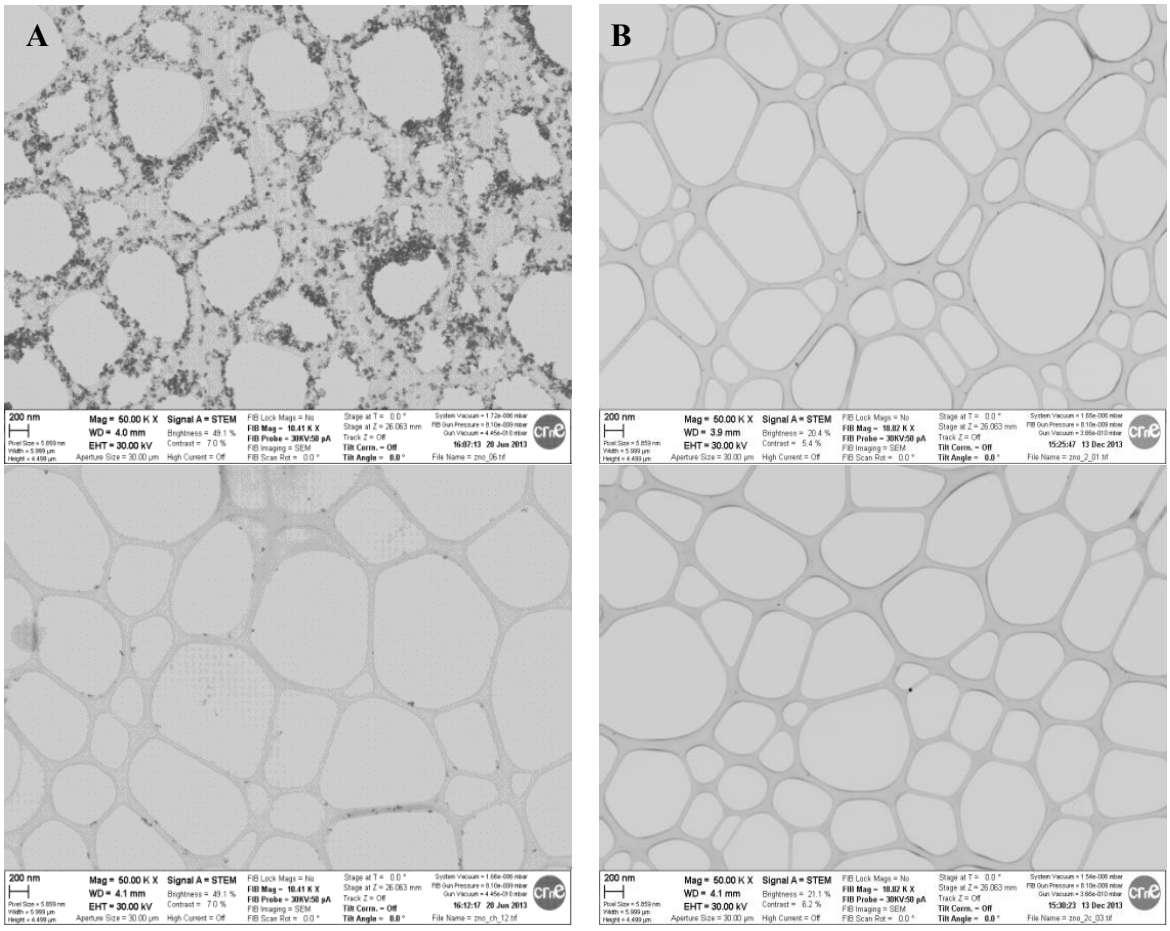

Figure 5.4 STEM images taken to evaluate: (A) the NPs presence in the remaining solutions after the sonochemical coating of cotton fabrics with 2 mM ZnO in absence (top image), and presence (bottom image) of 0.3 % (w/v) CS; and (B) the NPs leaching into a solution incubated with the fabrics coated with ZnO (top image), and ZnO/CS (bottom image).

5.1.3 Antibacterial activity

Both ZnO and CS are largely reported as efficient antibacterial agents. The most widely accepted mechanism of ZnO antibacterial action involves the oxide dissolution to Zn^{2+} further associated with oxidative stress in bacteria cells and generation of ROS.[129,301] ROS cause inhibition of cell enzymes, lysosomal and mitochondrial damage, and consequently cell death.[302] The antimicrobial effect of CS depends on its molecular weight and varies among different microorganisms.[303,304] Among the proposed mechanisms of CS antimicrobial action are: i) binding to the cell DNA to inhibit the protein synthesis, and ii) interaction with negatively charged microbial membranes to alter the cell permeability.[305,306] Recently, hybrid complexes of CS and metal ions showed several-fold enhancement of their

antibacterial activity as compared to the individual components.[182,298] In addition, the antibacterial activity was directly proportional to the amount of metal ions in these complexes.

In a next step, the antibacterial efficiency of the sonochemically generated on cotton fabrics hybrid Zn^{2+}/CS was evaluated against two medically relevant bacterial species and further compared to the effect of pure ZnO coatings. The Zn^{2+}/CS coatings reduced the viabilities of both *S. aureus* and *E. coli*, though to a different extent (Figure 5.5). As expected, the presence of chitosan enhanced the antibacterial effect of the coatings against both strains regardless of zinc concentration in the complex. However, the fabrics coated with the lowest NPs concentration (0.2 mM) in presence of CS brought about only 30 % reduction of bacteria viabilities. Increasing the amount of zinc in the coatings resulted in enhanced antibacterial effect. The coatings with 2 and 20 mM ZnO showed comparable antibacterial efficiency for both bacteria. Thus, all further experiments were carried out with the fabrics treated with 2 mM NPs, as this concentration was considered appropriate to produce efficient antimicrobial textiles.

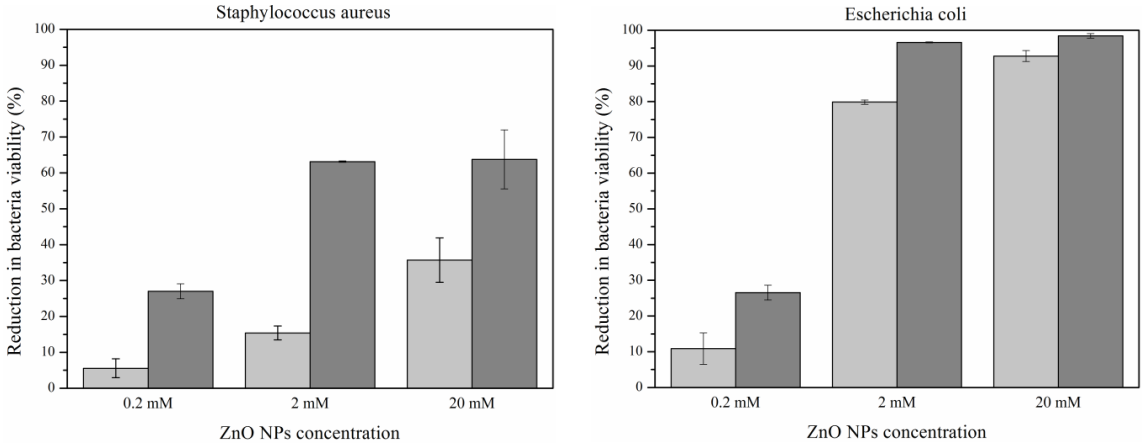

Figure 5.5 Antibacterial activity of ZnO (light grey bars) and Zn^{2+}/CS (dark grey bars) coated cotton fabrics towards S. aureus and E. coli after 15 min of contact.

In Table 5.1 the antibacterial activity of fabrics coated with 0.3 % (w/v) CS, 2 mM ZnO, and the corresponding hybrid is shown as a function of the incubation time. The hybrid coating led to 98 % reduction of bacteria growth for *S. aureus* after 60 min, whereas ZnO and CS alone reduced the bacteria growth by 61 and 31 %, respectively. It is worthy to mention that the CS coating reached its maximum activity against *S. aureus* already after 30 min, while

the longer incubation time resulted in improved antimicrobial effect for the coatings containing ZnO. In the case of *E. coli* a progressive improvement in antibacterial effect was observed for both CS and pure ZnO coatings. The different efficiency of the CS-containing coatings against *E. coli* (78 % after 60 min incubation) in comparison to *S. aureus* (31 %) could be due by the low Mw of the biopolymer (15 kDa) used in the study. Low Mw chitosans are reported to be more active against Gram-negative than against Gram-positive bacteria.[304] On the other hand, the hybrid coating reduced the bacterial viability by more than 96 % even after 15 min of incubation. Nearly 100 % reduction was observed for both fabrics treated with ZnO and the hybrid coating after 60 min incubation.

Table 5.1 Antibacterial activity of the coated fabrics against S. aureus and E. coli after different incubation time.

Staphylococcus aureus			
	Reduction in viability, %		
Coating	15 min	30 min	60 min
CS	26.84 ± 4.07	33.00 ± 1.94	30.99 ± 1.81
2 mM ZnO NPs	15.39 ± 1.93	41.50 ± 2.12	60.77 ± 0.16
2 mM ZnO NPs/CS	63.15 ± 0.23	81.62 ± 3.58	98.48 ± 0.22

Escherichia coli			
	Reduction in viability, %		
Coating	15 min	30 min	60 min
CS	25.18 ± 1.02	72.66 ± 1.02	78.06 ± 0.51
2 mM ZnO NPs	79.88 ± 0.60	89.81 ± 1.31	99.86 ± 0.02
2 mM ZnO NPs/CS	96.60 ± 0.12	96.72 ± 0.18	99.88 0.04

5.1.4 Durability of antibacterial effect

Despite the advances in antimicrobial finishing, the hospital textiles still become contaminated at use.[307] Frequent laundering is therefore necessary in order to entirely prevent the transfer of pathogens. In order to evaluate the durability of the antimicrobial coatings, the fabrics were subjected to 10 washing cycles at 75 ºC and their antibacterial performance was assessed afterwards against the selected bacterial strains. The results

are expressed in percentage of remaining biocide activity compared to non-washed fabrics (Figure 5.6A). The ZnO coating retained about 50 % of its initial activity against both strains, whereas the hybrid coating preserved about 70 % and 85 % of the efficacy against *S. aureus* and *E. coli*, respectively (illustrated at Figure 5.6B). It is the presence of CS that improved the washing stability of the hybrid coating, as the individual CS coating was showed to maintain between 85 and 90 % of its initial activity. The sonochemical deposition of polymers onto solid surfaces usually results in their stable embedding on the substrate.[308] Under ultrasound irradiation of liquids, the microjets and shock waves produced after cavitation collapse are able to drive the biopolymers at such high velocities towards a solid surface that fusion and strong adherence by physical or chemical interactions with the fabric occurs during collision.[309] Conversely, sonochemically deposited metal oxides are not particularly stable and additional pre-treatment of the solid substrate are required for improved coating stability.[141]

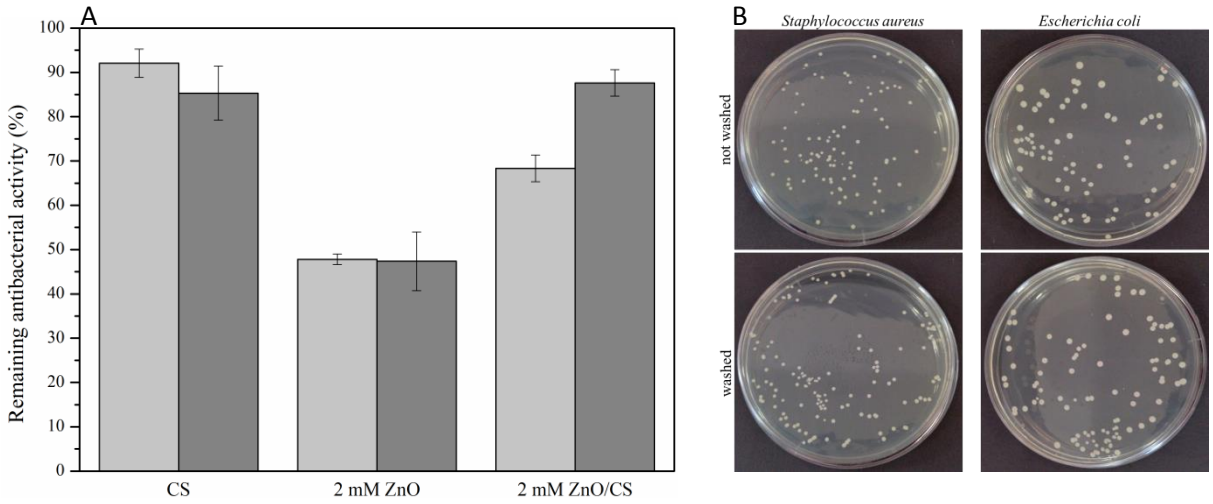

Figure 5.6 (A) Percentage of remaining antibacterial activity of the coatings after 10 washing cycles at 75 °C against S. aureus (light grey bars) and E. coli (dark grey bars), after 15 min of contact. (B) Images of antibacterial activities of the Zn^{2+}/CS fabrics before and after washing.

5.1.5 Cell viability

Although zinc and copper oxides are safer alternatives to more toxic silver, the studies continue to highlight their biological toxicity using soil and aquatic organisms[310] and mammalian cell lines.[311,312] The toxic action of metal and MeO NPs is mainly a consequence of the release of cytotoxic metal ions from such systems.[301,313] Since ZnO NPs partially dissolve in water, their dissolution in aqueous systems is expected to involve both ionic and particulate species. Solubilized Zn^{2+} proved to contribute substantially to the cytotoxicity of ZnO NPs.[165,310] Another assumption claims that ZnO produces toxic species associated with its photocatalytic property. ROS generated under environmentally relevant UV radiation increase significantly the toxicity of these systems to human cells.[301] Some studies even report the generation of ROS in absence of photo-chemical energy.[314,315] It is therefore crucial to evaluate the potential toxicity to humans of the systems comprising ZnO.

After optimizing the ZnO concentration in the antimicrobials-coated textiles, the potential cytotoxicity of these systems was evaluated for medical application requiring contact with human skin. Indirect contact method was used to determine the potential toxicity that CS, ZnO or hybrid nano-coatings might induce to fibroblasts cell culture. During the first 24 h the cultured cells were metabolically active with no difference in cell viability observed among the experimental groups. However, after one week of contact with the ZnO coated fabric cell viability dropped to less than 5 %. In contrast, the CS and the hybrid coating did not induce considerable cell toxicity even after one week. As in the case of bacteria killing, ZnO NPs induce oxidative stress in human cells through the generation of free radicals and ROS.[316] The reason for the lower cytotoxicity value in the case of the hybrid coating could be the lower amount of ZnO impregnated on the fabric compared to the fabric treated with ZnO alone (Figure 5.1A). It could be also hypothesized that the CS inhibits the generation of ROS below the threshold of oxidative stress due to its antioxidant capacity.[317]

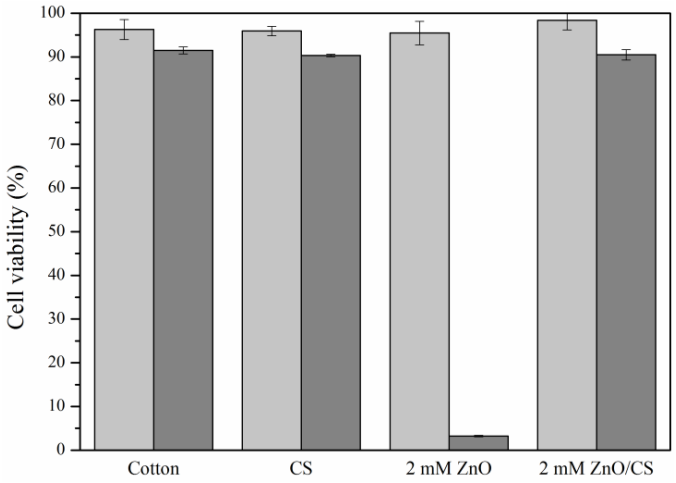

Figure 5.7 Human skin fibroblasts viability after 24 h (light grey bars) and 1 week (dark grey bars) contact with the coated cotton fabrics.

5.1.6 Conclusions

Hybrid antimicrobial coatings were generated on cotton fabrics via a one-step sonochemical deposition of ZnO NPs in presence of chitosan. The process was optimized in terms of ZnO concentration and ultrasound irradiation time towards obtaining highly efficient and non-cytotoxic antibacterial textiles for use in hospitals. The synergy between ZnO NPs and chitosan resulted in enhanced antibacterial efficiency against *S. aureus* and *E. coli* even at low ZnO concentration, compared to the individual ZnO and chitosan coatings. The antimicrobial effect of the treated fabrics was resistant to multiple washing cycles at 75 ºC according to the laundry regimes used in hospitals. Moreover, the presence of chitosan substantially improved the biocompatibility of the ZnO coatings avoiding the risk of adverse effects on human health. The sonochemically generated antimicrobial textiles showed potential, in terms of easiness of the process coupled to enhanced antimicrobial effect and high washing stability, for uses in hospital environment to prevent the spread of nosocomial infection.

5.2 Simultaneous sono-enzymatic coating of medical textiles with antibacterial ZnO nanoparticles

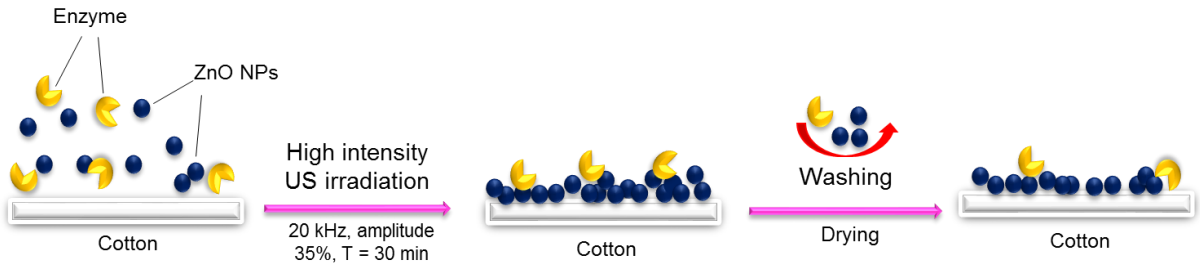

This section is based on the following publication:

Petkova P, Francesko A, Perelshtein I, Gedanken A, Tzanov T, Simultaneous sonochemical-enzymatic coating of medical textiles with antibacterial ZnO nanoparticles. *Ultrasonics Sonochemistry*, 2016, 29, pp 244 - 250

5.2.1 Introduction

The antimicrobial finishing is a must for production of medical textiles, aiming at reducing the bioburden in clinical wards and consequently decreasing the risk of hospital-acquired infections. The production of durable antibacterial textiles embedded with inorganic nanoparticles (NPs) often requires time-consuming fabric pretreatments such as chemical or plasma activation, in addition to subsequent coating stabilization using different cross linking technique.[318–320] Using enzymes, as tools for activation of textile surfaces, would avoid the use of harsh chemicals and allow to impart new functionalities to the fibrous substrates at mild processing conditions.[321]

The objective of this work is to combine biocatalysis and physicochemical processing in a single-step, industry-attractive technology for durable coating of medical textiles with antibacterial NPs. The coating consists in embedding of ZnO NPs onto cotton fabrics in a 30 min simultaneous sonochemical/enzymatic process. The ultrasound (US) is employed to boost the rate of the enzymatic (cellulase) hydrolysis and create on the cotton surface a larger number of reducing sugar ends for better NPs adhesion and durability of the antibacterial effect. The activity of the fabrics is evaluated against the clinically relevant bacteria *Staphylococcus aureus* (*S. aureus*) and *Escherichia coli* (*E. coli*) after multiple washing cycles with a non-ionic detergent at hospital laundry regimes (75 °C).

5.2.2 Cellulase activity at the processing conditions

Cellulases catalyze the hydrolysis of 1,4-β-glucosidic bonds in cellulose substrates. These enzymes are widely used in the textile industry to reduce the surface hairiness and improve the evenness of cotton fabrics in a process called biopolishing. During this process, and as a result of cellulose hydrolysis, novel reducing sugar ends appear on the fibers surface providing anchoring points for further functionalization. The efficiency of the activation process depends on the mass transfer from the processing liquid towards the surface of the textile material, usually intensified by high level of mechanical agitation.[322,323] It was demonstrated that controlled US accelerates this mass transfer without damaging the fibers, and results in better uniformity of the enzymatic treatment over a shorter period of time.[324] Thus, to illustrate the surface effect of the simultaneous US-enzymatic treatment, the morphology of the fibers after 30 min of sonication (amplitude 35 %, intensity 17.30 W/cm^2, 55 °C) alone and in presence of cellulase was observed via HRSEM. The biopolishing effect of the cellulase in terms of removal of the protruding after the US treatment fibrils (Figure 5.8A) was confirmed in Figure 5.8B.

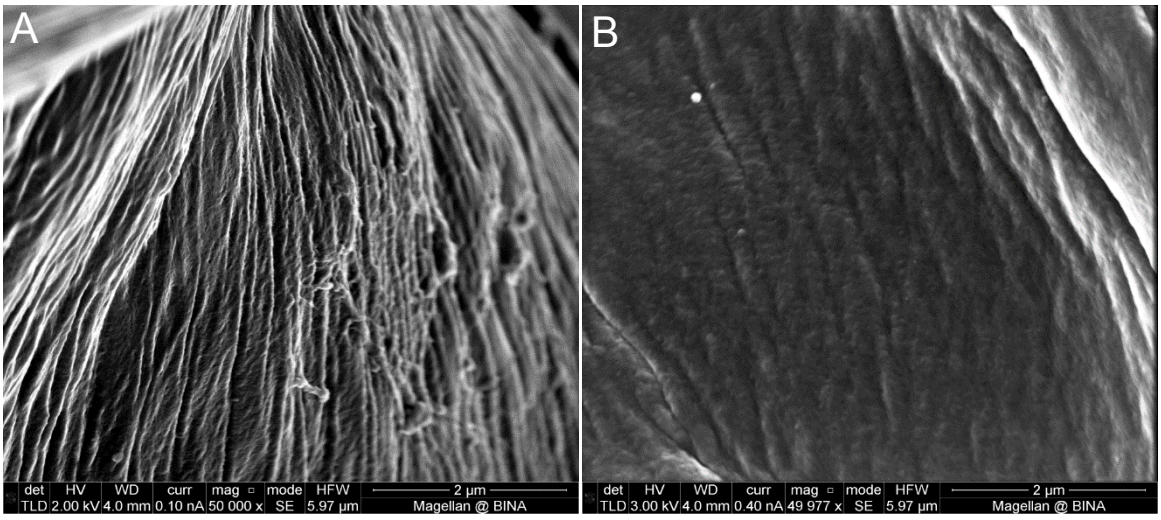

Figure 5.8 HRSEM image of cotton fabrics after 30 min of US irradiation (amplitude 35 %, intensity 17.30 W/cm^2, 55^{o}C) in absence (A) and presence (B) of enzyme.

Thereafter, as a prerequisite for efficient enzymatic activation of the fabric surface, we studied the cellulase activity as a function of the temperature and the enzyme stability in the ultrasonic field. The temperature profile of cellulase activity at temperatures ranging from 20 to 65 ºC showed a maximum at 55 °C (Figure 5.9A).

During US irradiation free hydroxyl and hydrogen radicals created by the high localized pressure and temperature could inactivate the enzyme.[325] To verify whether the cellulase activity would be affected by the US applied in the sonochemical coating process, an aqueous cellulase solution without substrate was exposed for 30 min to US irradiation at different temperatures. Thereafter, filter paper samples were incubated with aliquots of this solution, and the amount of reducing sugars was determined. The residual enzyme activity was calculated as a percentage of the activity of the enzyme not exposed to US irradiation. Only 10 to 20 % activity loss was detected after the US treatment regardless of the temperature in the cell (Figure 5.9A), suggesting that the simultaneous sono-enzymatic process would be feasible without compromising significantly the activity of the enzyme.

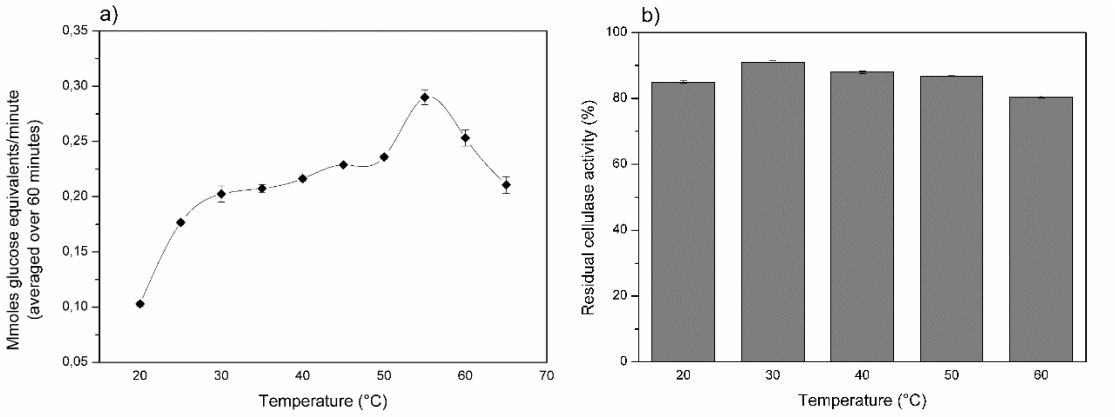

Figure 5.9 Temperature profile of cellulase (Kappacell ETU 39) activity (A) and the residual cellulase activity after 30 min of US irradiation (amplitude 35 %, intensity 17.30 W/cm^2) as a function of temperature (B). The residual activity was calculated as a percentage of the activity of the enzyme not exposed to US at 55 °C for 1 h in presence of Whatman No. 1 filter paper as a substrate.

The hydrolytic potential of the cellulase used in our experiments was studies under ultrasonic irradiation with different amplitudes/intensities. Figure 4.10 compares the final reducing sugar concentrations after 30 min of enzymatic hydrolysis on a model cellulose substrate at various amplitudes. The highest amount of reducing sugars released during the enzymatic process was obtained when the US amplitude and intensity were 35 % and 17.30 W/cm^2, respectively. Thus, all further experiments were carried out at these conditions, considered as the optimal for the enzyme performance in presence of US irradiation.

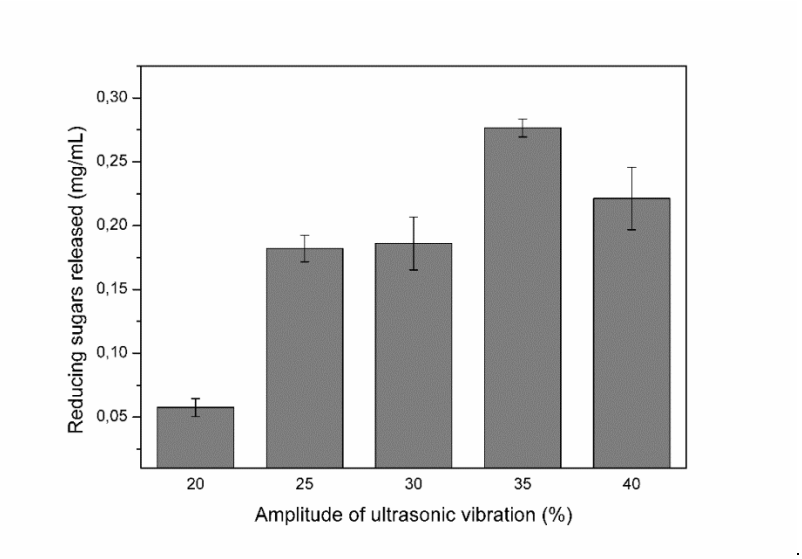

Figure 5.10 Reducing sugars released under different US amplitudes after 30 min of US irradiation at 55 °C in presence of Whatman No. 1 filter paper as a substrate. The US amplitudes of 20, 25, 30, 35 and 40 % correspond to the US intensities of 6.90, 10.40, 13.10, 17.30 and 30.80 W/cm^2, respectively.

Thereafter, the enzyme activity at the selected processing conditions (amplitude of 35 % and intensity of 17.30 W/cm^2) in terms of reducing sugars released during the 30 min sonication process in the presence of filter paper substrate (0.5 g) was determined and compared to the activity of the enzyme upon mechanical stirring (110 rpm). The assay was performed at the temperature of maximum enzyme activity (55 °C), used further for the enzyme/US coating of cotton with ZnO NPs. A 3-fold increase of the released reducing sugars, and thus, cellulase activity, was observed upon sonication (0.311 ± 0.01 mg/mL) in comparison to mechanical stirring (0.096 ± 0.02 mg/mL), due to the intensified mass transport.[324] In addition, changes in the molecular structure of the enzyme reported by others [326] to explain its increased activity were not observed in the fluorescence spectra of cellulase before and after sonication (Figure 5.11).

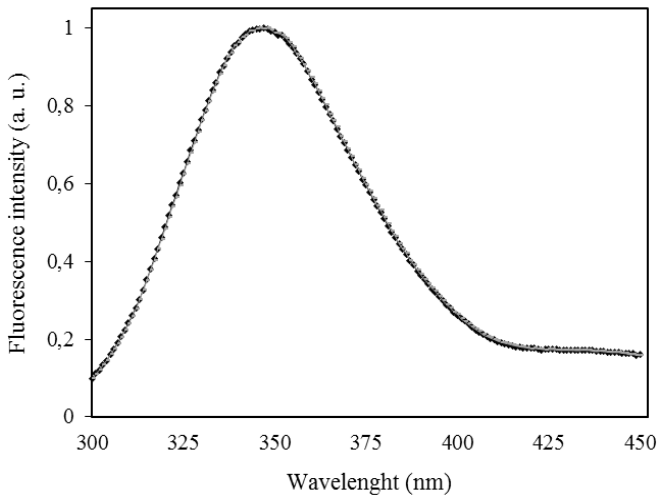

Figure 5.11 Intrinsic fluorescence spectra of untreated (black chart line) and ultrasound treated for 30 min cellulase (gray chart line).

5.2.3 Simultaneous sonochemical/enzymatic coating of cotton with ZnO NPs

Cotton fabrics were coated with antibacterial ZnO NPs in a simultaneous enzyme/US process carried out with both active and denatured enzyme as a control. ICP - AES measurements were further performed for quantifying the amount of ZnO on the treated fabrics (Table 5.2). Similar amount of ZnO was deposited sonochemically in the processes using either active or denatured cellulase. In addition to determining the amount of ZnO NPs embedded onto the fabrics, we also examined the durability of the coatings subjected to 10 washing cycles at 75 °C in presence of non-ionic surfactant. The fabrics treated with the active enzyme resisted better the applied washing cycles, though ~67 % of the initially deposited ZnO were removed after the washings. At the same time, 95 % of the ZnO on the fabrics coated in presence of denatured enzyme was washed-off. Greater resistance to washings of the NPs on the samples treated with active enzyme demonstrates the significance of the enzymatic activation of the fibers surface for improved NPs adhesion and more durable treatment. The hydrolytic bio-treatment of the cotton fibers generates free hydroxyl groups on their surface, serving as anchoring points for NPs deposition.[141]

Table 5.2 Amount of ZnO deposited on the cotton fabrics in a simultaneous sono-enzymatic process (experimental error ± 10 %).

Sample	**ZnO, % wt (per 100 g of fabric) after coating**		**ZnO on the fabrics after 10 washing cycles (%)**
	Non-washed	Washed	
Enzyme	0.8048	0.2690	33.4
Denatured enzyme	0.8533	0.0428	5.0

The HRSEM surface analysis of the coated samples showed that NPs agglomeration was observed regardless of the enzyme used in the coating process (active or denatured). However, the tendency of the particles to form aggregates was more pronounced for the fabric coated in presence of denatured protein (Figure 5.12A, B). More uniformly distributed NPs were observed on the cotton surface coated in presence of active cellulase (Figure 5.12E, F). This was additionally confirmed from the size histograms of the NPs deposited on both fabrics (Figure 5.13A, B), showing more narrow distribution of the deposited NPs when the active enzyme was used. These observations corroborate our previous findings that the enzymatic activation of cotton surface leads to uniformly dispersed along the fibers NPs.[141] In the current study a similar effect was achieved using a single-step sono-enzymatic process. The morphology of the fabrics treated in presence of denatured and active cellulase after subjecting to 10 washing cycles is shown in Figure 5.12C, D and Figure 5.12G, H, respectively. On the surface of the fabric coated in presence of denatured enzyme few NPs were found after the washings, while still a dense NPs layer is observed on to the surface of the enzyme treated samples. These observations were in a good agreement with the ICP – AES findings (Table 5.2), namely NPs improved stability when deposited in a simultaneous sono-enzymatic process.

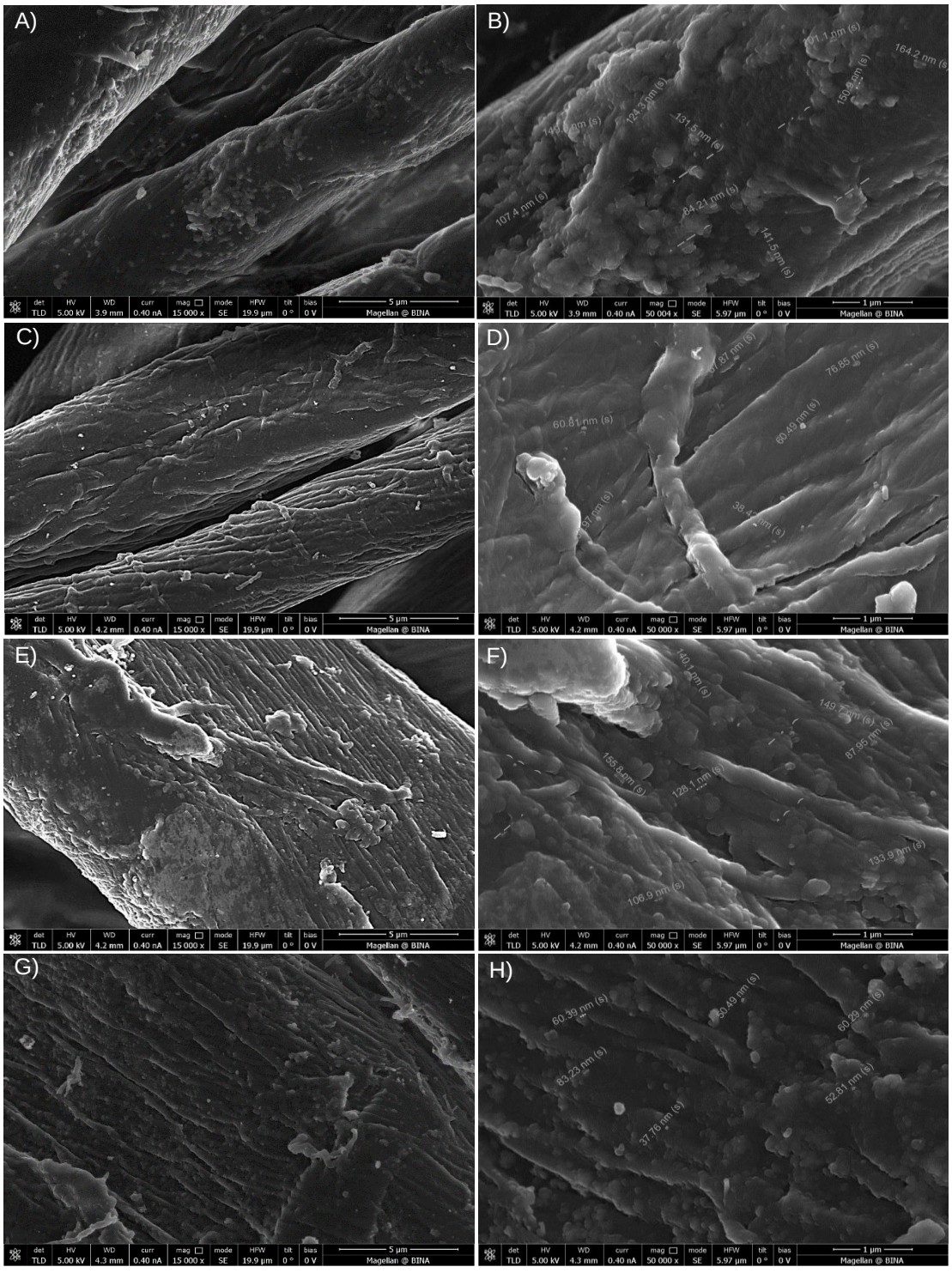

Figure 5.12 Representative HRSEM micrographs of cotton fabrics coated with 1 mM of ZnO NPs at 55 °C in presence of denatured enzyme before (a, b) and after 10 washing cycles (c, d) and in presence of cellulase before (e, f) and after10 washing cycles (g, h). The images on the left were taken with 15000x, whereas the right-side images were taken with 50000x magnification.

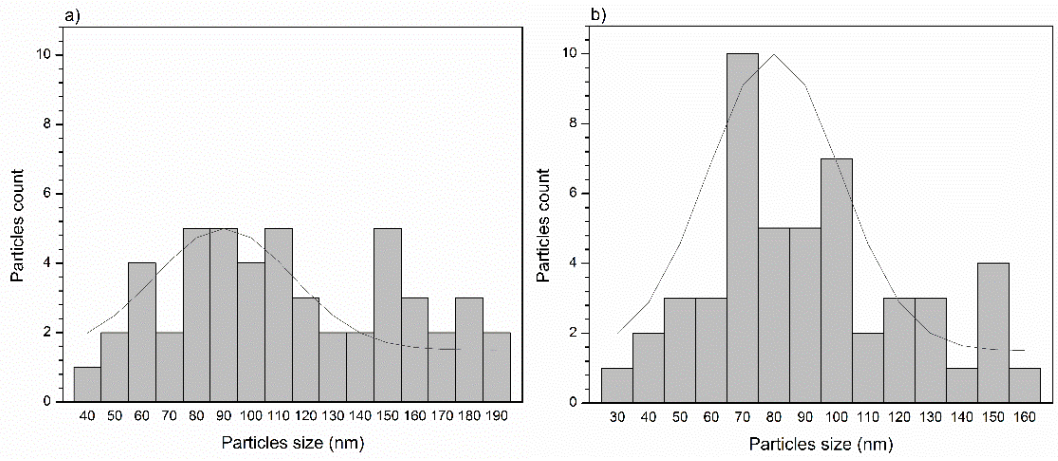

Figure 5.13 Size histograms (fitted by Gaussian curves (solid line)) of the ZnO NPs deposited on the fabric in presence of denatured enzyme (a) and cellulase (b) associated with Fig. 5.12b and 5.12f, respectively.

5.2.4 Antibacterial activity

ZnO NPs are largely reported as efficient antibacterial agents against both Gram-positive and Gram-negative bacteria. The antibacterial efficiency of the fabrics coated with ZnONPs was evaluated against *S. aureus* and *E. coli.* The non-washed fabrics treated with active or denatured cellulase showed comparable antibacterial performances (~70 % reduction in bacteria viability) toward *S. aureus* (Figure 5.14a). However, after 10 washings the coatings obtained in presence of denatured enzyme lost entirely their antibacterial efficacy toward this bacterial strain. On the other hand, the coating deposited in presence of the active enzyme retained ~50 % of its initial antibacterial activity, which is in good agreement with the amount of remaining ZnO on this fabric.

All non-washed fabrics were more efficient against *E. coli*, and the samples obtained in presence of active or denatured protein reduced the bacterial viability by 98 % and 90 %, respectively. After washing, however, the antibacterial performance of the coating obtained in presence of active cellulase was maintained. The sample coated in presence of denatured enzyme lost more than 30 % of its initial antibacterial efficiency (Figure 5.14b), though the ZnONPs amount for this sample was reduced by 95 % after the washings. A possible explanation for these results could be that the amount of the ZnONPs needed to inhibit the *E. coli* growth is much lower than the one initially deposited on to the fabric. On the other hand, the ZnO concentration on the fabrics after the washings is considerably reduced and it is below the concentration needed for full kill of this bacterium but still enough to inhibit 50

% of its growth. These findings reconfirmed that the cellulase treatment improved the durability of the coating effect. The higher resistance of *S. aureus* to ZnONPs in comparison with *E. coli* is due to the thicker peptidoglycan layer in the cell wall of Gram-positive bacteria, which makes them less susceptible to MeO NPs.[137,327] The results also showed that the durability of the antibacterial effect of the ZnO NP coating obtained in the one step sono-enzymatic coating approach against *E. coli* was higher compared to the already reported durability of the coating obtained in the two step-process (consisting of enzymatic pre-treatment of the cotton textiles followed by sonochemical deposition of ZnO NPs).[141]

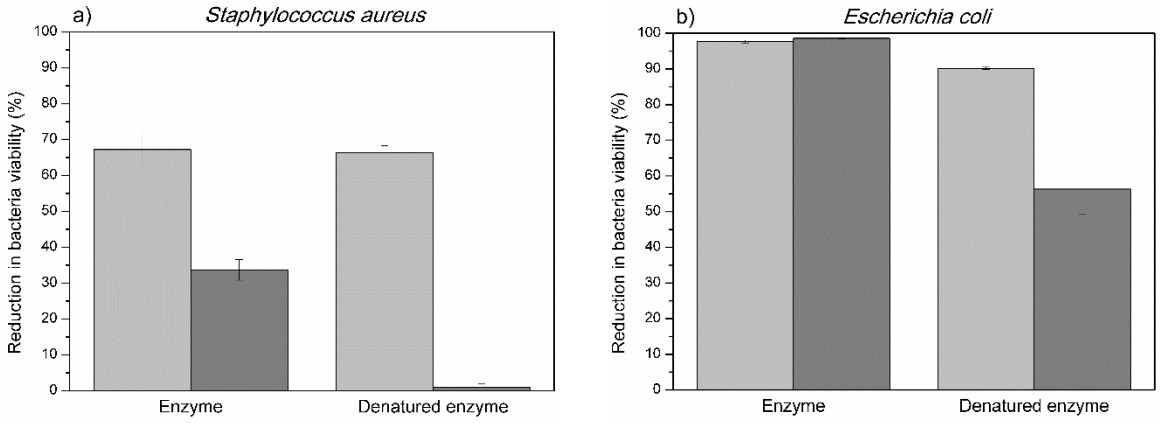

Figure 5.14 Antibacterial activity of the fabrics coated with 1 mM of ZnONPs: light gray bars represent non-washed fabrics, whereas dark gray bars show the antibacterial activity of the fabrics after 10 washing cycles at 75°C. The assays were performed with S. aureus (a) and E. coli (b), after 1 h of contact with the fabrics.

5.2.5 Conclusions

Novel industry-attractive technologies are required for the manufacturing of antibacterial medical textiles used to reduce the risk of hospital-acquired infections. In this study we assessed the feasibility of a single-step sono-enzymatic process for durable coating of cotton fabrics with antibacterial ZnO NPs. The coating procedure resulted in the uniform multilayer deposition of ZnO NPs onto the fibers. As a consequence of the boosted cellulase activation of the fabric surface during sonication, the adhesion of the coated NPs was improved and thus, the antibacterial performance was ensured. Although the outer NP layers were not firmly fixed on the textiles, 33 % of the initially deposited ZnO NPs remained on the surface after multiple intensive washing cycles. The remaining after washings NPs still exhibited nearly 100 % reduction of the viability of *E. coli*, whereas the efficiency toward *S. aureus* decreased by 50 %. In summary, the one-step sono-enzymatic process is an attractive alternative to the currently used technologies for antibacterial textile functionalization that rely on aggressive and time-consuming chemical pre-treatments to achieve durable antimicrobial fabrics.

5.3 Enzyme-assisted functionalization of cork surface with antibacterial biopolymer/silver hybrid nanoparticles

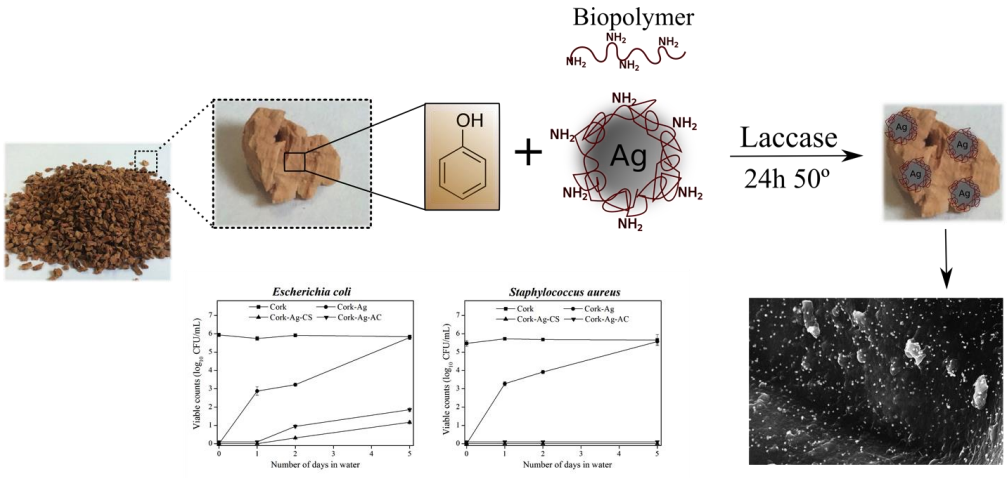

This section is based on the following publication:

Francesko A, Blanón L, Vázquez M, **Petkova P**, Morató J, Pfeifer A, Heinze T, Mendoza E, Tzanov T, Enzymatic functionalization of cork surface with antimicrobial hybrid biopolymer/silver nanoparticles. *Applied Materials & Interfaces*, 2015, 7(18), pp 9792-9799

5.3.1 Introduction

In this work, antibacterial silver nanoparticles (AgNPs) colloidal dispersions were synthesized by reduction of silver nitrate ($AgNO_3$) with sodium borohydride ($NaBH_4$) and simultaneously doped with two amino-functional biopolymers: CS and AC. In this reaction the chemical reagent can be omitted because both chitosan (CS) and aminocellulose (AC) have been used as combined reducing and capping agents.[328,329] However, $NaBH_4$ is used as a fast reducing agent in order to avoid high temperatures in the reaction and/or the assistance of an additional technology required for the Ag^+ reduction.

The employment of CS and AC is considered advantageous for stabilization of the AgNPs providing in the same time the particles with amino functionalities for immobilization on different solid substrates and thus, facilitating the NPs recovery and reuse.

Herein, laccase-assisted oxidation of the phenolic structures in cork is used to covalently immobilize the hybrid biopolymer-AgNPs on the cork surface via reaction with the amino groups in biopolymers. The antimicrobial activity of the green-functionalized cork is evaluated against *E. coli* and *S. aureus*, in order to assess its potential as a filter to reduce these common pathogenic indicators of pollution in constructed wetlands.

5.3.2 Characterization of AgNPs and AgNPs-biopolymers dispersions

AgNPs were synthesized by a chemical reduction of $AgNO_3$ with $NaBH_4$ in absence and presence of biopolymers. In order to confirm the interactions between CS and AC with AgNPs during their synthesis, the ζ potential of pure AgNPs and biopolymer-doped AgNPs was measured. AgNPs doped with biopolymers displayed positive ζ potential values due to the presence of amino groups in the macromolecules that are protonated at pH 5 – used for the AgNPs preparation (Table 5.3). Given that pure AgNPs display a negative potential, these results suggest the interactions between the AgNPs and the biopolymers.

The pure AgNPs also displayed notably smaller hydrodynamic radius than their homologues doped with biopolymers (Table 5.3). When measured by DLS, the increase in the NPs diameter in presence of biopolymers represents an indirect demonstration that the AgNPs are coated with macromolecules in thick layers.[184] This is the opposite to a thin layer doping of noble metal NPs in which case the change in the hydrodynamic radius is negligible.[10] Also, in our study it is probable that the similar Mw of the biopolymers used induced comparable size increase after the AgNPs doping.

Table 5.3 ζ potential and mean hydrodynamic radius of AgNPs synthesized in absence and presence of CS and AC.

Sample	ζ potential (mV)	Mean particle size (nm)
AgNPs	-25.3 ± 0.8	32.3 ± 1.7
AgNPs-CS	41.5 ± 0.7	239.6 ± 13.5
AgNPs-AC	26.2 ± 1.36	253.8 ± 20.0

The interactions between the AgNPs and biopolymers were further confirmed by STEM analysis. Without doping the AgNPs were abundant in the dispersion and most of the particles displayed the sizes ≤30 nm (Figure 5.15A). In contrast, the average sizes of the AgNPs doped with CS or AC, which were shaped in rod-like structures, exceeded 100 nm, thereby confirming the DLS findings (Figure 5.15B and C). The doped particles were well dispersed in the biopolymer templates forming aggregated complexes, apparently as a result of their sticking upon drying of the sample. The pure AgNPs precipitated in a matter of hours leaving very few particles in the dispersion (Figure 5.15D). This is expected since

the synthesis of NPs by strong chemical reduction often results in agglomeration and precipitation of the colloids. In contrast, the hybrid structures of the biopolymer-doped AgNPs were stable and resisted the aggregation in dispersion and precipitation (Figure 5.15E and F). STEM images together with the macroscopic observation of the dispersions (inset images) provided a clear proof that both CS and AC stabilized the AgNPs dispersions through the passivation of the particles surface.

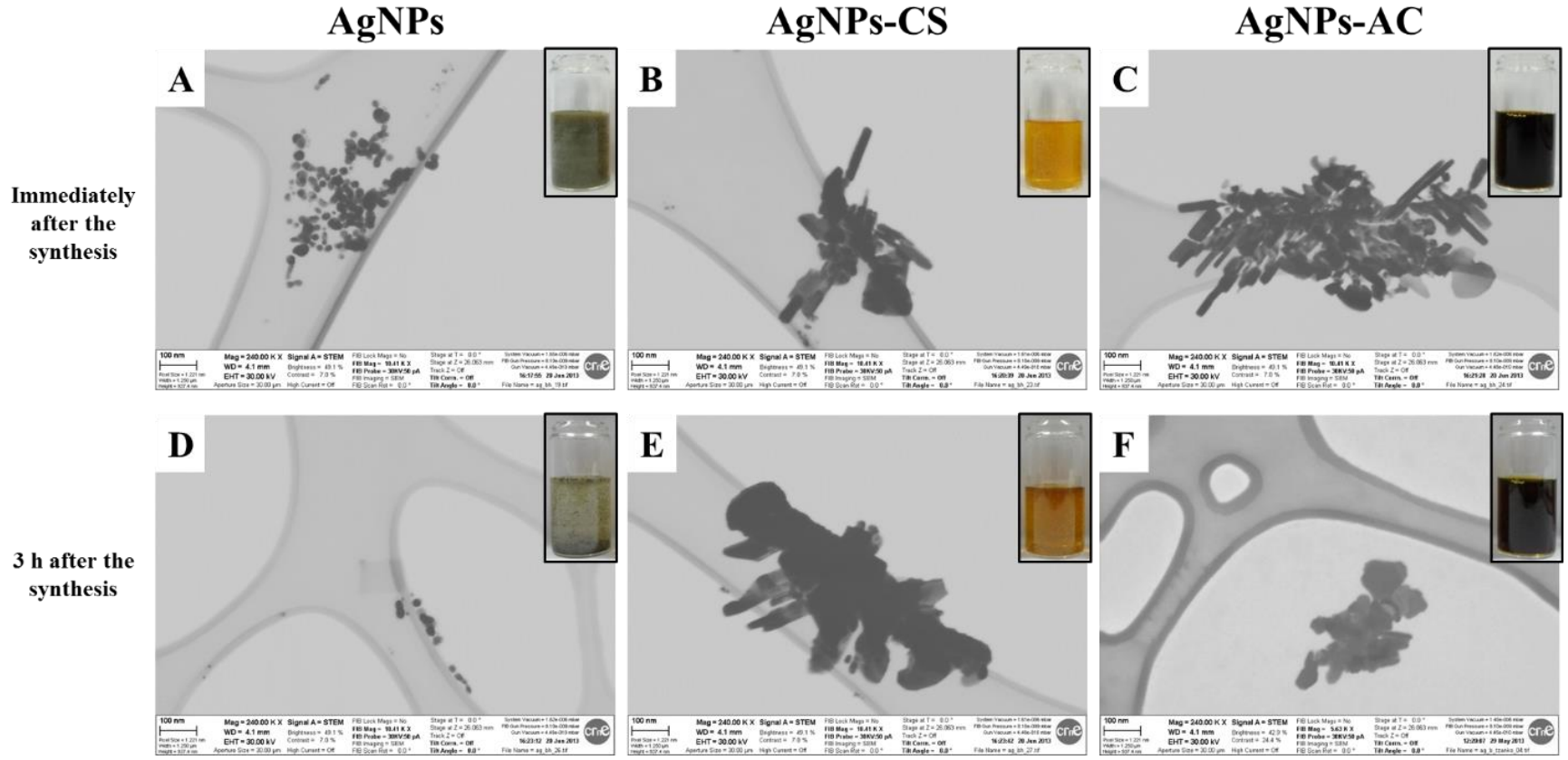

Figure 5.15 STEM images of the AgNPs dispersions synthesized in absence and presence of CS and AC. The images were taken to evaluate the presence of NPs in the dispersions immediately after the synthesis of the particles (images A, B and C) and after 3 h of their preparation (images D, E and F). The inset photographs represent the analyzed dispersions.

UV-Vis spectra were recorded for the pure AgNPs and the dispersions doped with CS and AC after 72 h of their synthesis. Since the dispersion prepared in absence of biopolymers was unstable and entirely precipitated during this time leaving the above solution clear, no characteristic for AgNPs absorption is observed in its spectrum in the 300-500 nm range (Figure 5.16). In contrast, the SPR band was detected for the stable AgNPs dispersions prepared in presence of both CS and AC. The change in color of the dispersion and the consequent appearance of the bands between 400 nm (for AgNPs-AC) and 425 (for AgNPs-CS) implies the interaction between the biopolymers and AgNPs surface which modify their interaction with light.[330]

Besides the different wavelength position of the SPR peak, the intensity of AgNPs-AC was around 3 times higher than that of AgNPs-CS. The intensity of the band in the AgNPs systems where biopolymers are used as particle stabilizers varies as a function of the preparation conditions, as well as the amount of a biopolymer used for the particles doping. Nevertheless, despite the higher peak intensity of the AgNPs-AC system and the same starting concentrations of AC and CS, it still could not be concluded that this macromolecule interacts better with silver compared to CS, especially in the case where the reduction of Ag^+ to elemental silver solely depends on the chemical compound ($NaBH_4$). Although the peak intensities are directly proportional to the amount of the AgNPs-biopolymer hybrids, these can only be compared between different samples of the same system (obtained varying the preparation conditions). For example, certain biopolymer concentrations can decrease the silver particles surface exposure to light, which may be the reason for decrease or even the absence of the SPR band in such systems.[331] If such scenario is applied to our case, we may even speculate on a better coverage of the AgNPs surface by CS compared to AC due to their strong interactions. Nevertheless, the strength of the organic-inorganic interactions as a function of the biomaterial structure goes beyond the scope of this manuscript.

Important from the technological point of view, the uniform color distribution throughout both AgNPs-CS and AgNPs-AC dispersions means that these hybrid systems were uniformly distributed in the dispersions, which broadens their application potential and facilitates exploitation of their functional properties. In addition, no precipitation was observed during several weeks after their synthesis, revealing sufficient stability of the systems for e.g. further surface functionalization of different materials.

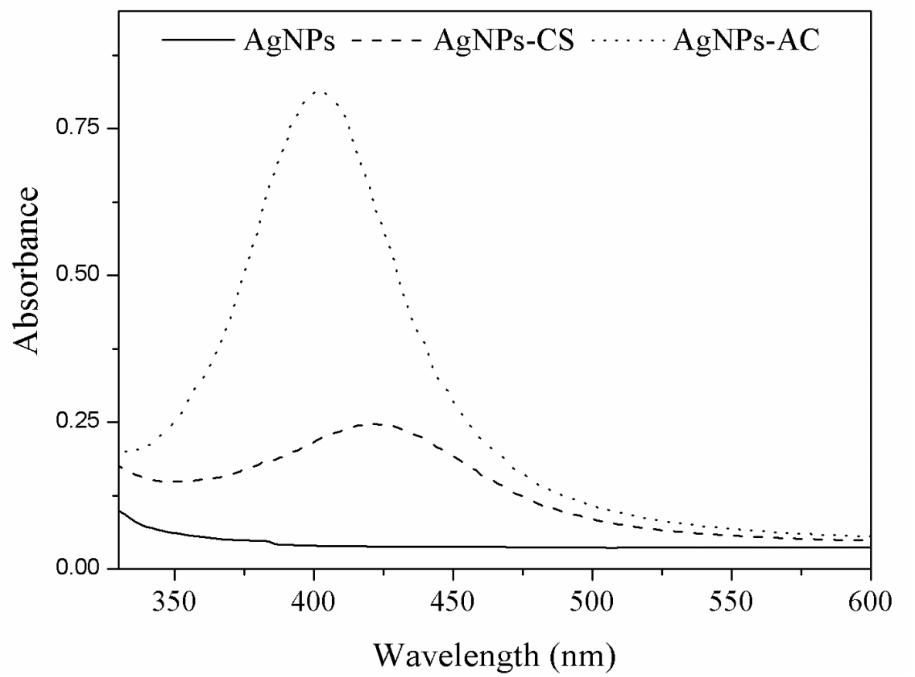

Figure 5.16 UV-Vis spectra obtained for the pure AgNPs dispersion and the dispersions doped with CS and AC after 72 h of their synthesis.

5.3.3 Enzymatic grafting of hybrid biopolymer-AgNPs on cork

The characterization of the AgNPs and hybrid biopolymer-AgNPs using ζ potential, DLS, UV-Vis and STEM analysis, indicated that interactions between the particles and CS or AC occur. Doping of the AgNPs with these biopolymers provides the amino moieties on the particles surface necessary for the enzyme-catalyzed covalent immobilization of NPs onto cork. The used enzymatic immobilization approach is complex and may involve different interactions/reactions between the cork surface and used macromolecules, such as electrostatic interactions, hydrogen bonding and covalent linking between the laccase-activated cork moieties and CS or AC. In this work we targeted covalent bonding in order to permanently functionalize the cork surface with biopolymer-doped AgNPs using laccase-assisted immobilization which necessarily comprises: i) oxidation of the cork phenol groups (from suberin and lignin) to reactive quinones, and ii) reaction of the quinones with nucleophilic moieties (amino groups) in biopolymers through 1,4-Michael addition or Schiff base formation,[332] as illustrated on Scheme 5.1.

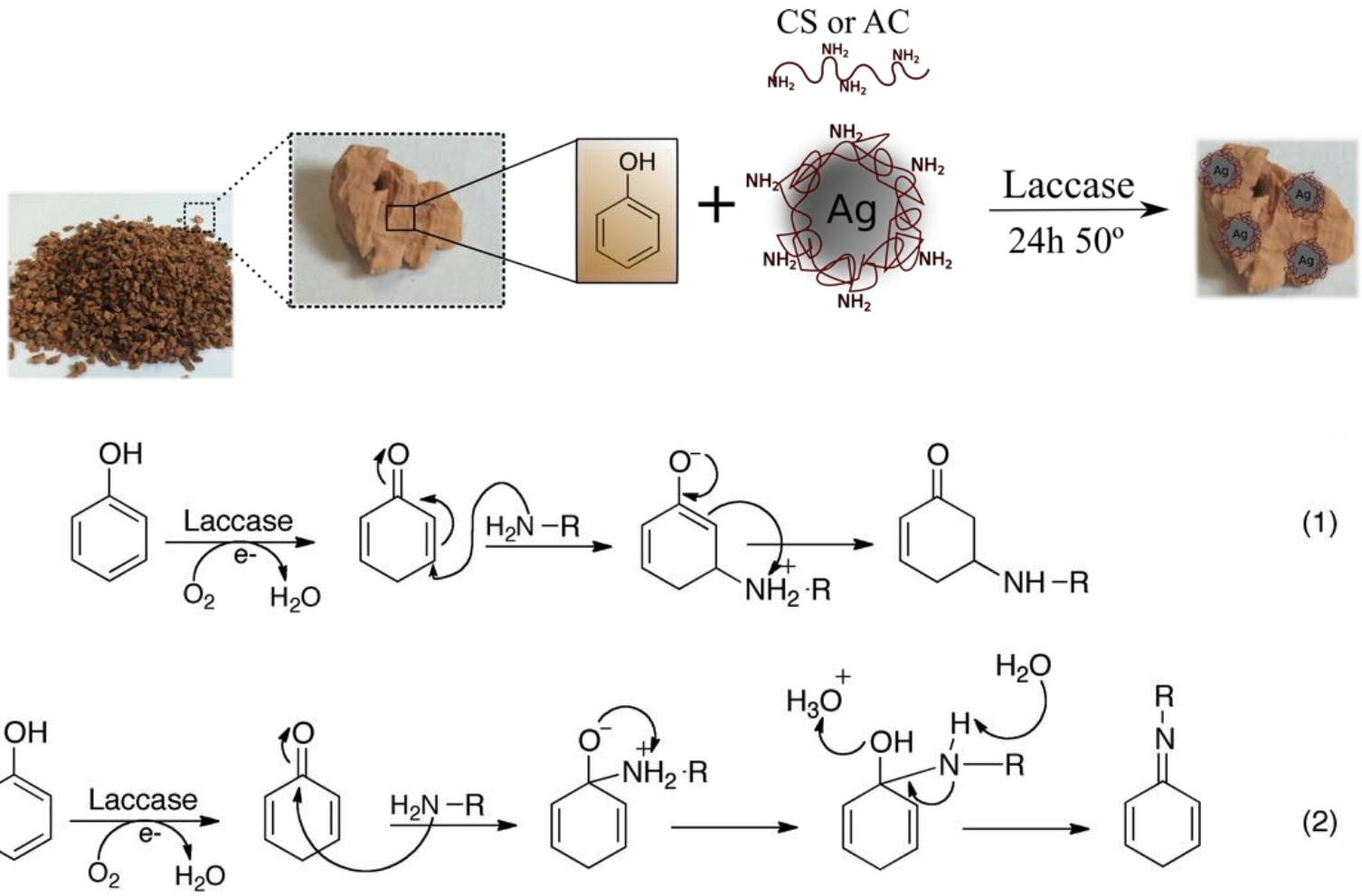

Scheme 5.1 Mechanism of immobilization of the hybrid AgNPs-biopolymers onto cork. Mechanisms above the scheme, show two possibilities of reaction: (1) Michael addition, (2) Schiff base formation.

FTIR spectra were recorded to verify whether the functionalization of the cork surface was successful. Prior to analysis, unmodified cork, cork enzymatically treated with pure AgNPs (immediately after their preparation) and cork treated with the hybrid biopolymer-AgNPs were subjected to thorough washing during which the samples were immersed in distilled water and vigorously stirred for 5 days. The water was changed each 24 h and the remaining solutions were checked for the presence of NPs by optical microscopy using a Nikon Eclipse Ti microscope, with a 100x oil-immersion objective. After 4 days in water, no particles were detected in any of the remaining solution meaning that after this time there was no AgNPs leaching from the samples.

The unmodified cork and cork treated with pure AgNPs displayed characteristic for cork spectra with some of the most prominent bands as markers of: i) suberin at 1462 cm^{-1}, 1236 cm^{-1} and 1157 cm^{-1}, its aliphatic chains at 2918 cm^{-1} and 2852 cm^{-1}, and its ester groups at 1735 cm^{-1} and 721 cm^{-1}, ii) lignin aromatics at 1600 cm^{-1}, 1510 cm^{-1} and 849 cm^{-1}, and iii) cork polysaccharides at 1096 cm^{-1} and 1035 cm^{-1} (Figure 5.17).[333] Clear and comparable differences were found in the spectra of the cork treated with AgNPs-biopolymer hybrids. All peaks attributed to the cork suberin including the bands constituting the typical suberin fingerprint (1462 cm^{-1}, 1236 cm^{-1} and 1157 cm^{-1})[334] decreased considerably after the enzymatic functionalization. Also the bands representing the lignin aromatics decreased or completely disappeared. Thus, both suberin and lignin from cork were involved in the functionalization reaction. At the same time, the differences in the spectra in polysaccharide regions between 1532 – 1681 cm^{-1} and 900 – 1120 cm^{-1} suggest a successful biopolymer grafting, but this regions are rather complicated for deeper analysis. Instead, a shoulder peak was noticed at 1260 cm^{-1} in the spectra of the treated cork (especially pronounced for the cork treated with AgNPs-CS), which could be attributed to C-N stretching of aryl amides formed via Michael addition.[332] Therefore, the FTIR spectra confirmed that the phenolic moieties from suberin and lignin in cork were covalently linked with CS or AC, where the reaction occurred predominantly via Michael addition.

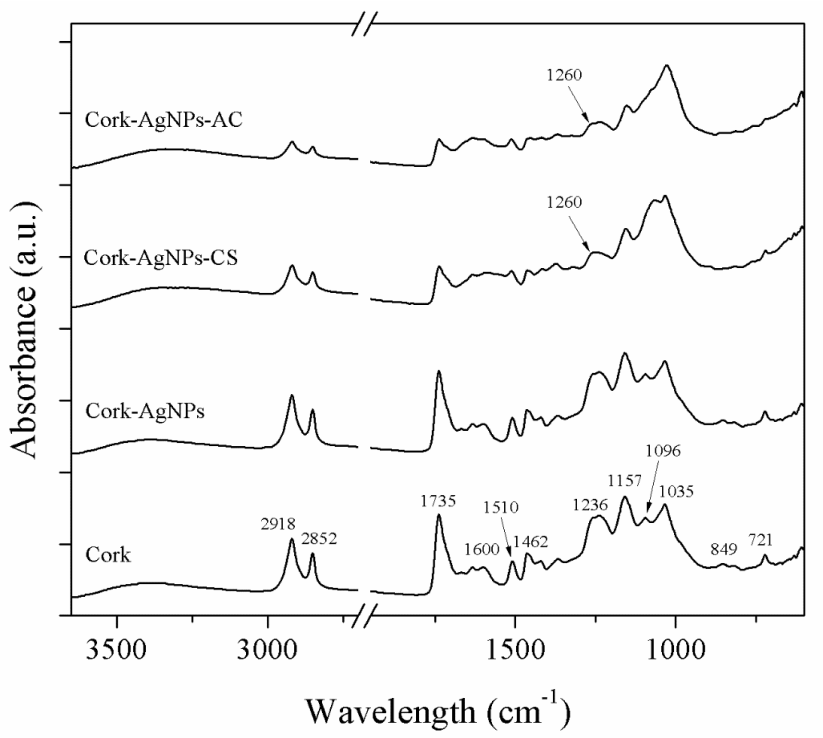

Figure 5.17 FTIR-ATR spectra of untreated and enzymatically functionalized cork with AgNPs, AgNPs-CS and AgNPs-AC dispersions.

SEM analysis was carried out in order to confirm the presence of AgNPs on the cork surface after the enzymatic treatment. On average, cork cells rarely exceed 50 µm height, with a hexagonal face of 15-20 µm and a thickness of 1-2 µm.[17] SEM images were thus taken inside the cells, first for the untreated cork without the NPs (Figure 5.18A). The cell surface was not smooth and appeared granulated, where the remaining deposits, not removed during the cleaning procedure, were noticed. The same deposits were observed on the cork treated in presence of laccase with the AgNPs immediately after their synthesis (Figure 5.18B). The AgNPs were thus not fixed on the cork surface or were removed during the immersion in water for 5 days. In contrast, particles and macromolecular structures were observed on the cork enzymatically embedded with the hybrid AgNPs-biopolymer systems even after extensive washing with water (Figure 5.18C and D). This was especially the case of AgNPs-CS treated cork, which displayed a large amount of NPs on the surface. Both individual submicron particles and larger agglomerates could be visualized. A lower number of AgNPs was observed on the cork surface treated with AgNPs-AC system (marked with red arrows on Figure 5.18D), but these were still fixed strong enough to resist the removal

by thorough washing. A larger number of permanently deposited AgNPs was achieved via the laccase-assisted grafting of CS on cork.

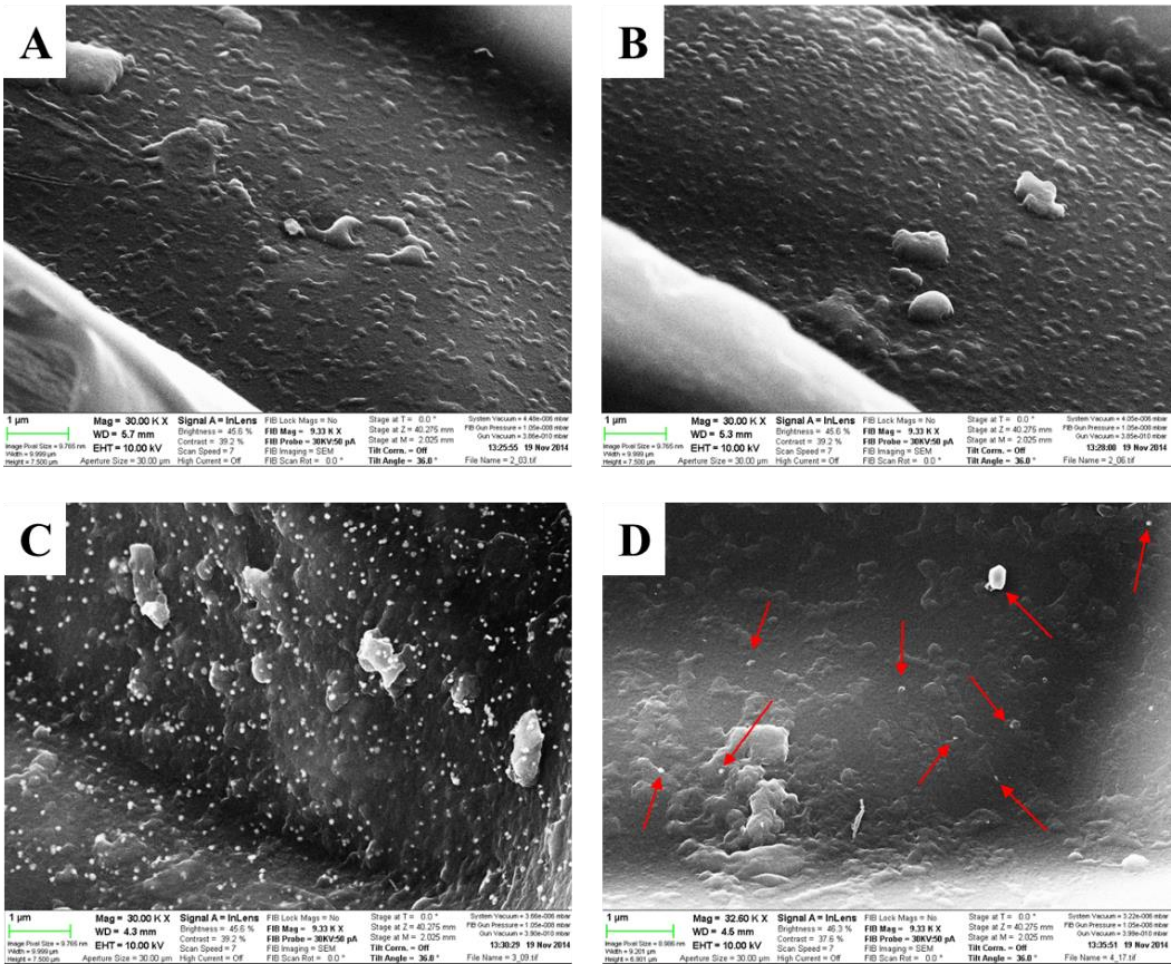

Figure 5.18 SEM images of cork surface enzymatically treated in absence (A) and presence of NPs: (B) pure AgNPs, (C) AgNPs-CS, and (D) AgNPs-AC.

5.3.4 Antimicrobial activity of AgNPs-embedded cork matrices

The antibacterial activity of cork matrices functionalized with biopolymer-doped AgNPs was evaluated at different time points after immersing the materials in water up to 5 days. The results of the time-kill experiments showed that the cork matrices treated with pure Ag-NPs (immediately upon their preparation) fully inhibited the bacterial growth for both *E. coli* and *S. aureus* if no washing procedure was performed (Figure 5.19). Although not expected in such extent, the antibacterial effect of cork-AgNPs sample could be explained by a moderate

adsorption capacity of cork towards silver.[335] In contrast, other materials such as nanoclay have been associated with AgNPs in absence of auxiliary molecules to impart diffusion-controlled antimicrobial activity, with long term impact.[336] Adsorption of metals onto different sorbents may occur by physiosorption and chemisorption.[337,338] Considering that the chemisorption involves the permanent modification through generation of new chemical bonds at the surface of a material and the progressive loss of the antibacterial effect of cork-AgNPs during 5 days in water, it is logical to conclude that this material maintained the activity whereas the physically adsorbed particles persisted on its surface. On the other hand, the cork matrices functionalized with AgNPs-CS and AgNPs-AC hybrids preserved most of the antibacterial effect (against *E. coli*) or fully retained the effect (against *S. aureus*) during the extensive washing procedure. Although it is probable that some of the hybrid structures were also physically adsorbed on surface (reflected in somewhat lower effect of the cork-AgNPs-CS and AgNPs-AC in case of *E. coli* after 5 days of washing), these results indirectly confirm the FTIR and SEM findings for the permanent functionalization of cork with AgNPs-biopolymer hybrids using the laccase-assisted approach.

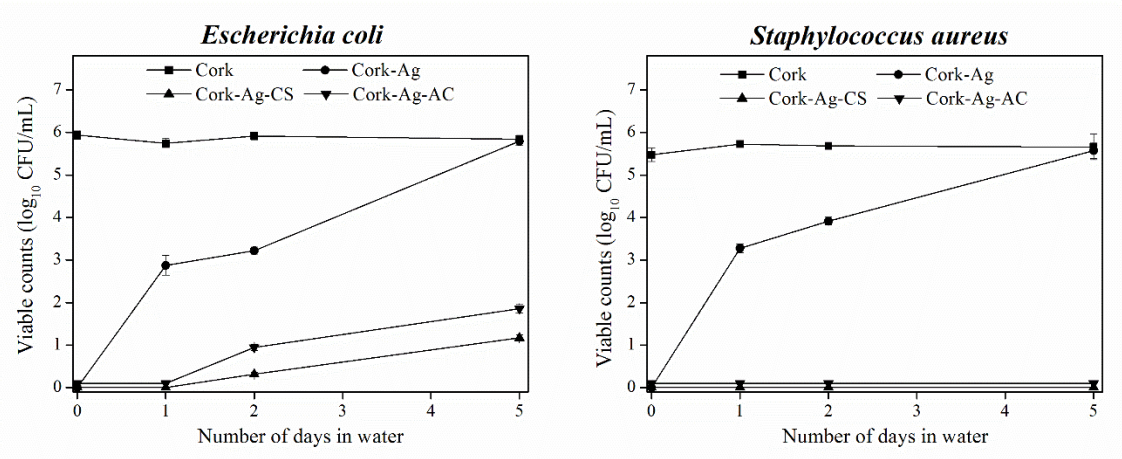

Figure 5.19 Antimicrobial activity of untreated and enzymatically functionalized cork with AgNPs, AgNPs-CS and AgNPs-AC dispersions. The materials were subjected to the washing treatment in water (stirring 100 rpm) for up to 5 days, during which the antibacterial activity is evaluated at different time points.

The antimicrobial effect of cork-AgNPs-CS and cork-AgNPs-AC after 5-day washing was also compared to the matrices enzymatically functionalized with only CS and AC (without AgNPs), in order to reveal if the effect of the biopolymers was restricted only to the material functionalization. Calculated in percentage of bacterial inhibition compared to the effect of

untreated cork, the matrices with enzymatically embedded hybrid AgNPs-CS and AgNPs-AC reduced respectively by 99.6 % and 85.3 % the growth of *E. coli*, whereas showing the full kill potential in the case of *S. aureus* (Table 5.4). Although the SEM images showed more AgNPs particles immobilized on cork in the case of AgNPs-CS, the antimicrobial efficiency of these two materials were comparable for the used bacteria inoculums. Such scenario did not allow to clearly distinguish the individual effects of AgNPs on one side and intrinsically antimicrobial CS or AC on another. Indeed, CS is a known while AC (a more economical substitute of CS) is an emerging antimicrobial macromolecule in different forms.[339,340] Cork treated with CS and AC in absence of AgNPs did not show activity against *E. coli*, whereas the efficiency for *S. aureus* reduction was of 10.2 % and 4.3 %, respectively. The antibacterial potential of these matrices is measured in the assay optimized to distinguish the effect of the cork embedded with AgNPs (small amount of the material and high bacteria count), which certainly possess higher antibacterial activity than the biopolymers. Thus, the absence or the low extent of the antibacterial potential of the matrices treated only with biopolymers is explained with the assay conditions applied. Moreover, a slightly higher antibacterial potential of the CS- treated compared to the matrices containing AC is attributed to better grafting of CS macromolecule compared to AC (concluded from the SEM images). Overall, the antibacterial efficiency of the cork grafted with hybrid AgNPs-biopolymers is largely dependent on the presence of silver. Nevertheless, some synergistic antibacterial effect of the AgNPs and the intrinsically antibacterial amino-functional biopolymers could still be envisaged, though the enhancement of antimicrobial activity in hybrid nanoscale architectures based on silver for long-term effect is not a new concept.[341]

Table 5.4 Antibacterial activity of enzymatically modified cork against Escherichia coli and Staphylococcus aureus after 5 days washing in water. The results are expressed in % of bacteria reduction compared to the untreated cork.

Sample	*E. coli* reduction (%)	*S. aureus* reduction (%)
Cork-AgNPs- CS	99.6	100
Cork-AgNPs-AC	85.3	100
Cork-CS	0	10.2
Cork-AC	0	4.3

In order to better understand the effect of the hybrid nano-coating on the bacteria, we further studied (by SEM) the surface morphology of the cork granules (natural cork or functionalized with AgNPs-CS complex) after incubation in water inoculated with *E. coli*. The SEM analysis revealed the presence of accumulated *E. coli* on the cork surface (Figure 5.20). However, the morphology of the bacteria found on the untreated cork and on the cork-AgNPs-CS composite was very different. Proliferating bacteria with well-formed flagella were observed on the surface of the untreated cork (Figure 5.20 A, B), whereas the *E. coli* found on the functionalized with AgNPs-CS cork granules were not flagellated (Figure 5.20 C, D). Apparently, the hybrid nanocomposite affected the bacteria structure and could prevent their attachment and proliferation on the surface. More bacteria were attached on the surface of the unmodified cork than on the surface of the cork-AgNPs-CS composite. The loss of flagella in *E. coli* after water disinfection with TiO_2-based photocatalyst was previously reported.[342] The presence or absence of flagella is important to bacterial survival and growth, since these appendages are not only driving cell locomotion, but also allow the bacteria to attach to surfaces or to epithelial cells.[343] It is well established that flagellar-mediated motility and the ability to produce a number of pili are essential for biofilm formation [344] and contribute to the virulence of pathogenic bacteria.[345]

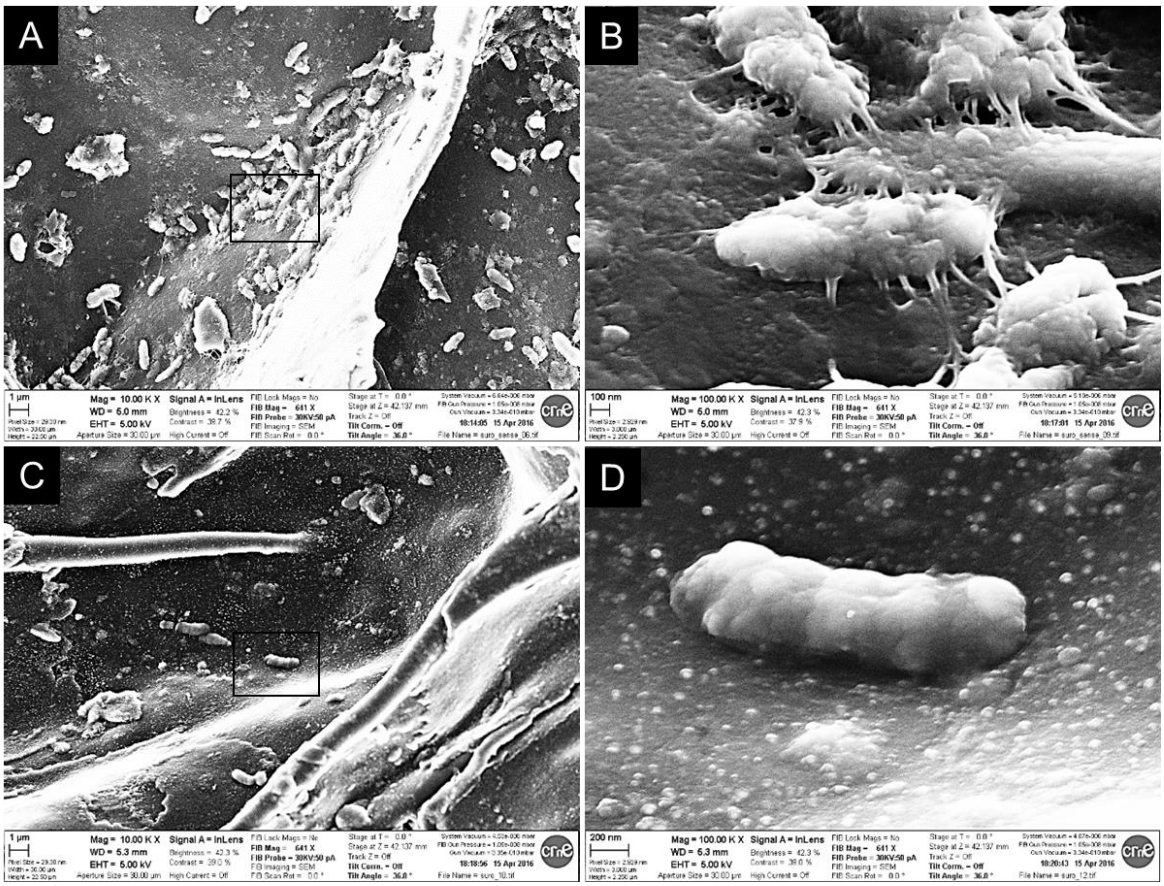

Figure 5.20 SEM images of E. coli accumulated on the surface of unmodified cork (A, B) and on the CS/AgNPs-cork composite (C, D) after 16 h of contact with E. coli suspension. The images on the left were taken with 10000×, whereas the right-side images were taken with 100000× magnification.

As a next step, the viability of the bacteria accumulated on the cork surface was tested by placing the cork pieces on Coliform agar plates specific for *E. coli*. The results showed that the flagellated bacteria observed on Figure 5.20A and B on the surface of the unmodified cork samples were viable, while bacteria growth was not observed for the cork-AgNPs–CS samples on which surface the bacteria were without flagella (Figure 5.21D). Therefore, the bacteria found observed on Figure 5.20 C and D were not viable, demonstrating the disinfection potential of the designed material.

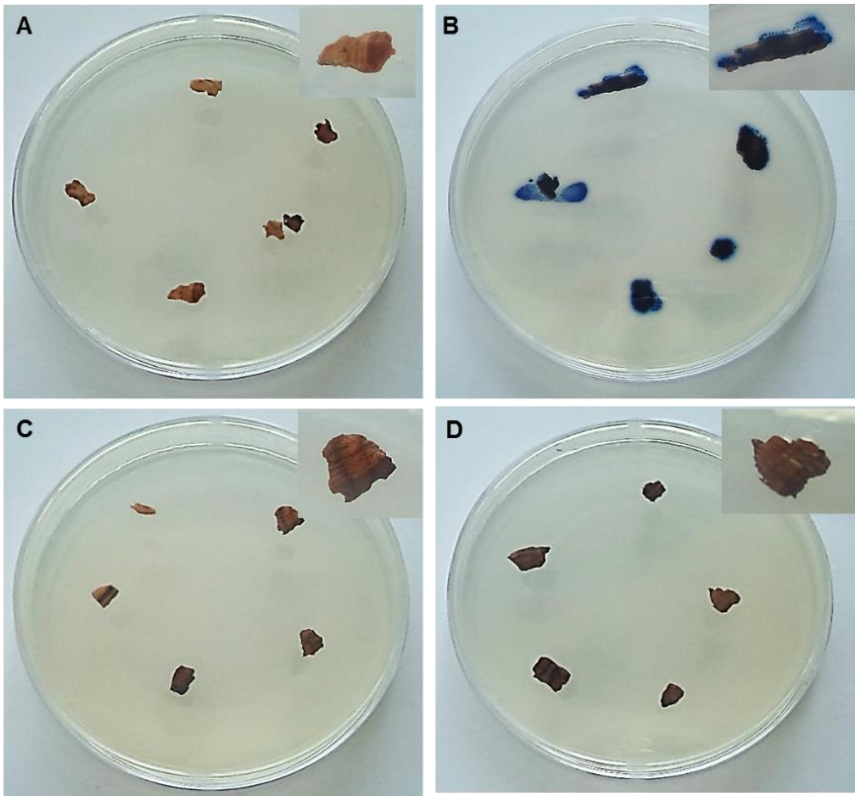

Figure 5.21 Images of natural cork granules after incubation in sterile distilled water (A) and water inoculated with *E. coli* (B); and cork-AgNPs-CS composite after incubation in sterile distilled water (C) and water inoculated with *E. coli* (D) for 16 h at room temperature. The images B and D are related to Figure 5.20 A, B and Figure 5.20 C, D, respectively.

5.3.5 Conclusions

In this study, the laccase oxidation of the phenol moieties in cork into reactive quinones and their further reaction with nucleophilic amino groups in CS- or AC-doped AgNPs was exploited to impart durable antibacterial activity onto cork matrices. The role of CS and AC biopolymers in the hybrid NPs structures was three-fold in order to: (i) stabilize the AgNPs and prevent their aggregation, (ii) serve as an interface for permanent grafting of AgNPs on cork, and iii) synergistically improve the AgNPs antibacterial effect. The biocatalytically functionalized cork matrices with AgNPs-CS and AgNPs-AC efficiently reduced the *Escherichia coli* and *Staphylococcus aureus* growth during the course of 5 days. Such long-term stability and durability of the antimicrobial effect in conditions of continuous water flow, suggest the potential application of the functionalized cork matrices in constructed wetlands as an adsorbent for removal of wastewater impurities at the same time avoiding microbial contaminations.

5.4 Enzyme-assisted formation of nanoparticles-embedded hybrid biopolymer hydrogels for wound healing

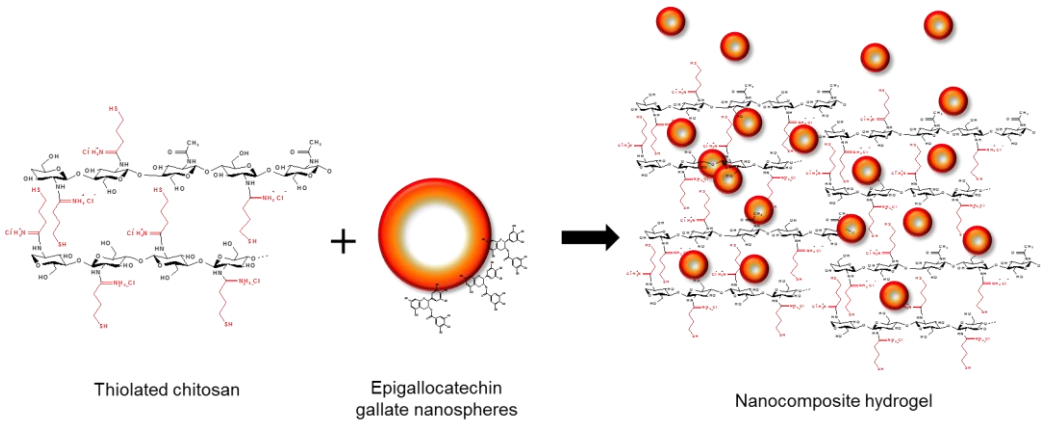

This section is based on the following publication:

Petkova P, Francesko A, Tzanov T., Enzyme-assisted formation of hybrid biopolymer hydrogels incorporating active phenolic nanospheres., *Engineering in Life Sciences*, 2015, 15 (4), pp 416–424

5.4.1 Introduction

This study reports on the synthesis of hybrid nanocomposite hydrogels comprising a thiolated chitosan (TC) platform that incorporates epigallocatechin nanospheres (EGCG NSs) as active polyphenolic agents for wound healing applications. The phenolic nanospheres (NSs) were prepared using an industry-attractive, low-cost and fast sonochemical technology, whereas the gel formation was achieved via a green approach involving the enzymatic cross-linking with horse-radish peroxidase (HRP), avoiding the use of chemical cross-linkers. In the hybrid material, the EGCG NSs will integrate the structural role to reinforce the hydrogel network with the healing function in chronic wound therapy.

The chronic wound environment is normally colonized with bacteria,[346] and characterized with high concentrations of reactive oxygen species (ROS) and elevated levels of (myeloperoxidase) MPO and collagenases, that altogether impair the normal wound healing process. Thus, the NSs functional properties will be evaluated for their potential to inhibit the chronic wound enzyme (MPO and collagenase) activities and their antibacterial and antioxidant properties prior to their loading into the TC matrix. The NSs release profile from the hybrid hydrogel material and the cytotoxicity of the system to human foreskin fibroblasts will be also assessed.

5.4.2 Nanospheres preparation and characterization

Some of the most common techniques used to prepare biodegradable NPs (nanospheres and nanocapsules) however the selection of an appropriate route depends on different factors including the particle size, their thermal, chemical and physiological stability, and the requirement of an organic solvent and surfactants in the reaction, both being associated with the biocompatibility of the final product. The EGCG NSs were prepared by ultrasound technology as this is surfactant free method for designing of nano/micro-scale materials due to the rapid reaction rates, relatively uniform size distribution and high purity of the obtained particles.[347] Moreover, the sonochemistry has been successfully applied for formation of various polymeric micro- and nano-spheres without compromising the intrinsic functional properties.[340] These structures may serve as bioactive compound itself or can encapsulate various drugs.

The cumulant (Z-average) hydrodynamic size of the sonochemically generated EGCG NSs (Scheme 5.2) was measured by DLS and was found to be 270±21 nm (Figure 5.22A). The results showed that the obtained NSs suspension is monomodal (only one peak), spherical (Figure 5.22B) and with PDI of 0.044±0.007 considered monodisperse (PDI < 0.1).[348]

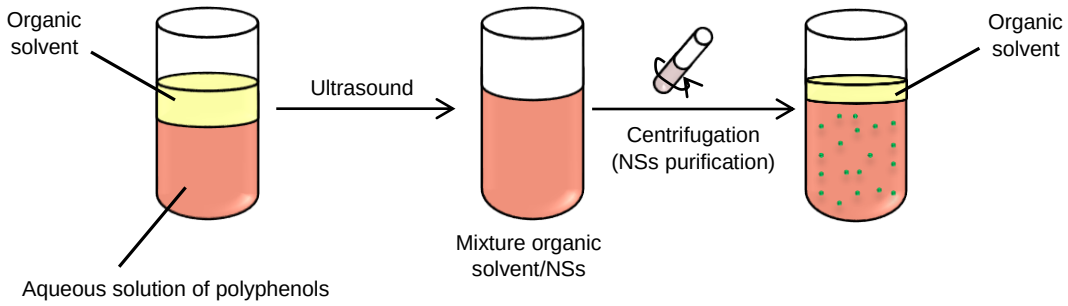

Scheme 5.2 Sonochemical synthesis of EGCG NSs preparation and their purification.

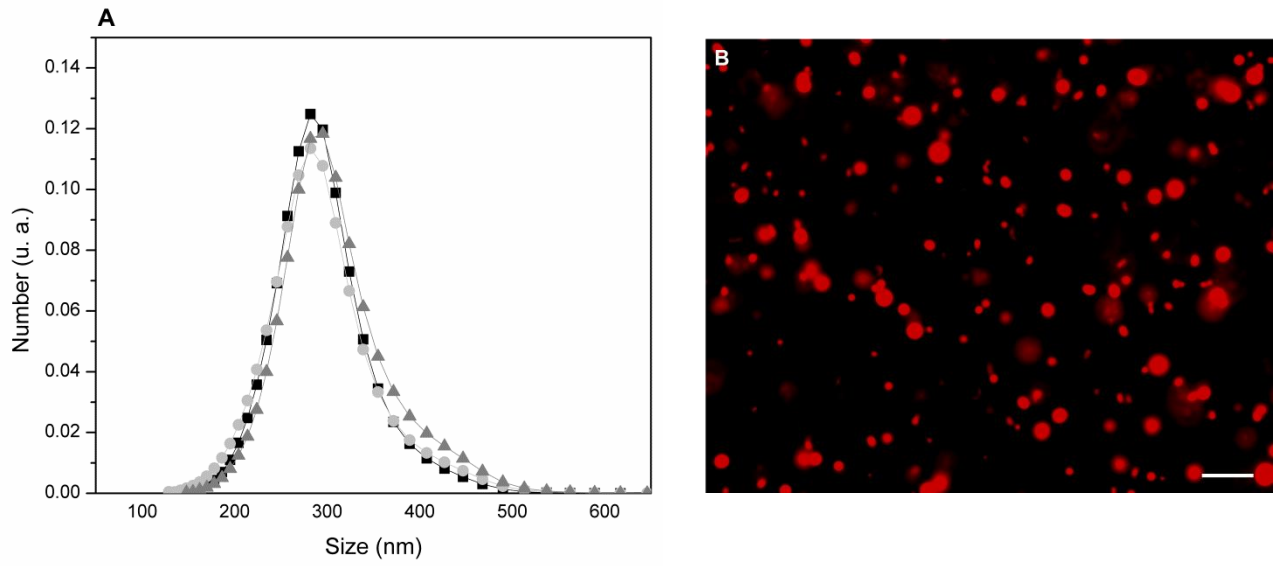

Figure 5.22 Data of EGCG NSs hydrodynamic radius (at 25 ° C) (n=3) (A), and fluorescence microscopy image of the spheres filled with Nile red (B). Scale bar 2 µm.

The obtained phenolic NSs were further studied for their suitability for application as active compounds for chronic wounds management. To this end, their antibacterial properties, antioxidant capacity and ability to inhibit MPO and collagenase enzymes were evaluated prior to the inclusion into biopolymer hydrogels.

5.4.3 Inhibition of chronic wound enzymes

The capacity of the NSs and the EGCG in solution to inhibit MPO (the anti-inflammatory potential) and collagenase (the antiprotease capacity) activities was studied. The EGCG NSs showed higher anti-inflammatory activities in comparison with the EGCG in solution (Figure 5.23A). As expected, more diluted EGCG solutions/NSs suspensions displayed lower inhibition capacities compared to more concentrated ones. Nevertheless, the NSs in the lowest concentration tested (0.001 mM) still inhibited nearly 50 % of the MPO activity, whereas at the same concentration the EGCG solution did not inhibit the enzyme. The same tendency was observed in the study evaluating the ability of EGCG NSs and solution to inhibit collagenase. In all tested concentrations the NSs showed better properties compared to the EGCG solution (Figure 5.23B). The highest concentration of polyphenolic NSs (0.5

mM) displayed close to 100 % inhibition. The higher enzyme inhibition capacity of the EGCG NSs compared with the one of the EGCG in free form could be explained by occluding the enzyme active site substrate entrance by the NSs.[349] Additionally, the high surface to volume ratio, i.e. large surface area of the NSs allows a better contact of the structures with the enzyme active site.[350] Comparing between the two enzymes, the inhibition of collagenase activity required higher concentrations (or less dilution) of both EGCG NSs and free solution by nearly 70 fold (the IC_{50} values for MPO and collagenase were 0.001 mM and 0.07 mM, respectively), already noticed in our previous work.[246]

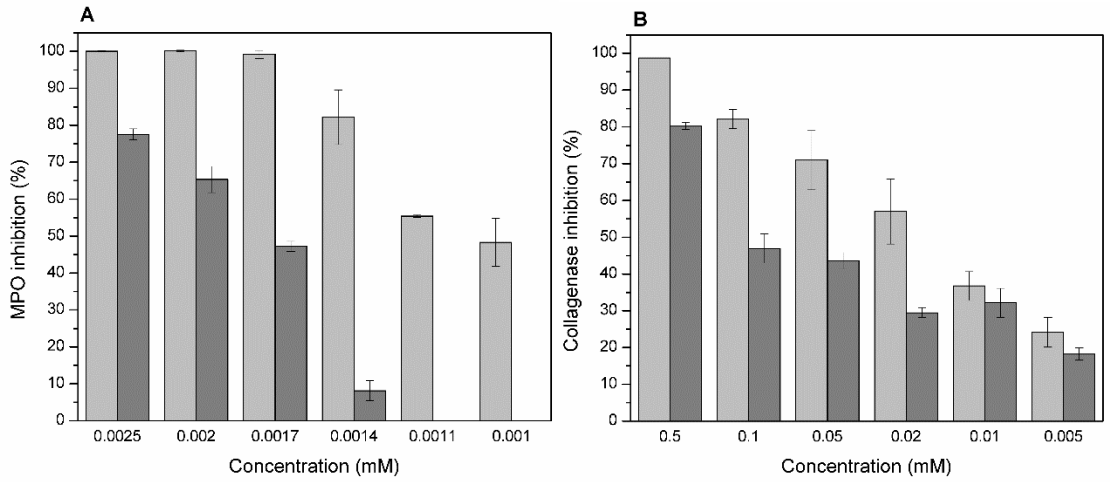

Figure 5.23 Functional properties of EGCG NSs (light grey bars) and free solution (dark grey bars). Inhibition of the activity of MPO (A) and collagenase (B). All results are reported as mean values ± standard deviation (n=3).

The activity of proteases in normal wounds is tightly regulated at the cellular level by the controlled expression of protease inhibitors. A failure at any level of this control mechanism would result in an increase in proteolytic activity, a trait of chronic wounds. The acute and chronic wound fluids biochemical and molecular profiles are different, where chronic wounds contain high levels of MPO, and proteolytic matrix metalloproteinases (MMPs), with the most abundant being collagenases. In the persistent inflammatory environment the MPO-generated hypochlorous acid (HOCl) oxidizes most biological molecules, adversely affecting the tissue regeneration. In addition, HOCl also triggers the MMPs activation[351] to further contribute the tissue deterioration. Therefore, the chronic wounds treatment should include

control over MPO and MMPs activities (total inhibition is not required), in order to provide favorable for the healing and extracellular matrix reconstruction conditions.

The current therapies aiming to modulate the activity of major chronic wound enzymes involve the application of anti-inflammatory agents as persistent inflammation is often a key to impaired wound healing. Alkaloids,[352] plants polyphenol extracts,[353] synthetic polymers with hydroactive properties,[354] oleic acid[355] and peptides[356] are therapeutic agents that through different mechanisms stimulate healing of chronic wounds. In the most recent attempts, chitosan and collagen based dressings were previously upgraded with bioactive phenolic compounds to simultaneously control MPO and collagenase activities *in vitro.*[246,278]

5.4.4 Radical scavenging activity

The DPPH assay was used to study the antioxidant capacity of EGCG NSs and EGCG in solution. In contrast to the inhibition of enzymes, no differences in the radical scavenging activities between NSs and free solution were observed (Figure 5.24). The antioxidant properties of phenols are linked with their chemical structure as their efficiency increases with increasing the number of OH groups. In the case of nano-scaled materials radical scavenging activity depends on a surface reaction since only the surface comes in contact with the free radicals.[357] Thus, our results suggest that the amount of phenolic groups is similar in the NSs and free solution, meaning that these are not involved in the sonochemical stabilization of the nanospheres. The latter was confirmed by evaluating the total phenol content, which was 0.176 ± 0.006 and 0.173 ± 0.004 mM GAE, respectively for the EGCG NSs and free solution. In addition, the surface contact with the functional groups is probably not crucial in the case of DPPH scavenging, as in the case of the enzyme inhibition.

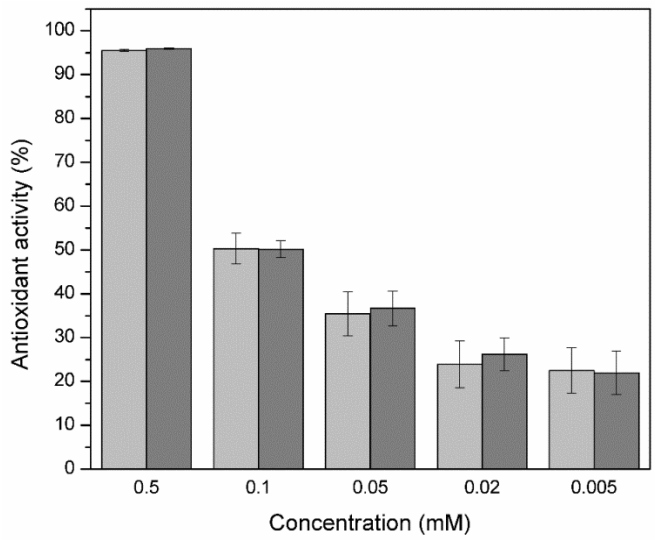

Figure 5.24 The antioxidant activity of EGCG NSs (light grey bars) and free solution (dark grey bars). All results are reported as mean values ± standard deviation (n=3).

5.4.5 Antibacterial activity

The loss of skin integrity and the exposure of the cutaneous tissue in chronic wounds provide a favorable environment for bacteria to colonize and proliferate. The antimicrobial activity of the NSs suspension/solution was therefore evaluated against the Gram-positive *S. aureus* - being one of the most commonly found pathogen in chronic wounds associated with changes to wound healing times.[358]

The results demonstrated that the EGCG NSs have better antibacterial performance than free solution, for all tested dilutions (Figure 5.25). Whereas the highest concentrations of NSs and free solution showed comparable antibacterial properties, their dilution led to different behavior in terms of inhibition of the *S. aureus* growth. The NSs displayed no changes in their performance down to 0.1 mM, whereas the EGCG solution did not show any antibacterial capacity at this concentration. The better antibacterial performance of the EGCG NSs could be attributed to the improved biophysical interactions between the NSs and bacteria including the NSs biosorption and bacterial uptake.[359] It has been also reported that the size and shape of the NPs could affect their antibacterial performance, usually following the rule that smaller structures of spherical shape are better antibacterials than bigger NPs with elongated shapes.[350] The small size of the NPs and the high surface to volume ratio aid to their interaction with the bacteria and the enhanced antimicrobial potential.

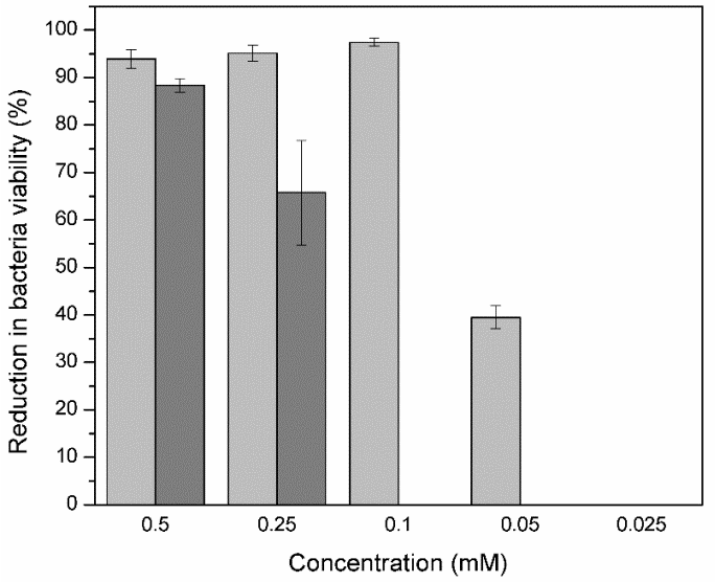

Figure 5.25 The antibacterial activity of EGCG NSs (light grey bars) and free solution (dark grey bars) towards Staphylococcus aureus. All results are reported as mean values ± standard deviation (n=3).

5.4.6 Enzyme-assisted hydrogel formation

The hydrogel preparation was achieved via HRP-mediated coupling reaction of thiol groups in TC (serving as a nucleophile) in presence and absence of phenolic NSs (Scheme 5.3). The ability to control the gelation time by varying the concentration of H_2O_2 used in the reaction was demonstrated regardless of the EGCG NSs presence (Figure 5.26). As expected, the gelation times decrease from 660 to 46 sec and 420 to 23 sec in presence and absence of NSs respectively, as the H_2O_2 concentrations increase from 0.05 wt % to 1.0 wt %. After the addition of HRP and H_2O_2, the thiols are susceptible to oxidization and are coupled to each other to give disulfide (-S-S-) bonds. The system consists of two interdependent reactions: the HRP/H_2O_2 mediated oxidation of thiols to thiyl radicals and later non-enzymatic transformation of these radicals to disulfides.[360]

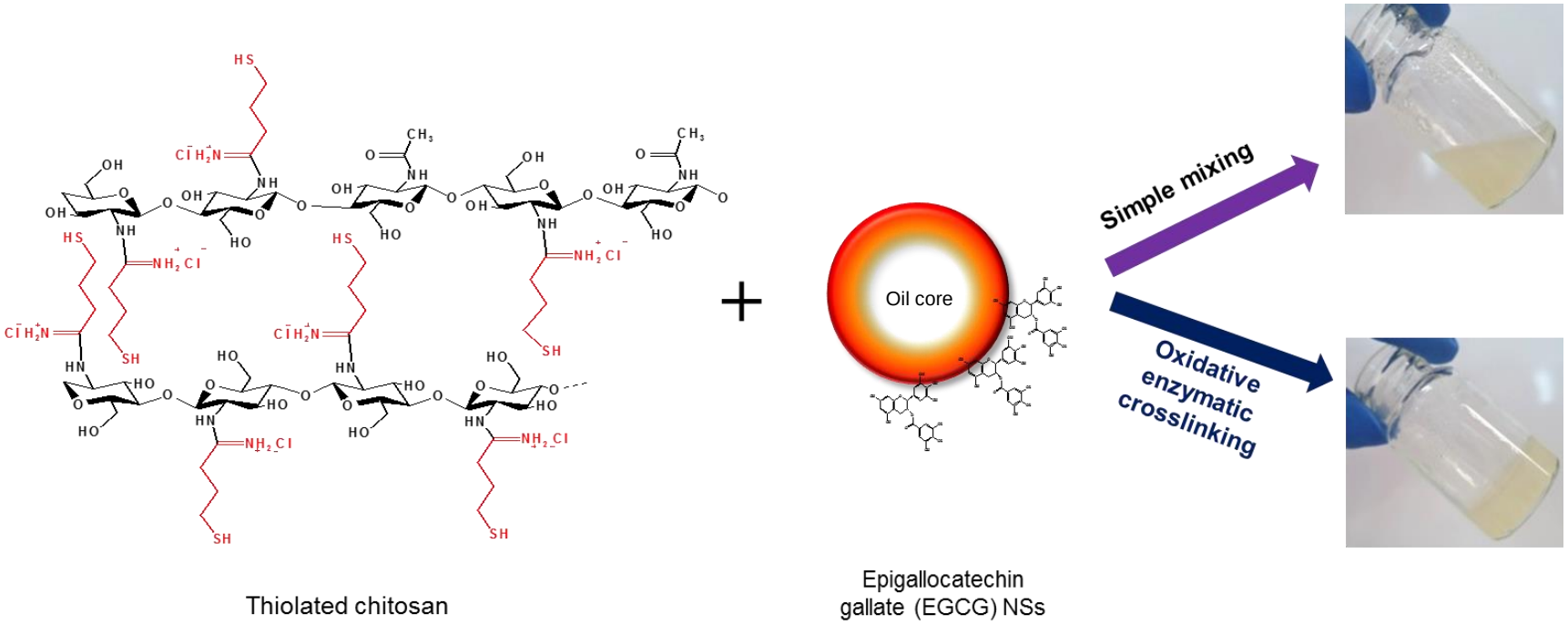

Scheme 5.3 EGCG NSs loading into TC hydrogels.

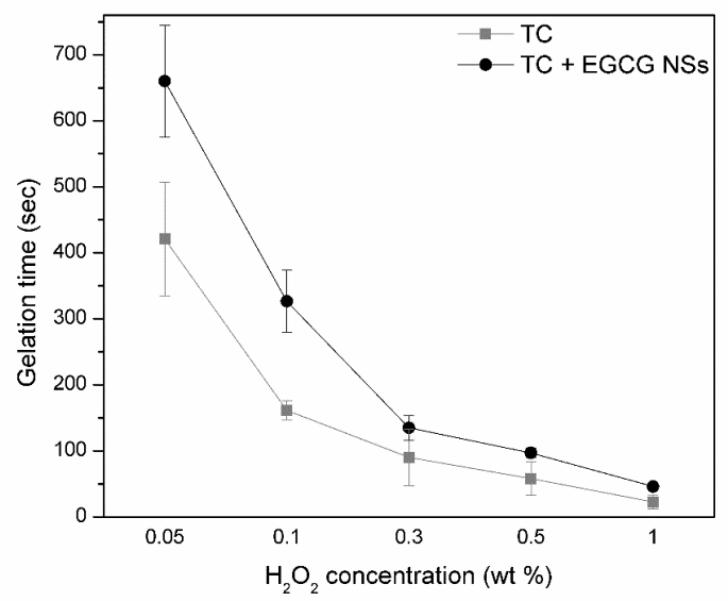

Figure 5.26 In situ gel formation of TC/EGCG hydrogels in the presence of HRP (9.65 U/mL) and different concentrations of H_2O_2. Data of the mean time of gelation ± standard deviation (n=3) are reported.

To study the behavior of the thiolated chitosan hydrogels when placed in aqueous environment, their swelling and degradation properties prior the NSs inclusion were evaluated. The swelling capacity of the TC hydrogels revealed that half of the total water uptake was absorbed within the first hour (34 %), while the swelling progressively continued reaching 66 % after 24 h, and then increased slowly to its maximum of 74 % at day 3 (Figure 5.27A). The results for hydrogel degradation indicated that after 3 weeks the hydrogels only lost ~25 % of their initial weight (Figure 5.27B). The weight loss was more pronounced during the first week as the weight of the samples decreased by 15 %, suggesting that during this period the non-cross linked polymer is released into the aqueous medium. When a hydrogel material is placed in an aqueous solution, water molecules penetrate into the polymer network. The water molecules are expected to occupy the free space in the network meshes, which will start to expand, allowing other water molecules to enter. The most important parameters influencing the biopolymer constructs swelling and stability are the hydrophilicity of its constituents and the extent of cross-linking in the matrix.

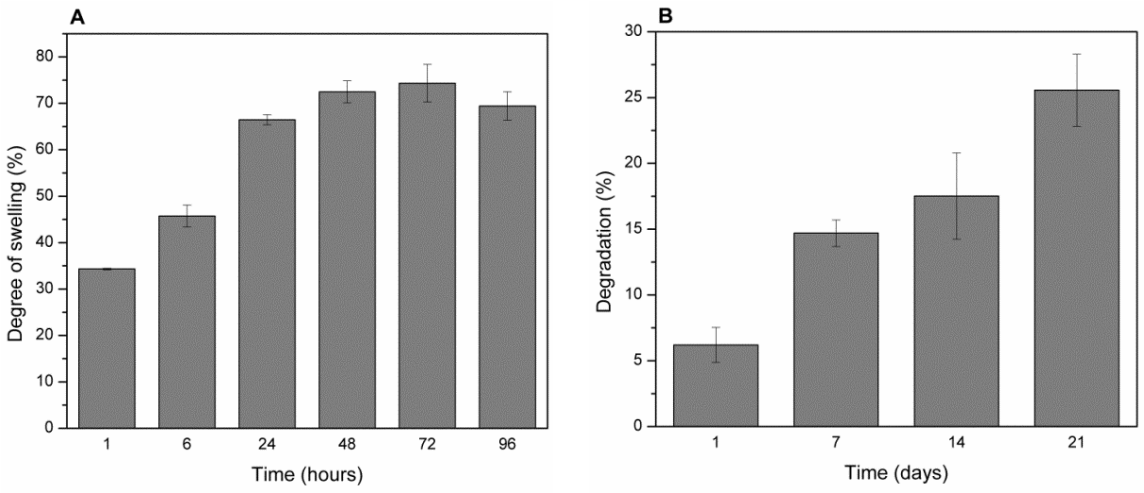

Figure 5.27 TC hydrogels swelling ratio (A) and degradation (B). The results show the mean hydrogel swelling and degradation of each experimental group ± standard deviation (n=6 for each time point).

The oxidative enzymes, such as the HRP, can also convert phenol groups in the EGCG to reactive quinones, which subsequently undergo non-enzymatic reactions with a variety of nucleophiles including the available free thiols and/or amino groups. It is generally accepted that the phenolic compounds are promoters of the peroxidase-catalyzed thiol oxidation by reducing the rate-limiting HRP intermediate and/or by oxidation of thiols by free radicals of phenols.[360,361] It was therefore expected that in presence of phenolic NSs, the enzyme-mediated gelation will be faster in comparison with the control (absence of phenolic NSs). Instead, the time of gelation increased with the nanospheres inclusion (Figure 5.26). The conventional peroxidase cycle involves reaction with H_2O_2, which is reduced to water while phenols are oxidized to phenoxy radicals that dimerize. On the other hand, when the thiols are oxidized by peroxidases (reactions characterized with the oxygen consumption) the process is yielding H_2O_2. The higher the concentration of H_2O_2 is, the more decomposition of H_2O_2 and more thiyl radicals are produced. The additional production of the oxidizing agent (H_2O_2) during the -S-S- bonds formation could be the reason why the gelation time in absence of phenols (which will reduce the H_2O_2 concentration) is faster.[360] Similarly to the findings reported by Sakai et al. (2014), namely decreased gelation time with decreasing of phenol groups content of chitosan/phenol system, was observed in our case by addition of the phenol NSs formulations of lower concentrations (Table 5.5).[362]

Table 5.5 Hydrogels time of gelation at room temperature using horseradish peroxidase (9.65 U/mL) and different concentrations of hydrogen peroxide and EGCG NSs:TC ratios.

EGCG NSs:TC ratio (v/v)	H_2O_2 concentration (%)	Time of gelation (sec)
1/99	0.3	83
10/90	0.3	150
1/99	0.5	60
10/90	0.5	90

5.4.7 Hydrogel morphology

The SEM of the inner section of the hydrogels loaded with the EGCG NSs confirmed the spheres incorporation into the material. The NSs were also intact after their incorporation into the gel matrix (Figure 5.28). The presence of a few bigger than 1 µm NSs is probably due to the nanospheres aggregation (Figure 5.28B, inset image).

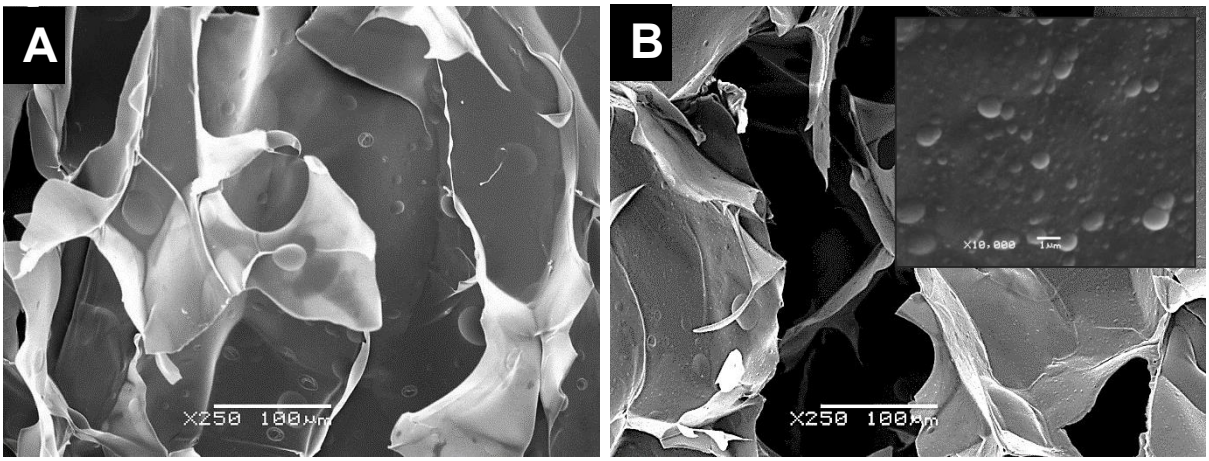

Figure 5.28 Hydrogels morphology (A) TC and (B) TC hydrogels loaded with EGCG NSs.

5.4.8 *In vitro* release study

After being loaded into the TC hydrogels, the EGCG NSs release profile from the biopolymer matrices was studied. The results (obtained after measuring the turbidity of the incubation solution) showed a potential of the obtained hydrogels for the sustained delivery of the intact

EGCG NSs. Nearly 50 % of the incorporated EGCG NSs were released during the course of 6 days in close to linear regime (Figure 5.29). The evaluation period of 6 days was chosen as a maximum and desirable period for the wound dressing change. Beyond this time the cells at the wound bed strongly adhere and proliferate within the material, which would impede the dressing removal.[363] On the other hand, the lower frequency of dressing change is costly while the strategy to maintain the environment moist in order to facilitate the wound-healing process through prevention of tissue dehydration and cell death is compromised. Moreover, the extent of the enzyme inhibition could be easily controlled by applying the hydrogel dressing on the wound site for different time periods.

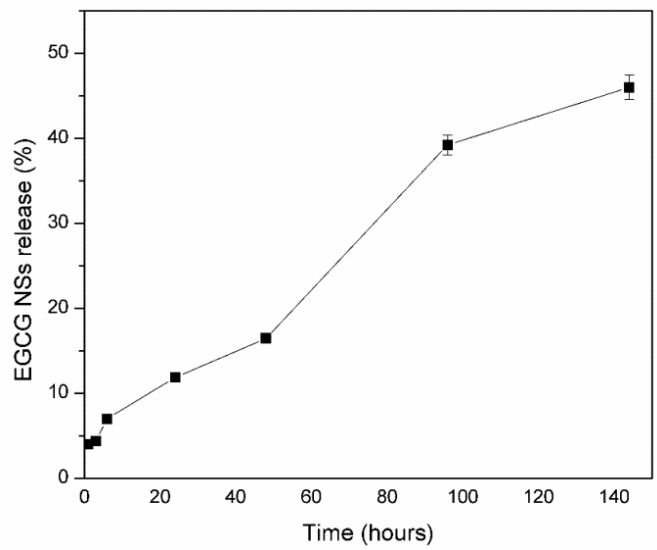

Figure 5.29 Time-dependent release of EGCG NSs from TC hydrogels. Three samples were evaluated for each time point and data are reported as mean EGCG NSs release (%) ± standard deviation.

5.4.9 Cytotoxicity

There is a notable rise in the number of publications discussing the toxicity of nanomaterials, based on their size, safe dose administration, and material constituents. Hence, the evaluation of their biocompatibility properties is highly recommendable, especially when such materials are aimed for medical applications. Thus, the toxicity of TC, EGCG NSs and their mixture to human foreskin fibroblasts cell line was assessed. All materials displayed good biocompatibility (above 90 % compared with the control), indicating that the application of the generated hydrogels as drug delivery devices would be safe (Figure 5.30).

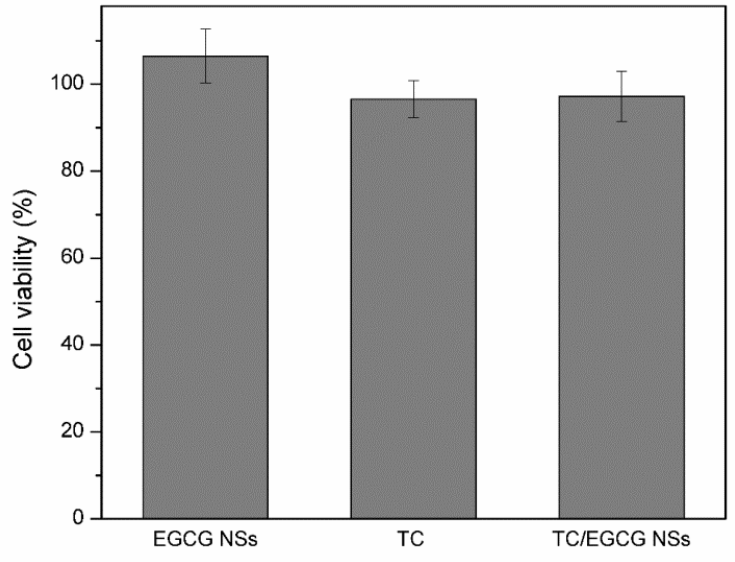

Figure 5.30 Cytotoxicity of EGCG NSs, TC and their mixture to human cell fibroblasts. The results show the mean cytotoxicity values of 3 independent assays ± standard deviation (n=6).

CS is a nontoxic polymer and widely applied as a drug delivery material. In addition, EGCG has been reported to have high antitumor activity,[364] and also ability to protected human normal bronchial epithelial BEAS-2B cells from Cr(VI)-induced cell death and apoptosis.[365] However, it was also reported that low concentrations of EGCG have inhibited the DNA damage induced by reactive oxygen and nitrogen species, while higher concentrations of the compound may itself result in damage to cellular DNA.[366] The EGCG conjugation with other materials (as in our case) is also a way to reduce its harmful effect.[367]

5.4.10 Conclusions

EGCG nanospheres were successfully generated via a one-step sonochemical process and further incorporated into the TC hydrogel platforms prepared by enzyme-mediated gelation without compromising the particles integrity. By optimizing the H_2O_2 concentration, the enzymatic gelation can be controlled to occur within less than 1 min. The potential of the phenolic NSs as chronic wound healing promoters was demonstrated via the improved antibacterial and chronicity factors inhibition compared to the EGCG in solution. Moreover, the intact EGCG NSs were released from the highly biocompatible hybrid hydrogel in a sustained manner over 6 days, suggesting potential for prolonged usage and low frequency of dressing change for wound healing applications.

6 Final conclusions

A range of multifunctional nano-structured materials aiming at controlling the bacterial transmission and thus, prevent the spread of infection diseases were develop during the realization of this thesis. Different environment friendly strategies based on sonochemical or enzymatic techniques (avoiding the use of solvents and harsh chemicals), were adopted for the development of these materials. The designed nanocomposites share a common feature, namely high antibacterial performance against hospital relevant bacteria species. It was also demonstrated that the use of intrinsically antimicrobial polymers improves the nanocomposites durability at use, enhances their antibacterial performance and improves their biocompatibility.

This thesis developed a platform of antibacterial materials and surfaces comprising:

Antibacterial medical textiles via one-step sonochemical process:

Simultaneous sonochemical coating of cotton with antibacterial zinc oxide/chitosan hybrid nanoparticles

- The presence of chitosan in the hybrid biopolymer-metal oxide nanoparticles coatings generated on cotton fabrics improves the textiles antibacterial properties, durability of the antibacterial effect to washing, and biocompatibility (in comparison to zinc oxide nanoparticles coatings alone).
- The synergistic effect of both chitosan and zinc oxide nanoparticles allowed for a high antibacterial performance of the hybrid coatings at minimum metal concentration.

Simultaneous sono-enzymatic coating of cotton with antibacterial zinc oxide nanoparticles

- Ultrasound-boosted enzymatic coating of cotton with zinc oxide nanoparticles improved the coating stability to washing and thus, ensure the fabric antibacterial properties.

Hybrid biopolymer-metal based nanoparticles and nanocomposites for water disinfection:

- Permanent modification of the cork matrices is achieved via enzymatically grafting of amino-functionalized biopolymers (chitosan or aminocellulose) doped silver nanoparticles.
- The biopolymers contributed to the antibacterial properties of the silver nanoparticles.
- The antibacterial hybrid nanoparticles-cork composite demonstrated long-term stability and durability of the antimicrobial effect in conditions of continuous water flow.

Hybrid nanocomposite hydrogels comprising of thiolated chitosan and epigallocatechin gallate nanospheres for wound healing applications.

- Green approach involving the enzymatic cross-linking with horseradish peroxidase is accomplished for the formation biocompatible nanocomposite hydrogel.
- The time of enzymatic gelation process is controllable through variation in the reagents' concentrations.
- Sustained delivery of intact phenolic nanospheres from the polymeric matrix is achieved.
- The developed material showed potential to provide free of bacteria environment at the wound site while exhibiting control over the chronic wound enzymes activities.

7 Future perspectives

Imparting antibacterial properties to the materials and surfaces is a key for achieving of bacteria-free environment in health care facilities and public areas. The results of this thesis have demonstrated that a wide variety of surface nanostructured 2D and 3D polymer-based materials for medical and industrial applications can be developed by applying an innovative combination of versatile sonochemical and enzymatic nano-coating technologies.

The development of the antibacterial medical textiles (sections 5.1 and 5.2) was carried out under the scope of the large scale European project SONO - A pilot line of antibacterial and antifungal medical textiles based on a sonochemical process, FP7-228730, which was acknowledged as a “Success Story” by the European Commission. Within this project a pilot line for the production of medical antibacterial textiles based on the scale-up of the sonochemical coating process was developed. The antibacterial efficiency of the produced textiles, e.g. hospital sheets, medical coats and bandages was proven in a clinical trial carried out in the Multi-profile Hospital for Active Medical Treatment and Emergency Medicine "N.I.Pirogov" in Sofia, Bulgaria. In a further step, the sonochemical pilot will be brought to a pre-commercial level and demonstrated in relevant industrial environment for coating of antibacterial substrates such as medical textiles, upholstery, and water/air membranes among others.

The disinfection efficacy of the developed at biopolymer/silver nanoparticles cork composites (section 5.3) will be evaluated at the level of a point-of-use water filtration device (water volume up to 2 L/day) prior constructing of larger disinfection installations e.g. point-of-entry systems (disinfection capacity of 100 - 150 L water per day). In addition, the hybrid biopolymer/silver nanoparticles cork material can be used as disinfection element in already existing water purification systems as it is facile to manipulate.

The efficiency of developed nanocomposite hydrogels (section 5.4) will be further tested *ex vivo* with real wound exudates and biofilms, prior to *in vivo* evaluation. In the production of nano-functionalized materials, nanotoxicology studies will ensure the safety of the workers, end users and the environment.

A large number of applications can be foreseen based on the outcomes and the knowledge derived from this thesis. A variety of nano-sized actives can be generated via ultrasound irradiation e.g. nano-antibiotics, enzyme nano-particles, and hybrid nano-antibiotics, among others, and further incorporated, by employing different biotechnological approaches in polymer matrices to obtain antibacterial and antibiofilm materials.

Acknowledgements

At the end of my thesis I would like to thank all people who made this thesis possible and an unforgettable experience for me.
First, I would like to sincere gratitude my supervisor Dr. Tzanko Tzanov for his patient guidance, encouragement and useful critiques during my research. I know there is a lot more to learn. Thanks for giving me the opportunity to participate in European projects and international congresses, to gain experience and know people from all parts of the world.

My sincere thanks also goes to Dr. Antonio Francesko who was helping me with his advices and knowledge during my studies and I would say was sharing (more than anyone else) with me my "scientific ups and downs" almost to the end of my PhD. Хвала пуно, Тони!

I acknowledge my gratitude to prof. Aharon Gedanken (Bar-Ilan University) and prof. Georg Gubitz (University of Natural Resources and Life Sciences) and the members of their groups (Betina, Anjani, Gregor, Kartin and Katrin, Barbara, the "container team" (Ale, Dani, Sara and Martin)) and all the rest gorgeous people I met in Tel-Aviv and Vienna for helping me to spent unforgivable time during my stay there. Special thanks to Dr. Ilana Perelshtein for her advices and cooperation whenever I needed during my PhD. I cannot miss to say thanks to Dr. Jamie Beddow (Coventry University) who introduce me to the field of microbiology.

Thanks to all my colleagues Carlos, Guillem, Margarida, Sonia, Kamelia, Teresa, Rosa, Elisabetta, Eva, Ivaylo, Silvia, Diana and Javi for the nice moments we shared the last years, without you and your support and help this journey won't be the same. Specially *Moltes, moltes gràcies* to Carlos and Eva per seva ajuda! You were always willing to help me in the lab and especially in arranging, translating and fixing the documents (in catalan and castellano) knowing better than me all the administrative steps I needed to do.
Thanks and to Krisi (I will not forget you) for being my friend (before all) and colleague. I still remember when we met (and Stanimir next to you) ….almost 11 years ago in this big auditorium and „Ти коя група си? ☺".
Криси и Мири, винаги е хубаво когато имаш някой от „вкъщи" когато си в чужбина, а когато този някой са някои и са твои приятели прави всичко много по-леко. Благодаря ви за подкрепата, вечерите, разходките, „обикалянето по магазините", приятелството (мога да изреждам още много). Без вас нищо не би било същото!

I would like to thank and to other part of our group members Dong, Lupita, Merce, Sundar,

and Miguel, supervised by Prof. Pere Garriga. I spent countless hours doing antimicrobial experiments in “your lab”. You tuned easily from my colleagues to my friends, sharing nice moments and talks which made me more familiar with your countries and cultures.

Thanks and to all my friends outside the laboratory and those I met in GAIA. Lina, Ricard, Ignacio and Giulio I will always remember our first dinner when you read a book in Catalan and spoke for some diodes (anyway I still do not like the physics). Shubham, thank you for being here after all the rest have left (good you got your grant after me). Kostas, it is always nice to have coffee and croissant with you. Alessandra, Alexia and Weiyi you were one of the best flat-mates/friends I could wish for.

Finally, I would like to thank to my family. My parents and sister, you are always there for me. Не бих могла да си пожелая по-прекрасни родители и сестра. Винаги сте ме подкрепяли безусловно във всяко мое начинание и това, което научих през годините е, че винаги, винаги трябва да се вслушвам в съветите, които ми давате. Мамо и тате, ние (аз и кака) сме това, което сме благодарение на вас и на всичко, което сте направили за нас, за да ни осигурите най-доброто каквото и да ви е струвало. Благодаря ви!

Bibliography:

(1) World Health Organization. Antimicrobial resistance http://www.who.int/mediacentre/factsheets/fs194/en/.

(2) Poehlsgaard Jacob; Douthwaite Stephen. *Nat. Rev. Microbiol.* **2005**, *3*, 870–881.

(3) Gale, E. F.; Folkes, J. P. *Biochem. J.* **1953**, *53*, 493–498.

(4) Wiedemann, I.; Breukink, E.; van Kraaij, C.; Kuipers, O. P.; Bierbaum, G.; de Kruijff, B.; Sahl, H. G. *J. Biol. Chem.* **2001**, *276*, 1772–9.

(5) Higgins, D. L.; Chang, R.; Debabov, D. V; Leung, J.; Wu, T.; Krause, K. M.; Sandvik, E.; Hubbard, J. M.; Kaniga, K.; Schmidt, D. E.; Gao, Q.; Cass, R. T.; Karr, D. E.; Benton, B. M.; Humphrey, P. P. *Antimicrob. Agents Chemother.* **2005**, *49*, 1127–34.

(6) Andersen, J. L.; He, G.-X.; Kakarla, P.; K C, R.; Kumar, S.; Lakra, W. S.; Mukherjee, M. M.; Ranaweera, I.; Shrestha, U.; Tran, T.; Varela, M. F. *Int. J. Environ. Res. Public Health* **2015**, *12*, 1487–547.

(7) Arias, C. A.; Murray, B. E. *Nat Rev Micro* **2012**, *10*, 266–278.

(8) Hidron, A. I.; Edwards, J. R.; Patel, J.; Horan, T. C.; Sievert, D. M.; Pollock, D. A.; Fridkin, S. K. *Infect. Control Hosp. Epidemiol.* **2008**, *29*, 996–1011.

(9) Hollenbeck, B. L.; Rice, L. B. *Virulence* **2012**, *3*, 421–569.

(10) McManus, M. C. *Am. J. Heal. Pharm.* **1997**, *54* , 1420–1433.

(11) World Health Organization. *Antimicrobial resistance: global report on surveillance*; 2014.

(12) World Health Organization. *Prevention of hospital-acquired infections*; 2002.

(13) Klevens, R. M.; Edwards, J. R.; Richards, C. L.; Horan, T. C.; Gaynes, R. P.; Pollock, D. A.; Cardo, D. M. *Public Health Rep.* **2007**, *122*, 160–166.

(14) Hughes, J. M. *Chemotherapy* **1988**, *34*, 553–561.

(15) No Title http://www.cdc.gov/nhsn/index.html.

(16) Visai, L.; De Nardo, L.; Punta, C.; Melone, L.; Cigada, A.; Imbriani, M.; Arciola, C. R. *Int. J. Artif. Organs* **2011**, *34*, 929–946.

(17) Visai, L.; de Nardo, L.; Punta, C.; Melone, L.; Cigada, A.; Imbriani, M.; Arciola, C. R. Titanium oxide antibacterial surfaces in biomedical devices. *International Journal of Artificial Organs*, 2011, *34*, 929–946.

(18) Gallo, J.; Holinka, M.; Moucha, C. S. *Int. J. Mol. Sci.* **2014**, *15*, 13849–13880.

(19) Zhao, L.; Seth, A.; Wibowo, N.; Zhao, C.-X.; Mitter, N.; Yu, C.; Middelberg, A. P. J. *Vaccine* **2014**, *32*, 327–37.

(20) Petros, R. A.; DeSimone, J. M. *Nat Rev Drug Discov* **2010**, *9*, 615–627.

(21) Arico, A. S.; Bruce, P.; Scrosati, B.; Tarascon, J.-M.; van Schalkwijk, W. *Nat Mater* **2005**, *4*, 366–377.

(22) Sobolev, K.; Flores, I.; Torres-Martinez, L. M.; Valdez, P. L.; Zarazua, E.; Cuellar, E. L. Bittnar, Z.; Bartos, P. J. M.; Němeček, J.; Šmilauer, V.; Zeman, J., Eds.; Springer Berlin Heidelberg: Berlin, Heidelberg, 2009; pp. 139–148.

(23) Daniel, M.-C.; Astruc, D. *Chem. Rev.* **2004**, *104*, 293–346.

(24) Salata, O. V. *J. Nanobiotechnology* **2004**, *2*, 1–6.

(25) Giljohann, D. A.; Seferos, D. S.; Daniel, W. L.; Massich, M. D.; Patel, P. C.; Mirkin, C. A. *Angew. Chemie Int. Ed.* **2010**, *49*, 3280–3294.

(26) Ediriwickrema, A.; Zhou, J.; Deng, Y.; Saltzman, W. M. *Biomaterials* **2014**, *35*, 9343–54.

(27) Kumari, A.; Yadav, S. C. S. K.; Yadav, S. C. S. K. *Colloids Surf. B. Biointerfaces* **2010**, *75*, 1–18.

(28) Lee, I. S.; Lee, N.; Park, J.; Kim, B. H.; Yi, Y.-W.; Kim, T.; Kim, T. K.; Lee, I. H.; Paik, S. R.; Hyeon, T. *J. Am. Chem. Soc.* **2006**, *128*, 10658–10659.

(29) Sekhon, B. S. *Nanotechnol. Sci. Appl.* **2014**, *7*, 31–53.

(30) Abramov, O. V; Gedanken, A.; Koltypin, Y.; Perkas, N.; Perelshtein, I.; Joyce, E.; Mason, T. J. *Surf. Coatings Technol.* **2009**, *204*, 718–722.

(31) Bangal, M.; Ashtaputre, S.; Marathe, S.; Ethiraj, A.; Hebalkar, N.; Gosavi, S. W.; Urban, J.; Kulkarni, S. K. *Hyperfine Interact.* **2005**, *160*, 81–94.

(32) Pelgrift, R. Y.; Friedman, A. J. *Adv. Drug Deliv. Rev.* **2013**, *65*, 1803–1815.

(33) Hajipour, M. J.; Fromm, K. M.; Akbar Ashkarran, A.; Jimenez de Aberasturi, D.; Larramendi, I. R. de; Rojo, T.; Serpooshan, V.; Parak, W. J.; Mahmoudi, M. *Trends Biotechnol.* **2012**, *30*, 499–511.

(34) Rao, J. P.; Geckeler, K. E. *Prog. Polym. Sci.* **2011**, *36*, 887–913.

(35) Pinto Reis, C.; Neufeld, R. J.; Ribeiro, A. J.; Veiga, F. *Nanomedicine* **2006**, *2*, 8–21.

(36) Shimanovich, U.; Bernardes, G. J. L.; Knowles, T. P. J.; Cavaco-Paulo, A. *Chem. Soc. Rev.* **2014**, *43*, 1361–1371.

(37) Suslick, K. S.; Price, G. J. *Annu. Rev. Mater. Sci.* **1999**, *29*, 295–326.

(38) Suslick, K. S.; Hammerton, D. A.; Cline, R. E. *J. Am. Chem. Soc.* **1986**, *108*, 5641–5642.

(39) Suslick, K. S. *Sci.* **1990**, *247* , 1439–1445.

(40) Leong, T.; Ashokkumar, Muthupandian Kentish, S. *Acoust. Aust.* **2011**, *39*, 54–63.

(41) BTO SAS - ULTRATECNO France. Les ultrasons, qu'est ce que c'est? http://www.ultratecno.fr/les-ultrasons/.

(42) Suslick, Kenneth S., Choe, Seok-Burm, Cichowlas, Andrzej A., Grinstaff, M. W. *Nature* **1991**, *353*, 414–416.

(43) Xu, H.; Zeiger, B. W.; Suslick, K. S. *Chem. Soc. Rev.* **2013**, *42*, 2555–2567.

(44) Hazra, C.; Bari, S.; Kundu, D.; Chaudhari, A.; Mishra, S.; Chatterjee, A. *Ultrason. Sonochem.* **2014**, *21*, 1117–31.

(45) Lorimer, J. P.; Mason, T. J. *Chem. Soc. Rev.* **1987**, *16*, 239–274.

(46) Safari, J.; Banitaba, S. H.; Khalili, S. D. *Ultrason. Sonochem.* **2012**, *19*, 1061–9.

(47) Safari, J.; Javadian, L. *Ultrason. Sonochem.* **2014**.

(48) Qiu, L.; Pol, V. G.; Calderon-Moreno, J.; Gedanken, A. *Ultrason. Sonochem.* **2005**, *12*, 243–7.

(49) Pol, V. G.; Motiei, M.; Gedanken, A.; Calderon-Moreno, J.; Mastai, Y. *Chem. Mater.* **2003**, *15*, 1378–1384.

(50) Li, Q.; Li, H.; Pol, V. G.; Bruckental, I.; Koltypin, Y.; Calderon-Moreno, J.; Nowik, I.; Gedanken, A. *New J. Chem.* **2003**, *27*, 1194–1199.

(51) Li, H.; Wang, R.; Hong, Q.; Chen, L.; Zhong, Z.; Koltypin, Y.; Calderon-Moreno, J.; Gedanken, A. *Langmuir* **2004**, *20*, 8352–8356.

(52) Jiang, L.-P.; Xu, S.; Zhu, J.-M.; Zhang, J.-R.; Zhu, J.-J.; Chen, H.-Y. *Inorg. Chem.* **2004**, *43*, 5877–5883.

(53) Arul Dhas, N.; Gedanken, A. *J. Mater. Chem.* **1998**, *8*, 445–450.

(54) Shafi, K. V. P. M.; Ulman, A.; Yan, X.; Yang, N.-L.; Estournès, C.; White, H.; Rafailovich, M. *Langmuir* **2001**, *17*, 5093–5097.

(55) Pinkas, J.; Reichlova, V.; Zboril, R.; Moravec, Z.; Bezdicka, P.; Matejkova, J. *Ultrason. Sonochem.* **2008**, *15*, 257–64.

(56) Alavi, M. A.; Morsali, A.; Joo, S. W.; Min, B.-K. *Ultrason. Sonochem.* **2014**.

(57) Cabanas-Polo, S.; Suslick, K. S.; Sanchez-Herencia, A. J. *Ultrason. Sonochem.* **2011**, *18*, 901–6.

(58) Alavi, M. A.; Morsali, A. *Ultrason. Sonochem.* **2010**, *17*, 441–6.

(59) Vidotti, M.; van Greco, C.; Ponzio, E. A.; Córdoba de Torresi, S. I. *Electrochem. commun.* **2006**, *8*, 554–560.

(60) Alavi, M. A.; Morsali, A. *Ultrason. Sonochem.* **2010**, *17*, 132–8.

(61) Jeevanandam, P.; Koltypin, Y.; Gedanken, A. *Nano Lett.* **2001**, *1*, 263–266.

(62) Askarinejad, A.; Morsali, A. *Chem. Eng. J.* **2009**, *150*, 569–571.

(63) Uzcanga, I.; Bezverkhyy, I.; Afanasiev, P.; Scott, C.; Vrinat, M. *Chem. Mater.* **2005**, *17*, 3575–3577.

(64) Koltypin, Y.; Cao, X.; Prozorov, R.; Balogh, J.; Kaptas, D.; Gedanken, A. *J. Mater. Chem.* **1997**, *7*, 2453–2456.

(65) Oxley, J. D.; Mdleleni, M. M.; Suslick, K. S. *Catal. Today* **2004**, *88*, 139–151.

(66) Hyeon, T.; Fang, M.; Suslick, K. S. *J. Am. Chem. Soc.* **1996**, *118*, 5492–5493.

(67) Shafi, K. V. P. M.; Gedanken, A.; Goldfarb, R. B.; Felner, I. *J. Appl. Phys.* **1997**, *81*.

(68) Suslick, R. B. and G. G. and T. H. and S. M. and D. M. and P. M. and K. S. *Phys. Scr.* **1995**, *1995*, 79.

(69) Suslick, K. S.; Hyeon, T.; Fang, M. *Chem. Mater.* **1996**, *8*, 2172–2179.

(70) Basnayake, R.; Li, Z.; Katar, S.; Zhou, W.; Rivera, H.; Smotkin, E. S.; Casadonte Dominick J.; Korzeniewski, C. *Langmuir* **2006**, *22*, 10446–10450.

(71) Bellissent, R.; Galli, G.; Hyeon, T.; Migliardo, P.; Parette, G.; Suslick, K. S. *J. Non. Cryst. Solids* **1996**, *205-207*, 656–659.

(72) Zhu, Y.; Li, H.; Koltypin, Y.; Hacohen, Y. R.; Gedanken, A. *Chem. Commun.* **2001**, 2616–2617.

(73) Zhu, J.; Koltypin, Y.; Gedanken, A. *Chem. Mater.* **1999**, *12*, 73–78.

(74) Aboutorabi, L.; Morsali, A. *Inorganica Chim. Acta* **2010**, *363*, 2506–2511.

(75) Hojaghani, S.; Akhbari, K.; Sadr, M. H.; Morsali, A. *Inorg. Chem. Commun.* **2014**, *44*, 1–5.

(76) Masjedi-Arani, M.; Salavati-Niasari, M.; Ghanbari, D.; Nabiyouni, G. *Ceram. Int.* **2014**, *40*, 495–499.

(77) Shafi, K. V. P. M.; Gedanken, A.; Prozorov, R.; Balogh, J. *Chem. Mater.* **1998**, *10*, 3445–3450.

(78) Vijayakumar, R.; Koltypin, Y.; Felner, I.; Gedanken, A. *Mater. Sci. Eng. A* **2000**, *286*, 101–105.

(79) Gao, T.; Li, Q.; Wang, T. *Chem. Mater.* **2005**, *17*, 887–892.

(80) Bang, J. H.; Suslick, K. S. *J. Am. Chem. Soc.* **2007**, *129*, 2242–2243.

(81) Sivakumar, M.; Gedanken, A. *Ultrason. Sonochem.* **2004**, *11*, 373–8.

(82) Abbasi, A. R.; Morsali, A. *Ultrason. Sonochem.* **2010**, *17*, 572–8.

(83) Abbasi, A. R.; Morsali, A. *Ultrason. Sonochem.* **2012**, *19*, 540–5.

(84) Esmaeili-Zare, M.; Salavati-Niasari, M.; Sobhani, A. *Ultrason. Sonochem.* **2012**, *19*, 1079–86.

(85) Mayers, B. T.; Liu, K.; Sunderland, D.; Xia, Y. *Chem. Mater.* **2003**, *15*, 3852–3858.

(86) Lu, S.; Sivakumar, K.; Panchapakesan, B. Sonochemical Synthesis of Platinum Nanowires and Their Applications as Electro-Chemical Actuators. *Journal of Nanoscience and Nanotechnology*, *7*, 2473–2479.

(87) Jiang, L.-P.; Xu, S.; Miao, J.-J.; Wang, H.; Zhu, J.-J. Sonochemical Synthesis of CdS and CdSe Nanowires. *Journal of Nanoscience and Nanotechnology*, *6*, 2584–2587.

(88) Zhang, S.-L.; Cho, B.-H.; Lee, D.-D.; Lim, J.-O.; Huh, J.-S. ZnO Nanorods, Nanotubes and Nanorings: Controlled Synthesis and Structural Properties. *Journal of Nanoscience and Nanotechnology*, *12*, 1521–1525.

(89) Miao, J.-J.; Fu, R.-L.; Zhu, J.-M.; Xu, K.; Zhu, J.-J.; Chen, H.-Y. *Chem. Commun.* **2006**, 3013–3015.

(90) Geng, J.; Hou, W.-H.; Lv, Y.-N.; Zhu, J.-J.; Chen, H.-Y. *Inorg. Chem.* **2005**, *44*, 8503–8509.

(91) Wang, H.; Lu, Y.-N.; Zhu, J.-J.; Chen, H.-Y. *Inorg. Chem.* **2003**, *42*, 6404–6411.

(92) Jevtić, M.; Mitrić, M.; Škapin, S.; Jančar, B.; Ignjatović, N.; Uskoković, D. *Cryst. Growth Des.* **2008**, *8*, 2217–2222.

(93) Avivi, S.; Mastai, Y.; Gedanken, A. *J. Am. Chem. Soc.* **2000**, *122*, 4331–4334.

(94) Jung, S.-H.; Oh, E.; Lee, K.-H.; Yang, Y.; Park, C. G.; Park, W.; Jeong, S.-H. *Cryst. Growth Des.* **2007**, *8*, 265–269.

(95) Avivi, S.; Mastai, Y.; Hodes, G.; Gedanken, A. *J. Am. Chem. Soc.* **1999**, *121*, 4196–4199.

(96) Krishnan, C. V; Chen, J.; Burger, C.; Chu, B. *J. Phys. Chem. B* **2006**, *110*, 20182–20188.

(97) Mishra, P.; Yadav, R. S.; Pandey, A. C. *Ultrason. Sonochem.* **2010**, *17*, 560–5.

(98) Wang, Y.; Tang, X.; Yin, L.; Huang, W.; Rosenfeld Hacohen, Y.; Gedanken, A. *Adv. Mater.* **2000**, *12*, 1183–1186.

(99) Perelshtein, I.; Applerot, G.; Perkas, N.; Grinblat, J.; Hulla, E.; Wehrschuetz-Sigl, E.; Hasmann, A.; Guebitz, G.; Gedanken, A. *ACS Appl. Mater. Interfaces* **2010**, *2*, 1999–2004.

(100) Perelshtein, I.; Applerot, G.; Grinblat, J.; Gedanken, A. *Chem. - A Eur. J.* **2012**, *18*, 4575–82.

(101) Perelshtein, I.; Applerot, G.; Perkas, N.; Wehrschetz-Sigl, E.; Hasmann, A.; Guebitz, G. M.; Gedanken, A. *ACS Appl. Mater. Interfaces* **2008**, *1*, 361–366.

(102) Kiel, S.; Grinberg, O.; Perkas, N.; Charmet, J.; Kepner, H.; Gedanken, A. *Beilstein J. Nanotechnol.* **2012**, *3*, 267–276.

(103) Perelshtein, I.; Ruderman, E.; Francesko, A.; Fernandes, M. M.; Tzanov, T.; Gedanken, A. *Ultrason. Sonochem.* **2013**.

(104) Pol, V. G.; Grisaru, H.; Gedanken, A. *Langmuir* **2005**, *21*, 3635–3640.

(105) Kotlyar, A.; Perkas, N.; Amiryan, G.; Meyer, M.; Zimmermann, W.; Gedanken, A. *J. Appl. Polym. Sci.* **2007**, *104*, 2868–2876.

(106) Anna, K.; Nina, P.; Yuri, K.; Meinhard, M.; Werner, Z.; Aharon, G. *Ultrason. Sonochem.* **2008**, *15*, 839–45.

(107) Dhas, N. A.; Zaban, A.; Gedanken, A. *Chem. Mater.* **1999**, *11*, 806–813.

(108) Gao, T.; Wang, T. *Chem. Commun.* **2004**, 2558–2559.

(109) Pol, V. G.; Gedanken, A.; Calderon-Moreno, J. *Chem. Mater.* **2003**, *15*, 1111–1118.

(110) Ye, X.; Zhou, Y.; Chen, J.; Sun, Y. *Appl. Surf. Sci.* **2007**, *253*, 6264–6267.

(111) Pol, V. G.; Srivastava, D. N.; Palchik, O.; Palchik, V.; Slifkin, M. A.; Weiss, A. M.; Gedanken, A. *Langmuir* **2002**, *18*, 3352–3357.

(112) Zhong, Z.; Mastai, Y.; Koltypin, Y.; Zhao, Y.; Gedanken, A. *Chem. Mater.* **1999**, *11*, 2350–2359.

(113) Perkas, N.; Amirian, G.; Dubinsky, S.; Gazit, S.; Gedanken, A. *J. Appl. Polym. Sci.* **2007**, *104*, 1423–1430.

(114) Applerot, G.; Perkas, N.; Amirian, G.; Girshevitz, O.; Gedanken, A. *EMRS Fall Meet. 2008 Curr. trends nanostructured Polym. sol-gel thin Film.* **2009**, *256*, S3–S8.

(115) Zheng, H.-Y.; An, M.-Z. *J. Alloys Compd.* **2008**, *459*, 548–552.

(116) Soloviev, M.; Gedanken, A. *Ultrason. Sonochem.* **2011**, *18*, 356–62.

(117) Friedman, A.; Perkas, N.; Koltypin, Y.; Gedanken, A. *Appl. Surf. Sci.* **2012**, *258*, 2368–2372.

(118) Meridor, D.; Gedanken, A. *Ultrason. Sonochem.* **2013**, *20*, 425–31.

(119) Qiu, G.; Wang, Q.; Nie, M. *Macromol. Mater. Eng.* **2006**, *291*, 68–74.

(120) Xia, Z.; Wang, G.; Tao, K.; Li, J. *J. Magn. Magn. Mater.* **2005**, *293*, 182–186.

(121) Morel, A.-L.; Nikitenko, S. I.; Gionnet, K.; Wattiaux, A.; Lai-Kee-Him, J.; Labrugere, C.; Chevalier, B.; Deleris, G.; Petibois, C.; Brisson, A.; Simonoff, M. *ACS Nano* **2008**, *2*, 847–856.

(122) Dang, F.; Enomoto, N.; Hojo, J.; Enpuku, K. *Ultrason. Sonochem.* **2010**, *17*, 193–9.

(123) Nikitenko, S. I.; Koltypin, Y.; Palchik, O.; Felner, I.; Xu, X. N.; Gedanken, A. *Angew. Chemie Int. Ed.* **2001**, *40*, 4447–4449.

(124) Zhang, L.; Lian, J.; Wu, L.; Duan, Z.; Jiang, J.; Zhao, L. *Langmuir* **2014**, *30*, 7006–7013.

(125) Singh, R.; Sripada, L.; Singh, R. *Mitochondrion* **2014**, *16*, 50–4.

(126) Stoimenov, P.; Klinger, R.; Marchin, G.; Klabunde, K. *Langmuir* **2002**, *18*, 6679–6686.

(127) Pelgrift, R. Y.; Friedman, A. J. *Adv. Drug Deliv. Rev.* **2013**, *65*, 1803–15.

(128) Brayner, R.; Ferrari-Iliou, R.; Brivois, N.; Djediat, S.; Benedetti, M. F.; Fiévet, F. *Nano Lett.* **2006**, *6*, 866–870.

(129) Applerot, G.; Lipovsky, A.; Dror, R.; Perkas, N.; Nitzan, Y.; Lubart, R.; Gedanken, A. *Adv. Funct. Mater.* **2009**, *19*, 842–852.

(130) Rozenzhak, S. M.; Kadakia, M. P.; Caserta, T. M.; Westbrook, T. R.; Stone, M. O.; Naik, R. R. *Chem. Commun.* **2005**, 2217–2219.

(131) Meghana, S.; Kabra, P.; Chakraborty, S.; Padmavathy, N. *RSC Adv.* **2015**, *5*, 12293–12299.

(132) Yacaman, J. R. M. and J. L. E. and A. C. and K. H. and J. B. K. and J. T. R. and M. J. *Nanotechnology* **2005**, *16*, 2346.

(133) Ananth, A.; Dharaneedharan, S.; Heo, M.-S.; Mok, Y. S. *Chem. Eng. J.* **2015**, *262*, 179–188.

(134) Perelshtein, I.; Lipovsky, A.; Perkas, N.; Gedanken, A.; Moschini, E.; Mantecca, P. *Nano Res.* **2014**, 1–13.

(135) Ruparelia, J. P.; Chatterjee, A. K.; Duttagupta, S. P.; Mukherji, S. *Acta Biomater.* **2008**, *4*, 707–16.

(136) Yoon, K.-Y.; Hoon Byeon, J.; Park, J.-H.; Hwang, J. *Sci. Total Environ.* **2007**, *373*, 572–5.

(137) Kim, J. S.; Kuk, E.; Yu, K. N.; Kim, J.-H.; Park, S. J.; Lee, H. J.; Kim, S. H.; Park, Y. K.; Park, Y. H.; Hwang, C.-Y.; Kim, Y.-K.; Lee, Y.-S.; Jeong, D. H.; Cho, M.-H. *Nanomedicine* **2007**, *3*, 95–101.

(138) Usman, M. S.; Zowalaty, M. E. El; Shameli, K.; Zainuddin, N.; Salama, M.; Ibrahim, N. A. *Int. J. Nanomedicine* **2013**, *8*, 4467–4479.

(139) Ren, G.; Hu, D.; Cheng, E. W. C.; Vargas-Reus, M. A.; Reip, P.; Allaker, R. P. *Int. J. Antimicrob. Agents* **2009**, *33*, 587–590.

(140) Salem, W.; Leitner, D. R.; Zingl, F. G.; Schratter, G.; Prassl, R.; Goessler, W.; Reidl, J.; Schild, S. *Int. J. Med. Microbiol.* **2015**, *305*, 85–95.

(141) Perelshtein, I.; Ruderman, Y.; Perkas, N.; Traeger, K.; Tzanov, T.; Beddow, J.; Joyce, E.; Mason, T. J.; Blanes, M.; Molla, K.; Gedanken, A. *J. Mater. Chem.* **2012**, *22*, 10736–10742.

(142) Ann, L. C.; Mahmud, S.; Bakhori, S. K. M.; Sirelkhatim, A.; Mohamad, D.; Hasan, H.; Seeni, A.; Rahman, R. A. *Ceram. Int.* **2014**, *40*, 2993–3001.

(143) Martinez-Gutierrez, F.; Olive, P. L.; Banuelos, A.; Orrantia, E.; Nino, N.; Sanchez, E. M.; Ruiz, F.; Bach, H.; Av-Gay, Y. *Nanomedicine* **2010**, *6*, 681–8.

(144) Foster, H. A.; Ditta, I. B.; Varghese, S.; Steele, A. *Appl. Microbiol. Biotechnol.* **2011**, *90*, 1847–1868.

(145) Jin, T.; He, Y. *J. Nanoparticle Res.* **2011**, *13*, 6877–6885.

(146) MubarakAli, D.; Thajuddin, N.; Jeganathan, K.; Gunasekaran, M. *Colloids Surf. B. Biointerfaces* **2011**, *85*, 360–5.

(147) Kim, H. W.; Kim, B. R.; Rhee, Y. H. *Carbohydr. Polym.* **2010**, *79*, 1057–1062.

(148) Jain, P.; Pradeep, T. *Biotechnol. Bioeng.* **2005**, *90*, 59–63.

(149) Esteban-Cubillo, A.; Pecharromán, C.; Aguilar, E.; Santarén, J.; Moya, J. S. *J. Mater. Sci.* **2006**, *41*, 5208–5212.

(150) Stevens, K. N. J.; Crespo-Biel, O.; van den Bosch, E. E. M.; Dias, A. A.; Knetsch, M. L. W.; Aldenhoff, Y. B. J.; van der Veen, F. H.; Maessen, J. G.; Stobberingh, E. E.; Koole, L. H. *Biomaterials* **2009**, *30*, 3682–90.

(151) Willcox, M. D. P.; Hume, E. B. H.; Vijay, A. K.; Petcavich, R. *J. Optom.* **2010**, *3*, 143–148.

(152) Ahn, S.-J.; Lee, S.-J.; Kook, J.-K.; Lim, B.-S. *Dent. Mater.* **2009**, *25*, 206–13.

(153) Eby, D. M.; Luckarift, H. R.; Johnson, G. R. *ACS Appl. Mater. Interfaces* **2009**, *1*, 1553–1560.

(154) Marslin, G.; Selvakesavan, R. K.; Franklin, G.; Sarmento, B.; Dias, A. C. P. *Int. J. Nanomedicine* **2015**, *10*, 5955–5963.

(155) Chen, C.-Y.; Chiang, C.-L. *Mater. Lett.* **2008**, *62*, 3607–3609.

(156) Moosavi, R.; Abbasi, A. R.; Yousefi, M.; Ramazani, A.; Morsali, A. *Ultrason. Sonochem.* **2012**, *19*, 1221–6.

(157) Krishnaraj, C.; Jagan, E. G.; Rajasekar, S.; Selvakumar, P.; Kalaichelvan, P. T.; Mohan, N. *Colloids Surf. B. Biointerfaces* **2010**, *76*, 50–6.

(158) Hebeish, A.; El-Rafie, M. H.; El-Sheikh, M. A.; Seleem, A. A.; El-Naggar, M. E. *Int. J. Biol. Macromol.* **2014**, *65*, 509–15.

(159) Dankovich, T. A.; Gray, D. G. *Environ. Sci. Technol.* **2011**, *45*, 1992–1998.

(160) Egger, S.; Lehmann, R. P.; Height, M. J.; Loessner, M. J.; Schuppler, M. *Appl. Environ. Microbiol.* **2009**, *75*, 2973–6.

(161) Boukherroub, O. F. and R. K. S. and M. R. D. and R. S. and L. M. and Y. C. and T. H. and M. M. and R. *Nanotechnology* **2013**, *24*, 495101.

(162) Vidic, J.; Stankic, S.; Haque, F.; Ciric, D.; Goffic, R.; Vidy, A.; Jupille, J.; Delmas, B. *J. Nanoparticle Res.* **2013**, *15*, 1–10.

(163) Heng, B. C.; Zhao, X.; Xiong, S.; Woei Ng, K.; Yin-Chiang Boey, F.; Say-Chye Loo, J. *Food Chem. Toxicol.* **2010**, *48*, 1762–1766.

(164) Gilbert, B.; Fakra, S. C.; Xia, T.; Pokhrel, S.; MÃ¤dler, L.; Nel, A. E. *ACS Nano* **2012**, *6*, 4921–4930.

(165) Xia, T.; Kovochich, M.; Long, M.; L., M.; Gilbert, B.; Shi, H.; I., Y. J.; Zink, J. I.; Nel, A. E. *ACS Nano* **2008**, *2*, 2121–2134.

(166) Shen, J.-M.; Tang, W.-J.; Zhang, X.-L.; Chen, T.; Zhang, H.-X. *Carbohydr. Polym.* **2012**, *88*, 239–249.

(167) Ding, F.; Nie, Z.; Deng, H.; Xiao, L.; Du, Y.; Shi, X. *Carbohydr. Polym.* **2013**, *98*, 1547–1552.

(168) Krishnaveni, R.; Thambidurai, S. *Ind. Crops Prod.* **2013**, *47*, 160–167.

(169) Li, L.-H.; Deng, J.-C.; Deng, H.-R.; Liu, Z.-L.; Li, X.-L. *Chem. Eng. J.* **2010**, *160*, 378–382.

(170) Kreibig, U.; Vollmer, M. *Optical Properties of Metal Clusters*; SpringerSeries in Material Science, 1995.

(171) Kumar, K. S.; Kumar, V. B.; Paik, P. *J. Nanoparticles* **2013**, *2013*, 1–24.

(172) Kreyling, W. G.; Abdelmonem, A. M.; Ali, Z.; Alves, F.; Geiser, M.; Haberl, N.; Hartmann, R.; Hirn, S.; de Aberasturi, D. J.; Kantner, K.; Khadem-Saba, G.; Montenegro, J.-M.; Rejman, J.; Rojo, T.; de Larramendi, I. R.; Ufartes, R.; Wenk, A.; Parak, W. J. *Nat Nano* **2015**, *10*, 619–623.

(173) Fresnais, J.; Yan, M.; Courtois, J.; Bostelmann, T.; Bée, A.; Berret, J.-F. *J. Colloid Interface Sci.* **2013**, *395*, 24–30.

(174) Pellegrino, T.; Manna, L.; Kudera, S.; Liedl, T.; Koktysh, D.; Rogach, A. L.; Keller, S.; Rädler, J.; Natile, G.; Parak, W. J. *Nano Lett.* **2004**, *4*, 703–707.

(175) Wang, H.; Song, X.; Liu, C.; He, J.; Chong, W. H.; Chen, H. *ACS Nano* **2014**, *8*, 8063–8073.

(176) Juan, J.; Cheng, L.; Shi, M.; Liu, Z.; Mao, X. *J. Mater. Chem. B* **2015**, *3*, 5769–5776.

(177) Flesch, C.; Unterfinger, Y.; Bourgeat-Lami, E.; Duguet, E.; Delaite, C.; Dumas, P. *Macromol. Rapid Commun.* **2005**, *26*, 1494–1498.

(178) Wang, D.; Astruc, D. *Chem. Rev.* **2014**, *114*, 6949–6985.

(179) Fratoddi, I.; Venditti, I.; Battocchio, C.; Polzonetti, G.; Cametti, C.; Russo, M. V. *Nanoscale Res. Lett.* **2011**, *6*, 1–8.

(180) Rabea, E. I.; Badawy, M. E.-T.; Stevens, C. V; Smagghe, G.; Steurbaut, W. *Biomacromolecules* **2003**, *4*, 1457–65.

(181) Kong, M.; Chen, X. G.; Xing, K.; Park, H. J. *16th CBL (Club des Bactéries Lact. Symp. May 2009, Toulouse, Fr.* **2010**, *144*, 51–63.

(182) Sanpui, P.; Murugadoss, A.; Prasad, P. V. D.; Ghosh, S. S.; Chattopadhyay, A. *Int. J. Food Microbiol.* **2008**, *124*, 142–146.

(183) Astilean, M. P. and E. J. and A. D. and O. P. and V. C. and S. *Nanotechnology* **2011**, *22*, 135101.

(184) Ali, S. W.; Rajendran, S.; Joshi, M. *Carbohydr. Polym.* **2011**, *83*, 438–446.

(185) Guo, Y.-B.; Wang, D.-G.; Liu, S.-H.; Zhang, S.-W. *Colloids Surfaces A Physicochem. Eng. Asp.* **2013**, *417*, 1–9.

(186) Juan, L. *Int. J. Nanomedicine* **2010**, 261.

(187) Shubayev, V. I.; Pisanic, T. R.; Jin, S. *Adv. Drug Deliv. Rev.* **2009**, *61*, 467–77.

(188) Pisanic, T. R.; Blackwell, J. D.; Shubayev, V. I.; Fiñones, R. R.; Jin, S. *Biomaterials* **2007**, *28*, 2572–81.

(189) Yeasmin, S.; Malik, D.; Das, T.; Bandyopadhyay, A. *RSC Adv.* **2015**, *5*, 39992–39999.

(190) Salgueiriño-Maceira, V.; Correa-Duarte, M. A. *Adv. Mater.* **2007**, *19*, 4131–4144.

(191) Darwish, M. S. A.; Nguyen, N. H. A.; Ševců, A.; Stibor, I.; Smoukov, S. K. *Mater. Sci. Eng. C* **2016**, *63*, 88–95.

(192) Kuo, W.-S.; Chang, C.-N.; Chang, Y.-T.; Yeh, C.-S. *Chem. Commun.* **2009**, 4853–4855.

(193) Singh, S.; Barick, K. C.; Bahadur, D. *Powder Technol.* **2015**, *269*, 513–519.

(194) Mody, V. V; Nounou, M. I.; Bikram, M. *Adv. Drug Deliv. Rev.* **2009**, *61*, 795–807.

(195) Mody, V.; Siwale, R.; Singh, A.; Mody, H. *J. Pharm. Bioallied Sci.* **2010**, *2*, 282–289.

(196) Zaleska-Medynska, A.; Marchelek, M.; Diak, M.; Grabowska, E. *Adv. Colloid Interface Sci.* **2015**, *229*, 80–107.

(197) Elzoghby, A. O.; Samy, W. M.; Elgindy, N. A. *J. Control. Release* **2012**, *161*, 38–49.

(198) Liu, L.; Ma, P.; Wang, H.; Zhang, C.; Sun, H.; Wang, C.; Song, C.; Leng, X.; Kong, D.; Ma, G. *J. Control. Release* **2016**, *225*, 230–239.

(199) Yadav, A.; Prasad, V.; Kathe, A. A.; Raj, S.; Yadav, D.; Sundaramoorthy, C.; Vigneshwaran, N. *Bull. Mater. Sci.* **2006**, *29*, 641–645.

(200) Selvam, S.; Rajiv Gandhi, R.; Suresh, J.; Gowri, S.; Ravikumar, S.; Sundrarajan, M. *Int. J. Pharm.* **2012**, *434*, 366–374.

(201) Kumar Bajpai, S.; Thomas, V.; Bajpai, M. *J. Eng. Fiber. Fabr.* **2011**, *6*, 73–81.

(202) AbdElhady, M. M. *Int. J. Carbohydr. Chem.* **2012**, *2012*, 1–6.

(203) Dastjerdi, R.; Montazer, M. *Colloids Surfaces B Biointerfaces* **2010**, *79*, 5–18.

(204) Perelshtein, I.; Applerot, G.; Perkas, N.; Wehrschuetz-Sigl, E.; Hasmann, A.; Guebitz, G.; Gedanken, A. *Surf. Coatings Technol.* **2009**, *204*, 54–57.

(205) Hadad, L.; Perkas, N.; Gofer, Y.; Calderon-Moreno, J.; Ghule, A.; Gedanken, A. *J. Appl. Polym. Sci.* **2007**, *104*, 1732–1737.

(206) Gedanken, I. P. and G. A. and N. P. and G. G. and S. M. and A. *Nanotechnology* **2008**, *19*, 245705.

(207) Perelshtein, I.; Ruderman, Y.; Perkas, N.; Beddow, J.; Singh, G.; Vinatoru, M.; Joyce, E.; Mason, T.; Blanes, M.; Mollá, K.; Gedanken, A. *Cellulose* **2013**, *20*, 1215–1221.

(208) Perelshtein, I.; Lipovsky, A.; Perkas, N.; Tzanov, T.; Arguirova, M.; Leseva, M.; Gedanken, A. *Ultrason. Sonochem.* **2015**, *25*, 82–88.

(209) Applerot, G.; Lellouche, J.; Perkas, N.; Nitzan, Y.; Gedanken, A.; Banin, E. *RSC Adv.* **2012**, *2*, 2314–2321.

(210) Abbasi, A. R.; Morsali, A. *Ultrason. Sonochem.* **2010**, *17*, 704–10.

(211) Abbasi, A. R.; Morsali, A. *Ultrason. Sonochem.* **2011**, *18*, 282–287.

(212) Abramova, A.; Gedanken, A.; Popov, V.; Ooi, E.-H.; Mason, T. J.; Joyce, E. M.; Beddow, J.; Perelshtein, I.; Bayazitov, V. *Mater. Lett.* **2013**, *96*, 121–124.

(213) Abramova, A. V; Abramov, V. O.; Gedanken, A.; Perelshtein, I.; Bayazitov, V. M. *Beilstein J. Nanotechnol.* **2014**, *5*, 532–536.

(214) Agudelo, R. M.; Peñuela, G.; Aguirre, N. J.; Morató, J.; Jaramillo, M. L. *Ecol. Eng.* **2010**, *36*, 1401–1408.

(215) GARCÍA, J.; ROUSSEAU, D. P. L.; MORATÓ, J.; LESAGE, E.; MATAMOROS, V.; BAYONA, J. M. *Crit. Rev. Environ. Sci. Technol.* **2010**, *40*, 561–661.

(216) Li, Y.; Zhu, G.; Ng, W. J.; Tan, S. K. *Sci. Total Environ.* **2014**, *468-469*, 908–932.

(217) Casas-Zapata, J. C.; Ríos, K.; Florville-Alejandre, T. R.; Morató, J.; Peñuela, G. *J. Environ. Sci. Heal. Part B* **2013**, *48*, 122–132.

(218) World Health Organization. No Title http://www.who.int/mediacentre/factsheets/fs391/en/.

(219) WHO Guidelines for Drinking Water Quality.

(220) WHO: Suministro Global de Agua y Saneamiento de Evaluación.

(221) Hunter, P. R. *J. Appl. Microbiol.* **2003**, *94 Suppl*, 37S–46S.

(222) Amar, P. K. *J. Pharm. Bioallied Sci.* **2010**, *2*, 253–66.

(223) WHO Guidelines for Drinking Water Quality.

(224) Li, Q.; Mahendra, S.; Lyon, D. Y.; Brunet, L.; Liga, M. V.; Li, D.; Alvarez, P. J. J. *Water Res.*

2008, *42*, 4591–4602.

(225) Richardson, S. D. *TrAC - Trends Anal. Chem.* **2003**, *22*, 666–684.

(226) Rodrigues, P. M. S. M.; Esteves da Silva, J. C. G.; Antunes, M. C. G. *Anal. Chim. Acta* **2007**, *595*, 266–274.

(227) Shannon, M. a.; Bohn, P. W.; Elimelech, M.; Georgiadis, J. G.; Mariñas, B. J.; Mayes, A. M. *Nature* **2008**, *452*, 301–310.

(228) Charrois, J. W. A. In *Encyclopedia of Analytical Chemistry*; John Wiley & Sons, Ltd, 2006.

(229) Wang, G.-S.; Deng, Y.-C.; Lin, T.-F. *Sci. Total Environ.* **2007**, *387*, 86–95.

(230) Motshekga, S. C.; Ray, S. S.; Onyango, M. S.; Momba, M. N. B. *Appl. Clay Sci.* **2015**, *114*, 330–339.

(231) Karumuri, A. K.; Oswal, D. P.; Hostetler, H. a.; Mukhopadhyay, S. M. *Mater. Lett.* **2013**, *109*, 83–87.

(232) Chou, W.-L.; Yu, D.-G.; Yang, M.-C. *Polym. Adv. Technol.* **2005**, *16*, 600–607.

(233) Zodrow, K.; Brunet, L.; Mahendra, S.; Li, D.; Zhang, A.; Li, Q.; Alvarez, P. J. J. *Water Res.* **2009**, *43*, 715–23.

(234) Cho, M.; Chung, H.; Choi, W.; Yoon, J. *Appl. Environ. Microbiol.* **2005**, *71*, 270–275.

(235) Sun, Y. *Chem. Soc. Rev.* **2013**, 2497–2511.

(236) Wang, L.; Wang, C.; Hsieh, C.; Shen, C. **2015**, 2685–2696.

(237) Loo SL, Krantz WB, Hu X, F. A. & L. T. *J. Colloid Interface Sci.* **2016**, *461*, 104–113.

(238) Gehrke, I.; Geiser, A.; Somborn-Schulz, A. *Nanotechnol. Sci. Appl.* **2015**, *8*, 1–17.

(239) Savage, N.; Diallo, M. S. *J. Nanoparticle Res. 7*, 331–342.

(240) Gelover, S.; Gómez, L. A.; Reyes, K.; Teresa Leal, M. *Water Res.* **2006**, *40*, 3274–80.

(241) Mpenyana-Monyatsi, L.; Mthombeni, N. H.; Onyango, M. S.; Momba, M. N. B. *Int. J. Environ. Res. Public Health* **2012**, *9*, 244–271.

(242) Don, T.-M.; Chen, C.-C.; Lee, C.-K.; Cheng, W.-Y.; Cheng, L.-P. *J. Biomater. Sci. Polym. Ed.* **2005**, *16*, 1503–1519.

(243) Yerushalmi, N.; Arad, A.; Margalit, R. *Arch. Biochem. Biophys.* **1994**, *313*, 267–73.

(244) Puolakkainen, P. A.; Twardzik, D. R.; Ranchalis, J. E.; Pankey, S. C.; Reed, M. J.; Gombotz, W. R. *J. Surg. Res.* **1995**, *58*, 321–9.

(245) Tian, J.; Wong, K. K. Y.; Ho, C.-M.; Lok, C.-N.; Yu, W.-Y.; Che, C.-M.; Chiu, J.-F.; Tam, P. K. H. *ChemMedChem* **2007**, *2*, 129–136.

(246) Francesko, A.; Soares da Costa, D.; Reis, R. L.; Pashkuleva, I.; Tzanov, T. *Acta Biomater.* **2013**, *9*, 5216–25.

(247) Drury, J. L.; Mooney, D. J. *Biomaterials* **2003**, *24*, 4337–4351.

(248) Dumitrescu, A. M.; Slatineanu, T.; Poiata, A.; Iordan, A. R.; Mihailescu, C.; Palamaru, M. N. *Colloids Surfaces A Physicochem. Eng. Asp.* **2014**, *455*, 185–194.

(249) Boateng, J. S.; Matthews, K. H.; Stevens, H. N. E.; Eccleston, G. M. *J. Pharm. Sci.* **2008**, *97*, 2892–2923.

(250) Gordon, N. C.; Wareham, D. W. *Int. J. Antimicrob. Agents* **2010**, *36*, 129–131.

(251) Sudheesh Kumar, P. T.; Lakshmanan, V.-K.; Anilkumar, T. V; Ramya, C.; Reshmi, P.; Unnikrishnan, A. G.; Nair, S. V; Jayakumar, R. *ACS Appl. Mater. Interfaces* **2012**, *4*, 2618–2629.

(252) Felice, F.; Zambito, Y.; Belardinelli, E.; D'Onofrio, C.; Fabiano, A.; Balbarini, A.; Di Stefano, R. *Eur. J. Pharm. Sci.* **2013**, *50*, 393–9.

(253) Sosnik, A.; Neves, J. das; Sarmento, B. *Prog. Polym. Sci.* **2014**.

(254) Hong, H.-J.; Jin, S.-E.; Park, J.-S.; Ahn, W. S.; Kim, C.-K. *Biomaterials* **2008**, *29*, 4831–7.

(255) Wijekoon, A.; Fountas-Davis, N.; Leipzig, N. D. *Acta Biomater.* **2013**, *9*, 5653–64.

(256) De Campos, A. *Eur. J. Pharm. Sci.* **2003**, *20*, 73–81.

(257) Pan, Y.; Li, Y.; Zhao, H.; Zheng, J.; Xu, H.; Wei, G.; Hao, J.; Cui, F. *Int. J. Pharm.* **2002**, *249*, 139–147.

(258) Bravo-Osuna, I.; Vauthier, C.; Farabollini, A.; Palmieri, G. F.; Ponchel, G. *Biomaterials* **2007**, *28*, 2233–43.

(259) Rho, K. S.; Jeong, L.; Lee, G.; Seo, B.-M.; Park, Y. J.; Hong, S.-D.; Roh, S.; Cho, J. J.; Park, W. H.; Min, B.-M. *Biomaterials* **2006**, *27*, 1452–61.

(260) Kirker, K. R.; Luo, Y.; Nielson, J. H.; Shelby, J.; Prestwich, G. D. *Biomaterials* **2002**, *23*, 3661–3671.

(261) Liu, Y.; Cai, S.; Shu, X. Z.; Shelby, J.; Prestwich, G. D. *Wound Repair Regen.* **2007**, *15*, 245–251.

(262) Park, S.-N.; Park, J.-C.; Kim, H. O.; Song, M. J.; Suh, H. *Biomaterials* **2002**, *23*, 1205–1212.

(263) Li, J.; Li, X.; Ni, X.; Wang, X.; Li, H.; Leong, K. W. *Biomaterials* **2006**, *27*, 4132–40.

(264) Hoffman, A. S. *Adv. Drug Deliv. Rev.* **2002**, *54*, 3–12.

(265) Garnier, C.; Axelos, M. A. V.; Thibault, J.-F. *Carbohydr. Res.* **1993**, *240*, 219–232.

(266) Renard, D.; Lefebvre, J. *Int. J. Biol. Macromol.* **1992**, *14*, 287–291.

(267) Achilli, M.; Mantovani, D. *Polymers (Basel).* **2010**, *2*, 664–680.

(268) Bhumkar, D. R.; Pokharkar, V. B. *AAPS PharmSciTech 7*, E138–E143.

(269) Li, J. *NPG Asia Mater* **2010**, *2*, 112–118.

(270) Bae, K. H.; Wang, L.-S.; Kurisawa, M. *J. Mater. Chem. B* **2013**, *1*, 5371–5388.

(271) Hoare, T. R.; Kohane, D. S. *Polymer (Guildf).* **2008**, *49*, 1993–2007.

(272) Teodorescu, M.; Negru, I.; Stanescu, P. O.; Drăghici, C.; Lungu, A.; Sârbu, A. *React. Funct. Polym.* **2010**, *70*, 790–797.

(273) Annabi, N.; Tamayol, A.; Uquillas, J. A.; Akbari, M.; Bertassoni, L. E.; Cha, C.; Camci-Unal, G.; Dokmeci, M. R.; Peppas, N. A.; Khademhosseini, A. *Adv. Mater.* **2014**, *26*, 85–124.

(274) Ekenseair, A. K.; Boere, K. W. M.; Tzouanas, S. N.; Vo, T. N.; Kasper, F. K.; Mikos, A. G. *Biomacromolecules* **2012**, *13*, 2821–2830.

(275) Vermonden, T.; Fedorovich, N. E.; van Geemen, D.; Alblas, J.; van Nostrum, C. F.; Dhert, W. J. A.; Hennink, W. E. *Biomacromolecules* **2008**, *9*, 919–926.

(276) Tanabe, Y.; Yasuda, K.; Azuma, C.; Taniguro, H.; Onodera, S.; Suzuki, A.; Chen, Y. M.; Gong, J. P.; Osada, Y. *J. Mater. Sci. Mater. Med.* **2007**, *19*, 1379–1387.

(277) Moreira Teixeira, L. S.; Feijen, P. dr. J.; Blitterswijk, P. dr. C. A. van; Dijkstra, D. P. J.; Karperien, P. dr. H. B. J. *Biomaterials* **2012**, *33*, 1281–1290.

(278) Rocasalbas, G.; Francesko, A.; Touriño, S.; Fernández-Francos, X.; Guebitz, G. M.; Tzanov, T. *Carbohydr. Polym.* **2013**, *92*, 989–96.

(279) Sakai, S.; Ashida, T.; Ogino, S.; Taya, M. *J. Microencapsul.* **2013**, *31*, 100–104.

(280) Sakai, S.; Yamada, Y.; Zenke, T.; Kawakami, K. *J. Mater. Chem.* **2009**, *19*, 230–235.

(281) Jin, R.; Moreira Teixeira, L. S.; Dijkstra, P. J.; Karperien, M.; van Blitterswijk, C. A.; Zhong, Z. Y.; Feijen, J. *Biomaterials* **2009**, *30*, 2544–51.

(282) Yung, C. W.; Bentley, W. E.; Barbari, T. A. *J. Biomed. Mater. Res. A* **2010**, *95*, 25–32.

(283) Rahn, K.; Diamantoglou, M.; Klemm, D.; Berghmans, H.; Heinze, T. *Angew. Makromol. Chemie* **1996**, *238*, 143–163.

(284) Ghose, T. K. *Pure Appl. Chem.* **1987**, *59*, 257–268.

(285) Scalbert, A.; Monties, B.; Janin, G. *J. Agric. Food Chem.* **1989**, *37*, 1324–1329.

(286) Bernkop-Schnürch, A.; Hornof, M.; Zoidl, T. *Int. J. Pharm.* **2003**, *260*, 229–237.

(287) Bravo-Osuna, I.; Teutonico, D.; Arpicco, S.; Vauthier, C.; Ponchel, G. *Int. J. Pharm.* **2007**, *340*, 173–81.

(288) Tran, N. Q.; Joung, Y. K.; Lih, E.; Park, K. D. *Biomacromolecules* **2011**, *12*, 2872–2880.

(289) Vold, I. M. N.; Vårum, K. M.; Guibal, E.; Smidsrød, O. *Carbohydr. Polym.* **2003**, *54*, 471–477.

(290) Peschel, D.; Zhang, K.; Fischer, S.; Groth, T. *Acta Biomater.* **2012**, *8*, 183–193.

(291) Nieto, J. M.; Peniche-Covas, C.; Del Bosque, J. *Carbohydr. Polym.* **1992**, *18*, 221–224.

(292) Wang, X.; Du, Y.; Fan, L.; Liu, H.; Hu, Y. *Polym. Bull.* **2005**, *55*, 105–113.

(293) Perelshtein, I.; Ruderman, E.; Perkas, N.; Tzanov, T.; Beddow, J.; Joyce, E.; Mason, T. J.; Blanes, M.; Molla, K.; Patlolla, A.; Frenkel, A. I.; Gedanken, A. *J. Mater. Chem. B* **2013**, *1*, 1968–1976.

(294) Du, W.-L.; Niu, S.-S.; Xu, Y.-L.; Xu, Z.-R.; Fan, C.-L. *Carbohydr. Polym.* **2009**, *75*, 385–389.

(295) Huang, H.; Yang, X. *Carbohydr. Res.* **2004**, *339*, 2627–2631.

(296) Huang, H.; Yang, X. *Biomacromolecules* **2004**, *5*, 2340–2346.

(297) Mudunkotuwa, I.; Rupasinghe, T.; Wu, M. V; Grassian, V. *Langmuir* **2012**, *28*, 396–403.

(298) Wang, X.; Du, Y.; Liu, H. *Carbohydr. Polym.* **2004**, *56*, 21–26.

(299) Rhazi, M.; Desbrières, J.; Tolaimate, A.; Rinaudo, M.; Vottero, P.; Alagui, A.; El Meray, M. *Eur. Polym. J.* **2002**, *38*, 1523–1530.

(300) Rhazi, M.; Desbrières, J.; Tolaimate, A.; Rinaudo, M.; Vottero, P.; Alagui, A. *Polymer (Guildf).* **2002**, *43*, 1267–1276.

(301) Ma, H.; Williams, P. L.; Diamond, S. A. *Environ. Pollut.* **2013**, *172*, 76–85.

(302) Fukui, H.; Horie, M.; Endoh, S.; Kato, H.; Fujita, K.; Nishio, K.; Komaba, L. K.; Maru, J.;

Miyauhi, A.; Nakamura, A.; Kinugasa, S.; Yoshida, Y.; Hagihara, Y.; Iwahashi, H. *Chem. Biol. Interact.* **2012**, *198*, 29–37.

(303) Mellegård, H.; Strand, S. P.; Christensen, B. E.; Granum, P. E.; Hardy, S. P. *Int. J. Food Microbiol.* **2011**, *148*, 48–54.

(304) Fernandes, J. C.; Tavaria, F. K.; Fonseca, S. C.; Ramos, O. S.; Pintado, M. E.; Malcata, F. X. *J. Microbiol. Biotechnol.* **2010**, *20*, 311–8.

(305) Tao, Y.; Qian, L.-H.; Xie, J. *Carbohydr. Polym.* **2011**, *86*, 969–974.

(306) Li, X.; Feng, X.; Yang, S.; Fu, G.; Wang, T.; Su, Z. *Carbohydr. Polym.* **2010**, *79*, 493–499.

(307) Fijan, S.; Turk, S. Š. *Int. J. Environ. Res. Public Health* **2012**, *9*, 3330–3343.

(308) Angel (Shimanovich), U.; Silva, C. M.; Cavaco-Paulo, A.; Gedanken, A. *Isr. J. Chem.* **2010**, *50*, 524–529.

(309) Suslick, K. S.; Price, G. J. *Annu. Rev. Mater. Sci* **1999**, *29*, 295–326.

(310) Aruoja, V.; Dubourguier, H.-C.; Kasemets, K.; Kahru, A. *Sci. Total Environ.* **2009**, *407*, 1461–1468.

(311) Cohen, D.; Soroka, Y.; Ma'or, Z.; Oron, M.; Portugal-Cohen, M.; Brégégère, F. M.; Berhanu, D.; Valsami-Jones, E.; Hai, N.; Milner, Y. *Toxicol. Vitr.* **2013**, *27*, 292–298.

(312) Demir, E.; Akça, H.; Kaya, B.; Burgucu, D.; Tokgün, O.; Turna, F.; Aksakal, S.; Vales, G.; Creus, A.; Marcos, R. *J. Hazard. Mater.* **2014**, *264*, 420–429.

(313) Auffan, M.; Rose, J.; Wiesner, M. R.; Bottero, J.-Y. *Behav. Eff. Nanoparticles Environ.* **2009**, *157*, 1127–1133.

(314) Li, Y.; Zhang, W.; Niu, J.; Chen, Y. *ACS Nano* **2012**, *6*, 5164–5173.

(315) Ma, H.; Kabengi, N. J.; Bertsch, P. M.; Unrine, J. M.; Glenn, T. C.; Williams, P. L. *Environ. Pollut.* **2011**, *159*, 1473–1480.

(316) Huang, C.-C.; Aronstam, R. S.; Chen, D.-R.; Huang, Y.-W. *Toxicol. Vitr.* **2010**, *24*, 45–55.

(317) Yen, M.-T.; Yang, J.-H.; Mau, J.-L. *Carbohydr. Polym.* **2008**, *74*, 840–844.

(318) Carosio, F.; Alongi, J.; Frache, A. *Eur. Polym. J.* **2011**, *47*, 893–902.

(319) El Shafei, A.; Shaarawy, S.; Hebeish, A. *Carbohydr. Polym.* **2010**, *79*, 852–857.

(320) Zhang, D.; Chen, L.; Zang, C.; Chen, Y.; Lin, H. *Carbohydr. Polym.* **2013**, *92*, 2088–94.

(321) Guebitz, G. M.; Cavaco-Paulo, A. *Trends Biotechnol.* **2008**, *26*, 32–38.

(322) Cavaco-Paulo, A.; Almeida, L.; Bishop, D. *Text. Res. J.* **1996**, *66* , 287–294.

(323) Azevedo, H.; Bishop, D.; Cavaco–Paulo, A. *Enzyme Microb. Technol.* **2000**, *27*, 325–329.

(324) Yachmenev, V. G.; Blanchard, E. J.; Lambert, A. H. *Ultrasonics* **2004**, *42*, 87–91.

(325) Yu, Z.-L.; Zeng, W.-C.; Zhang, W.-H.; Liao, X.-P.; Shi, B. *Ultrason. Sonochem.* **2014**, *21*, 930–936.

(326) Subhedar, P. B.; Gogate, P. R. *J. Mol. Catal. B Enzym.* **2014**, *101*, 108–114.

(327) Nair, S.; Sasidharan, A.; Divya Rani, V. V; Menon, D.; Nair, S.; Manzoor, K.; Raina, S. *J. Mater. Sci. Mater. Med.* **2009**, *20*, 235–241.

(328) Huang, H.; Yuan, Q.; Yang, X. *Colloids Surfaces B Biointerfaces* **2004**, *39*, 31–37.

(329) Cheng, F.; Betts, J. W.; Kelly, S. M.; Schaller, J.; Heinze, T. *Green Chem.* **2013**, *15*, 989.

(330) George, J.; Kumar, R.; Sajeevkumar, V. A.; Ramana, K. V.; Rajamanickam, R.; Abhishek, V.; Nadanasabapathy, S.; Siddaramaiah. *Carbohydr. Polym.* **2014**, *105*, 285–292.

(331) Tran, H. V.; Tran, L. D.; Ba, C. T.; Vu, H. D.; Nguyen, T. N.; Pham, D. G.; Nguyen, P. X. *Colloids Surfaces A Physicochem. Eng. Asp.* **2010**, *360*, 32–40.

(332) Rocasalbas, G.; Francesko, A.; Touriño, S.; Fernández-Francos, X.; Guebitz, G. M.; Tzanov, T. *Carbohydr. Polym.* **2013**, *92*, 989–996.

(333) Lopes, M. H.; Barros, A. S.; Pascoal Neto, C.; Rutledge, D.; Delgadillo, I.; Gil, A. M. *Biopolymers* **2001**, *62*, 268–277.

(334) Lopes, M. H.; Neto, C. P.; Barros, A. S.; Rutledge, D.; Delgadillo, I.; Gil, A. M. *Biopolymers* **2000**, *57*, 344–351.

(335) Hanzlík, J.; Jehlička, J.; Šebek, O.; Weishauptová, Z.; Machovič, V. *Water Res.* **2004**, *38*, 2178–2184.

(336) Girase, B.; Depan, D.; Shah, J. S.; Xu, W.; Misra, R. D. K. *Mater. Sci. Eng. C* **2011**, *31*, 1759–1766.

(337) Pintor, A. M. A.; Ferreira, C. I. A.; Pereira, J. C.; Correia, P.; Silva, S. P.; Vilar, V. J. P.; Botelho, C. M. S.; Boaventura, R. A. R. *Water Res.* **2012**, *46*, 3152–3166.

(338) Witek-Krowiak, A.; Szafran, R. G.; Modelski, S. *Desalination* **2011**, *265*, 126–134.

(339) Genco, T.; Zemljič, L. F.; Bračič, M.; Stana-Kleinschek, K.; Heinze, T. *Macromol. Chem. Phys.* **2012**, *213*, 539–548.

(340) Fernandes, M. M.; Francesko, A.; Torrent-Burgués, J.; Carrión-Fité, F. J.; Heinze, T.; Tzanov, T. *Biomacromolecules* **2014**, *15*, 1365–1374.

(341) Misra, R. D. K.; Girase, B.; Depan, D.; Shah, J. S. *Adv. Eng. Mater.* **2012**, *14*, B93–B100.

(342) Wu, P.; of Illinois at Urbana-Champaign, U. *Antimicrobial Materials for Water Disinfection Based on Visible-light Photocatalysts*; University of Illinois at Urbana-Champaign, 2007.

(343) Girón, J. A.; Torres, A. G.; Freer, E.; Kaper, J. B. *Mol. Microbiol.* **2002**, *44*, 361–379.

(344) Pratt, L. A.; Kolter, R. *Mol. Microbiol.* **1998**, *30*, 285–293.

(345) Ramos, H. C.; Rumbo, M.; Sirard, J.-C. *Trends Microbiol.* **2004**, *12*, 509–17.

(346) Fazli, M.; Bjarnsholt, T.; Kirketerp-Møller, K.; Jørgensen, B.; Andersen, A. S.; Krogfelt, K. A.; Givskov, M.; Tolker-Nielsen, T. *J. Clin. Microbiol.* **2009**, *47* , 4084–4089.

(347) Bang, J. H.; Suslick, K. S. *Adv. Mater.* **2010**, *22*, 1039–1059.

(348) Lim, J.; Yeap, S. P.; Che, H. X.; Low, S. C. *Nanoscale Res. Lett.* **2013**, *8*, 381.

(349) Innocenti, A.; Durdagi, S.; Doostdar, N.; Strom, T. A.; Barron, A. R.; Supuran, C. T. *Bioorg. Med. Chem.* **2010**, *18*, 2822–8.

(350) Simon-Deckers, A.; Loo, S.; Mayne-L'hermite, M.; Herlin-Boime, N.; Menguy, N.; Reynaud, C.; Gouget, B.; Carrière, M. *Environ. Sci. Technol.* **2009**, *43*, 8423–8429.

(351) Fu, X.; Kassim, S. Y.; Parks, W. C.; Heinecke, J. W. *J. Biol. Chem.* **2001**, *276*, 41279–87.

(352) Bensalem, S.; Soubhye, J.; Aldib, I.; Bournine, L.; Nguyen, A. T.; Vanhaeverbeek, M.; Rousseau, A.; Boudjeltia, K. Z.; Sarakbi, A.; Kauffmann, J. M.; Nève, J.; Prévost, M.; Stévigny, C.; Maiza-Benabdesselam, F.; Bedjou, F.; Van Antwerpen, P.; Duez, P. *J.*

Ethnopharmacol. **2014**, *154*, 361–9.

(353) Díaz-GonzáLez, M.; Rocasalbas, G.; Francesko, A.; Touriño, S.; Torres, J. L.; Tzanov, T. *Biocatal. Biotransformation* **2012**, *30*, 102–110.

(354) Eming, S.; Smola, H.; Hartmann, B.; Malchau, G.; Wegner, R.; Krieg, T.; Smola-Hess, S. *Biomaterials* **2008**, *29*, 2932–40.

(355) Edwards, J. V.; Howley, P.; Davis, R.; Mashchak, A.; Goheen, S. C. *Int. J. Pharm.* **2007**, *340*, 42–51.

(356) Barros, S. C.; Martins, J. A.; Marcos, J. C.; Cavaco-Paulo, A. *Enzyme Microb. Technol.* **2012**, *50*, 107–14.

(357) Vidhu, V. K.; Philip, D. *Spectrochim. Acta. A. Mol. Biomol. Spectrosc.* **2014**, *134C*, 372–379.

(358) Fazli, M.; Bjarnsholt, T.; Kirketerp-Møller, K.; Jørgensen, A.; Andersen, C. B.; Givskov, M.; Tolker-Nielsen, T. *Wound Repair Regen.* **2011**, *19*, 387–391.

(359) Priester, J. H.; Stoimenov, P. K.; Mielke, R. E.; Webb, S. M.; Ehrhardt, C.; Zhang, J. P.; Stucky, G. D.; Holden, P. A. *Environ. Sci. Technol.* **2009**, *43*, 2589–2594.

(360) Obinger, C.; Burner, U.; Ebermann, R. *PHYTON-HORN-* **1997**, *37*, 219–226.

(361) Goldman, R.; Stoyanovsky, D. A.; Day, B. W.; Kagan, V. E. *Biochemistry* **1995**, *34*, 4765–4772.

(362) Sakai, S.; Khanmohammadi, M.; Khoshfetrat, A. B.; Taya, M. *Carbohydr. Polym.* **2014**, *111*, 404–9.

(363) Kanokpanont, S.; Damrongsakkul, S.; Ratanavaraporn, J.; Aramwit, P. *Int. J. Pharm.* **2012**, *436*, 141–53.

(364) Lecumberri, E.; Dupertuis, Y. M.; Miralbell, R.; Pichard, C. *Clin. Nutr.* **2013**, *32*, 894–903.

(365) Wu, F.; Sun, H.; Kluz, T.; Clancy, H. A.; Kiok, K.; Costa, M. *Toxicol. Appl. Pharmacol.* **2012**, *258*, 166–75.

(366) Johnson, M. K.; Loo, G. *Mutat. Res. Repair* **2000**, *459*, 211–218.

(367) Hsieh, D.-S.; Wang, H.; Tan, S.-W.; Huang, Y.-H.; Tsai, C.-Y.; Yeh, M.-K.; Wu, C.-J. *Biomaterials* **2011**, *32*, 7633–40.